NEW KINASE-BASED MOLECULAR DIAGNOSTIC TOOLS FOR TARGET DISCOVERY, LIVE IMAGING, AND DRUG RESPONSE PROFILING IN CANCER

Alaa Omar Baryyan

Division of Experimental Medicine

Faculty of Medicine

McGill University

Montreal, Canada

August 2021

A thesis submitted to McGill University in partial fulfillment of the requirements of the degree of Doctor of Philosophy

First Date of Publication February 26, 2024

I ABSTRACT

Over the past two decades kinase inhibitors have revolutionized the therapy of cancer. This revolution was based on their target selectivity for specific oncogenes that drive cancer progression and resistance to classical chemotherapy. Despite their specificity, they bind to multiple targets of the same or other families of kinases (e.g. threonine and tyrosine kinases). While in the past this lack of selectivity was viewed negatively, it is now increasingly clear that the promiscuous inhibitors are more potent against resistance tumours. Their target profiling often includes several oncogenes associated with drug resistance. Here the target multiplicity of kinase inhibitors is exploited in two specific ways: a) to develop tools to read kinase signatures and evaluate their significance in chemotherapeutic drug response and, b) tagging the inhibitors with fluorescent labels in order to visualize their distribution and localization inside the cells. To achieve objective (a), we designed and synthesized two chemoprobes targeted to two receptor tyrosine kinases, which are amongst the most validated cancer targets of the past two decades: the epidermal growth factor receptor (EGFR) and the hepatocyte growth factor receptor MET. To achieve objective (b), we synthesized fluorescent labeled chemoprobes to visualize the subcellular distribution of these inhibitors and that of their targets EGFR or MET. Thus, based on structure activity relationships previously established in our laboratory, we built AB31 with a quinazoline warhead to target EGFR and a biotin tag for magnetic pull-down. Likewise, AB19 a biotin tagged chemoprobe linked to a crizotinib scaffold was designed with a crizotinib scaffold to target MET and a biotin tag for pull-down. The results showed that AB31 could pull-down its primary target EGFR, in addition to a small population of kinases and mitochondrial proteins in cell lysates. Studies with fluorescent probes AB20, AB63, and AB64 carrying the same warheads as AB19 and AB31 revealed that the cellular localization was primarily non-membranal but rather perinuclear. This

suggests that these fluorescent probes preferentially bind to EGFR or MET localized in the perinuclear region. As a more versatile probe than AB31, AB19 was capable of pulling down a broad spectrum of kinases, and was used to extensively answer two major questions: 1) are the kinase pull-down profiles produced by the chemical probes in all cells similar or cell specific? and 2) Do pull-down patterns from drug-treated and non-treated cells present the same kinase/protein profile? The results showed that kinase pull-down profiles significantly varied with cell types. By contrast, the profiles of cells treated with the chemotherapeutic drug paclitaxel, barely changed from drug treatment to no-treatment conditions. Increases in captured kinases (e.g. mTOR, AURKA) inspired the design of combination of paclitaxel + crizotinib, paclitaxel + torkinib (mTOR inhibitor) and paclitaxel + alisertib (AURKA inhibitor). Of all the combinations tested the paclitaxel + alisertib combination was the most synergistic. We further tested the ability of AB19 to profile human plasma samples collected from lung cancer patients treated with crizotinib. Our results *in toto* demonstrated that the chemoprobe AB19 could pull-down lipoproteins and specific proteins such as fibronectin. However, the linker of the chemoprobe appeared to be involved in their pull-down mechanism. Further studies on the approach may lead to the development of chemoprobes as liquid biopsy tools to guide cancer therapy.

II RESUME

Au cours des deux dernières décennies, les inhibiteurs de kinases ont révolutionné le traitement du cancer. Cette révolution a été basée sur leur sélectivité pour des oncogènes responsables de la progression tumorale et de la résistance à la chimiothérapie classique. Malgré leur spécificité, ils sont capables de cibler plusieurs protéines de la même famille et même, d'autres familles de kinases (par ex. thréonine et tyrosine kinases). Alors que par le passé, ce manque de sélectivité était perçu péjorativement, il est maintenant de plus en plus clair que l'efficacité des inhibiteurs multiciblés est supérieure à celle de ceux qui sont sélectifs. L'ensemble des cibles qu'ils atteignent comprend souvent plusieurs oncogènes associés à la résistance aux médicaments. Dans le contexte de ce travail, la multiplicité de cibles des inhibiteurs de kinases est exploitée de deux manières spécifiques : (a) développer des outils pour lire les signatures de kinases et évaluer leur importance dans la réponse aux antinéoplasiques et (b) marquer les inhibiteurs avec des marqueurs fluorescents afin de visualiser leur distribution et leur localisation à l'intérieur des cellules. Pour atteindre l'objectif (a), nous avons conçu et synthétisé deux sondes chimiques qui visent deux récepteurs de la classe des tyrosine kinases, qui sont parmi les cibles cancéreuses les plus validées au cours des deux dernières décennies : le récepteur du facteur de croissance épidermique (EGFR) et le récepteur du facteur de croissance des hépatocytes MET. Pour atteindre l'objectif (b), nous avons synthétisé des chimiosondes fluorescentes pour visualiser la distribution subcellulaire de ces inhibiteurs et celle de leurs cibles EGFR ou MET. Sur la base des relations structure-activité précédemment établies dans notre laboratoire, nous avons construit AB31 avec une tête de quinazoline pour cibler l'EGFR et une queue marquée à la biotine pour l'attraction magnétique. De même, AB19, une chimiosonde marquée à la biotine liée à un échafaudage crizotinib a été conçue avec un échafaudage crizotinib pour cibler MET et une étiquette biotine pour le captage

magnétique. Les résultats ont montré qu'AB31 pouvait capter sa cible principale EGFR, en plus d'une petite population de kinases et de protéines mitochondriales dans les lysats cellulaires. Des études avec des sondes fluorescentes AB20, AB63 et AB64 portant les mêmes ogives que AB19 et AB31 ont révélé que la localisation cellulaire était principalement non membranaire mais plutôt périnucléaire. Cela suggère que ces sondes fluorescentes se lient préférentiellement à l'EGFR ou au MET qui sont localisés dans la région périnucléaire. En tant que sonde plus polyvalente que AB31, AB19 était capable de capter un large spectre de kinases et a été utilisée pour répondre de manière approfondie à deux questions principales : 1) les profils de distribution de kinase captés parles sondes chimiques dans toutes les cellules sont-ils similaires ou spécifiques à une cellule ? et 2) les profils de distribution captés dans les cellules traitées sont-ils similaire ou différents? Les résultats ont montré que les profils de kinase obtenus variaient de manière significative avec les types de cellules. En revanche, les profils des cellules traitées avec l'antinéoplasique paclitaxel, ont à peine changé d'un traitement médicamenteux à l'autre. Par contre, L'augmentation de la quantité de kinases captées (par ex. mTOR, AURKA) a inspiré la conception de nouvelles formules de combinaison avec le paclitaxel: paclitaxel + crizotinib, paclitaxel + torkinib (inhibiteur de mTOR) et paclitaxel + alisertib (AURKA). De toutes les combinaisons testées, l'association paclitaxel + alisertib était la plus synergique. Nous avons également testé la capacité d'AB19 à profiler des échantillons de plasma humain prélevés sur des patients atteints de cancer du poumon traités par crizotinib. Nos résultats ont démontré dans la sonde chimique pouvait capter des lipoprotéines et des protéines spécifiques telles que la fibronectine. Cependant, l'espaceur des sondes chimiques semble être impliqué dans leur mécanisme d'attraction. D'autres études sur l'approche pourraient conduire au développement de sondes chimiques en tant qu'outils de biopsie liquide pour guider le traitement du cancer.

III ACKNOWLEDGEMENT

First and foremost, I am forever grateful to my parents, Fawziah and Omar, for their love, prayers, and sacrifices for educating and preparing me since day one. I am thankful to my children, Fatimah, Ahmed, and Sumaia, for their love, patience, and understanding throughout the toughest times of this journey.

I would like to express my deep and sincere gratitude to my research supervisor, Dr. Bertrand Jean-Claude, for giving me the golden opportunity to do research and providing invaluable guidance throughout my Ph.D. project. His vision, sincerity and motivation have deeply inspired me. I cannot thank him enough for taking the time to help me particularly during deadlines. It was a great privilege and honor to work and study under his guidance. I am extremely grateful for what he has offered me. I am extending my heartfelt thanks to his family for their acceptance and patience during the meetings I had with him on research work and thesis preparation.

I am very grateful to Dr. Kurt Dejgaard for his help and proteomics expertise that have significantly contributed to the success of this project.

I would like to thank my committee members, late Dr. Geoffery Henry, Dr. Suhad Ali, Dr. Siham Sabri, Dr. Jian Wu, and Dr. Jacques Lapointe.

I also would like to thank my labmates, and friends for their constant encouragement. Special thanks to Dr. Caterina Facchin for her help in fluorescence microscopy. My thanks go to all the people who have supported me to complete my Ph.D. research directly or indirectly.

Finally, my thanks go to the university of Umm Al-Qura for financially supporting me over the last six years, and to McGill university for opening their doors of knowledge to me.

IV SCHOLARLY CONTRIBUTION TO ORIGINAL KNOWLEDGE

Several elements of the this thesis are considered original scholarship and scholarly contribution to knowledge. There are described as follows:

- The feasibility of a chemoprobe carrying a unique quinazoline warhead (AB31) to pull down EGFR and other kinases from lysates of tumour cells, was demonstrated.
- The feasibility of magnetically pulling down this chemoprobe with its captured proteins was demonstrated.
- AB31 could pull down several kinases from different cell lines with a kinase targeting profile that was cell-specific and in most cells captured several mitochondrial proteins.
- AB19 was successfully synthesized as a probe designed to target MET, contained a crizotinib warhead, a linker, and a biotin tag directed at streptavidin beads for pull-down.
- Using cell lysates, AB19 showed its ability to bind to MET and to pull down several important oncoproteins such as SRC, LCK, and EPHA2 (receptor and non-receptor tyrosine kinases).
- Probing cells pre-treated with paclitaxel and arrested in M phase led to the identification of AURKA and mTOR as targets for modulating response to paclitaxel. Of all the targets tested, inhibiting AURKA appeared to be a synergistic event in prostate cancer cell pre-treated with paclitaxel.
- Designing probes to carry a fluorescent tag led to AB20 (green color), and AB64 (red color) to image A549 cells that co-express MET and EGFR.
- AB64 and AB20 were colocalized in the perinuclear region, and using an endogenously expressing full length EGFR cells A549, AB64 was found to be colocalized with EGFR in the perinuclear region but not in the membrane.

- AB19 could pull down proteins from patient samples with primarily a large content in lipoproteins and the most relevant oncoprotein was fibronectin.

V CONTRIBUTIONS OF AUTHORS

This manuscript-based thesis is composed of four manuscripts and the contributions of each author are stated below.

CHAPTER 2: DESIGN AND SYNTHESIS OF A NOVEL EPIDERMAL GROWTH FACTOR RECEPTOR (EGFR)-TARGETED PROBE: AFFINITY PULL-DOWN FROM CANCER CELLS

Dr. Kurt Dejgaard have analysed all proteomics samples, he also wrote the mass spectrometry and data analysis of proteomics raw files in methods section of the manuscript. I carried out the synthesis of the chemoprobes, the cell culture as well as the pull-down assays. I interpretated the data in this manuscript, I also helped with the preparation of the manuscript. Dr. Bertrand Jean-Claude revised the manuscript and made the necessary changes.

CHAPTER 3: DESIGN, SYNTHESIS, AND VALIDATION OF A MET-TARGETED CHEMOPROBE FOR IDENTIFYING KINASES TO BE TARGETED FOR SENSITIZING CELLS TO PACLITAXEL: A PROOF-OF-CONCEPT STUDY

Dr. Kurt Dejgaard have run all proteomics samples. He also wrote the mass spectrometry and data analysis of proteomics raw files in methods section of the manuscript. Dr. Alain Wagner (university of Strasbourg) has gifted us the biotin tag PEG5. I am also grateful to Dr. Karine Pasturaud who helped with the molecular modeling. I carried out the synthesis of the chemoprobes, the cell culture and the cell cycle experiments, the growth inhibition assay, the pull-down assay, and the drug combination experiments. I interpretated the data generated in this manuscript, I also

helped with the preparation of the manuscript. Dr. Bertrand Jean-Claude overlooked the proceedings of the experimental work and revised the manuscript.

CHAPTER 4: SYNTHESIS OF NOVEL EPIDERMAL GROWTH FACTOR RECEPTOR (EGFR) AND HEPATOCYTE GROWTH FACTOR RECEPTOR MET TARGETED INHIBITORS RATIONALLY DESIGNED TO CARRY A GREEN OR RED FLUORESCENT LABELS

I carried out the synthesis of the fluorescent-labeled probes. Dr. Caterina Facchin and I have contributed to the cell culture and live cell imaging experiments as well as the interpretated of the data in this chapter. I am also grateful to Dr. Ana Fraga Timiraos for upscaling the quantity of probe AB64. I have helped with the preparation of the manuscript, and Dr. Bertrand Jean-Claude made all the necessary comments and revised the manuscript.

CHAPTER 5: APPLICATION OF THE CHEMOPROBE APPROACH TO THE ANALYSIS OF CLINICAL SAMPLES: POTENTIAL DEVELOPMENT AS LIQUID BIOPSY TOOLS

I prepared the AB19 and AB22 probes. I performed sample preparation and pull-down experiments, while Dr. Kurt Dejgaard have run the proteomics analysis of the samples. I analysed and interpreted the proteomics data. Dr. Bertrand Jean-Claude helped with the design, conception and preparation of the manuscript.

Table of Contents

VI LIST OF ABBREVIATIONS

CML - chronic myelogenous leukemia

ATP - adenosine triphosphate

RTK - receptor tyrosine kinase

NRTK - non receptor tyrosine kinase

TK - tyrosine kinase

INSR - insulin receptor

EGFR - epidermal growth factor receptor

MAPK - mitogen-activated protein kinase

IGF1R - insulin-like growth factor R

ALK - Anaplastic Lymphoma Kinase

ADP - Adenosine diphosphate

EGF - epidermal growth factor

HGF – hepatocyte growth factor

GHR - growth hormone receptor

VEGF - vascular endothelial growth factor

TGFα - the growth factor α

AR - Amphiregulin

BTC - betacellulin

EPR - epiregulin

HB-EGF - heparin-binding EGF

NRG-1/2 - . Neurogulin-1 and -2 ligands

NSCLC - non-small cell lung cancer

TNBC - triple negative breast cancer

ER - endoplasmic reticulum

COPI - coat protein complex protein I

NLS - nuclear localization signals

ADAM - a disintegrins and metalloprotease

GFP - green fluorescent protein

NBD - p-nitrobenzoxadiazole

HBB - hemoglobin subunit beta

PCR - polymerase chain reaction

PTM - posttranslational modification

HTP - high throughput

SILAC - stable isotope labelling with amino acid

FGFR - fibroblast growth factor receptor

THF - tetrahydrofuran

HOBt – hydroxybenzotriazole

DMAP – dimethylaminopyridine

EDCI - 1-Ethyl-3-(3-dimethylaminopropyl)carbodiimide

DIEA - N,N-Diisopropylethylamine

TLC – thin layer chromatography

TBA - Tubulin binding agent

PEG - polyethylene glycol

SRB - sulforhodamine B

CI - Combination index

CHAPTER 1

INTRODUCTION

1.1 PREFACE

The past twenty years have seen development in genomics, transcriptomics, proteomics, metabolomics, and other high throughput analysis of biomolecules that now we refer to as Omics. High throughput characterization of gene expression profile has significantly contributed to the elucidation of several mechanisms that drive tumour progression and response to chemotherapeutic regimen. Among many diseases, cancer is the most studied pathology that utilized the Omics. As an example, the revolution marked by personalized medicine in cancer was triggered by the identification of specific mutants that characterize sensitivity to epidermal growth factor receptor inhibitors in 2004 (1, 2). This discovery could not have been achieved without the advances in the field of genomics and this was accompanied by developments in the field of proteomics that profile kinases and give rise to the field of phosphorproteomics. In the cancer therapeutic filed, the discovery of the role of kinases e.g. tyrosine, serine, threonine kinases etc. in the complex network of signaling that characterize cancer progression and reduce sensitivity to antitumour drugs has revolutionized cancer therapy with small molecules leading now to molecules that are called “targeted therapy”. In contrast to traditional chemotherapeutic agents targeting DNA or metabolic enzymes, drugs that inhibit specific kinases have emerged as more targeted and less toxic agents that can be administered daily (3). The first agent that marked the beginning of this new era was imatinib, a kinase inhibitor that block BCR-ABL kinase which is a target for chemotherapeutic intervention against chronic myelogenous leukemia (CML), these new targeted agents replace the highly toxic chemotherapeutic agents such as hydroxyurea, busulfan which are now irreversibly withdrawn from the clinical management of CML (4, 5). BCR-ABL represents a target that is the soul oncogene driving the resistance to apoptosis by the CML cancer cells. However, in most cancers the resistance mechanism is mediated by more complex

mechanisms involving many distinct signaling pathways that are controlled by multiple kinases (Figure 1.1). There are about 500 of these kinases inside the tumour cells and they formed what is now known as the kinome (6). Cancer is one of the diseases that is the most etiologically and therapeutically affected by disorders of the kinome. Overexpression and mutation of several kinases, most particularly receptor tyrosine kinases, characterize the progression of several tumour types, including breast, prostate, lung and this is associated with poor prognosis (7). From a therapeutic standpoint, because these disorders often lead to activation of anti-apoptotic signaling, they are associated with reduced sensitivity to anticancer drugs. Another phenomenon termed "signaling redundancy" leads to resistance to kinase inhibitors. This occurs when blockade of a receptor with a given inhibitor does not inhibit downstream signaling pathway due to the presence of other receptors that activate the same signaling pathway (8). As a result, kinase inhibitors are being developed with a strong focus on their ability to block multiple signaling pathways. The kinases have in common a little pocket that binds to ATP termed "ATP pocket". Because this pocket is conserved, a molecule targeting the ATP pocket may bind to many different kinases (9). Indeed, it has been found that most kinase inhibitors while having a conical target, can unspecifically bind to many other kinases and this termed kinase profiling (10, 11). The fundamental idea of this thesis is to use the ATP pocket as an anchorage point to pull-down the kinases and generate profiles that can be used to generate signatures of tumours under conditions where they are treated or non-treated with tumour drugs. This has been achieved by designing molecules termed chemoprobes that contain a head designed to bind to the ATP pockets and a tail used for attachment to a tag that can be used for pull-down or generating fluorescence for live imaging. The idea about pulling down probe-bound proteins and characterization by proteomics is now called chemical proteomics. Here our purpose is to make the proof of concept of the

chemoprobes as molecular diagnostic tools that can be used to probe biological fluids under pharmacological and clinical conditions. Prior to describing our results (chapters 2-5), here we discuss tyrosine kinases, kinase inhibitors, their role in cancer, principles underlying molecular diagnostic, and the background underlined previous efforts that led to our design and studies.

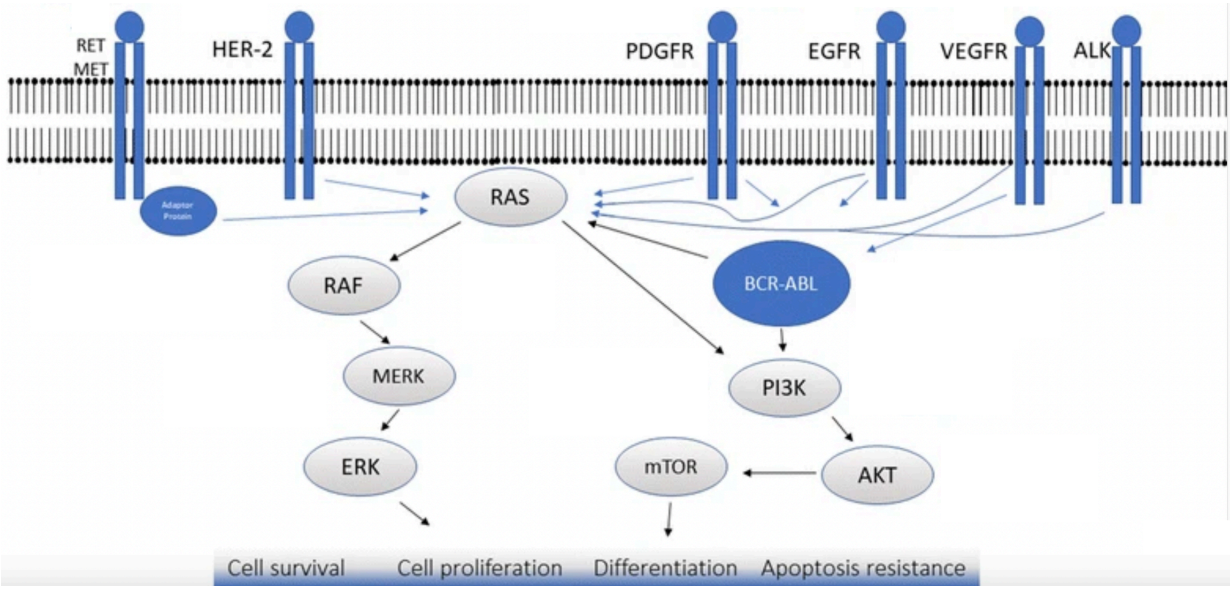

Figure 1.1 Schematic representation of receptor tyrosine kinases and downstream signaling pathways. Reprinted from "Receptor tyrosine kinases and downstream pathways as druggable targets for cancer treatment: the current arsenal of inhibitors". Copyright © 2018, *Molecular Cancer*. No special permission is required to reuse all or part of article published by the journal.

1.2 THE HUMAN KINOME

1.2.1 Definition

The Human kinome is a large set of kinases encoded by corresponding unique genomes, and are classified based on their substrates into protein and lipid kinases. Human genome sequencing led

to the identification of 518 protein kinases, which represent less than 2% of the total human genes, and about 20 lipid kinases (6). A schematic representation of the phylogenesis of human kinome is shown in Figure 1.2. Protein kinases are further classified based on the amino acid residue phosphorylated into serine/threonine, tyrosine, or histidine kinases. In addition to their role in controlling cellular processes such as metabolism and cell cycle, protein kinases also mediate signaling transduction in cells and modifying substrates activity. Protein phosphorylation play a key role in cell communication as a response to various biological processes such as homeostasis and alters proteins functional activity by different mechanisms. Studying protein kinases over the recent decades revealed the association between dysregulated kinases and diseases such as cancer and diabetes. Indeed, about 164 kinases are linked with amplicons regularly found in tumours. Thus, protein kinases are an attractive target in drug design and development field, and many kinase agonists and antagonists have been developing since then (12-14). Manning and his colleagues (6) classified protein kinases into 9 major groups based on sequence similarity in kinase domains. Among these groups are receptor tyrosine kinases (RTKs) located at the cell transmembrane, and non-receptor tyrosine kinases (NRTKs) located in the cytoplasmic region of the cell. TKs transduce signals among cellular pathways in response to external or internal stimuli, and meditating various biological processes such as cell growth, proliferation, migration, apoptosis, differentiation, cell cycle, and metabolism. These processes in total intend to maintain tissue homeostasis (6, 15). Signaling is a complex but well organized operation between cellular components including membrane receptors, cytoplasmic proteins, and transcription factors, to transduce signals from the outside the cell downstream to the DNA. Dysfunctioning TKs promote disease progression through various mechanisms including overexpression, point mutation, fusion, and relocation (6, 16-19). Next sections discuss TKs implication in cancer and targeted therapy.

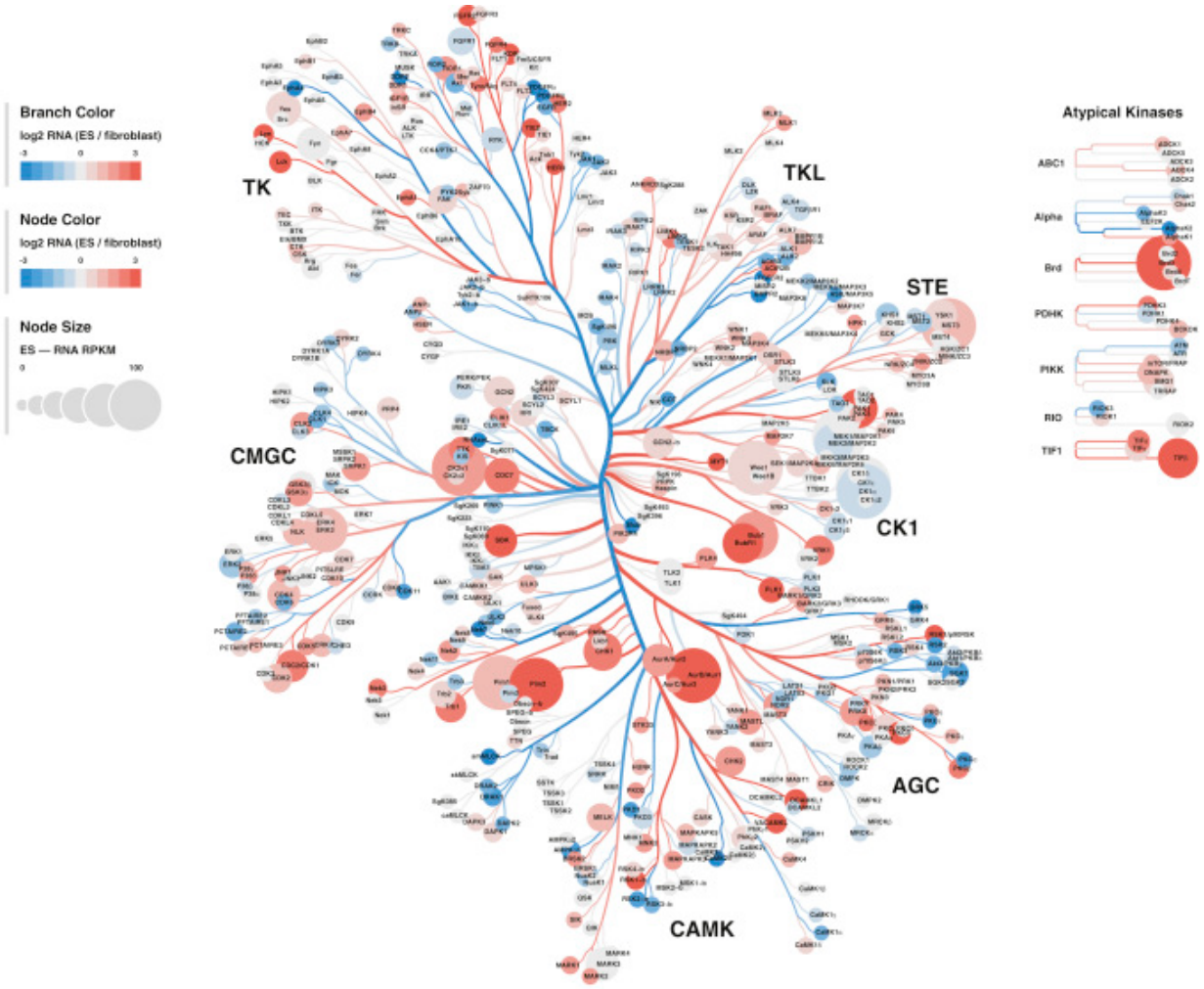

Figure 1.2 A phylogenetic tree of human kinome showing protein kinases. Reprinted from "Coral: Clear and Customizable Visualization of Human Kinome Data". Copyright © 2018, *Cell Systems*. License Number # 5187340896900.

1.2.2 Overview of the discovery of protein tyrosine kinases

The importance of phosphorylation and cell signaling was accumulated over the last century upon early discoveries in the field of cell biology. Protein phosphorylation was first reported in 1906 upon his discovery of phosphorylated vitellin protein. Protein phosphorylation research and their role in cellular functions became a phenomenon in biochemical laboratories back then (20-22). In

1943, glycogen phosphorylase was identified and an effort was made to hypothesize its mechanism of activation (23). Over the following decade, a consecutive work by various researchers was achieved and described multiple enzymes, particularly, the protein kinase activity in the presence of ATP molecule (24-27). Nevertheless, it was not until the late 1970s when the actual attention towards protein phosphorylation started and many signaling pathways have been identified. The first protein tyrosine kinase was discovered in 1979 by Hunter as a fortunate incidence in the lab that influenced our understanding about the biology of cancer ever since. Hunter was studying Rous sarcoma virus that causes cancer in chickens, and was attempting to understand the enzyme responsible for tumour growth. The separation of two amino acids, phosphor-tyrosine and phospho-threonine, on the electrophoresis plate ran in a slightly low pH buffer led to identification of that enzyme as a protein tyrosine kinase (c-Src) causing cancer in chickens (28). Concomitantly, Witte and his team (29) were studying Abelson virus causing leukemia in mice, and investigating the protein kinase triggering tumour growth. They reported that the phosphorylation of Abelson murine leukemia protein (P120) may be involved in activating the virus causing leukemia and sarcoma too. Similarly, EGFR and insulin receptor (INSR) were also identified as a protein tyrosine kinases and are activated upon EGF and insulin engagement, respectively (30, 31). Further studied were conducted on EGFR and revealed that the receptor can be phosphorylated exogenously as well as without the ligand involvement (32, 33). Likewise EGFR, MET was first identified in 1984 as a by-product of gene transforming in osteosarcoma cells until 1991 where it was indeed identified as a hepatocyte growth factor receptor known to promote the cellular hepatocyte growth (34-36). More investigations continued to explore other signaling pathways revealed some tyrosine and serine/threonine kinases, for example, phosphoinositide 3-kinase (PI3K) and mitogen-activated protein kinase (MAPK) pathways (24, 37).

1.2.3 Structure and function of protein tyrosine kinases

Human genome sequencing project has identified approximately 23,000 genes containing 90 tyrosine kinases genes that were further classified based on the kinase domain structure, kinase function, and cellular location into receptor tyrosine kinases (RTKs) and non-receptor tyrosine kinases (NRTKs) (38). The next two sub-sections will highlight the structure and function of the two types protein tyrosine kinases.

1.2.3.1 Receptor tyrosine kinases (RTKs)

RTKs are transmembrane glycoproteins have been divided based on extracellular structural features and sequence homology into 20 subfamilies (Figure 1.3). In common, they transduce signals from extracellular part of the cells cytoplasmic part upon ligand binding to their cognate receptor by phosphorylating tyrosine residues on the receptor itself and on cytoplasmic signaling proteins. RTKs activation is a fundamental process in cellular communication by which they activate different signaling pathways within cells leading to cell proliferation, migration, differentiation, or metabolic changes. Ligand-receptor signaling adopt various mechanisms depending on the cell type as well as ligands and receptors involved. For example, the binding of the epidermal growth factor (39), growth arrest specific gene-6 (Gas6), and insulin ligands to their corresponding receptors EGFR, AXL, and insulin receptor (INSR), respectively. The biding occurs as a response to a growth stimulus in response to glucose homeostasis process (40-42).

Most RTKs share similar intracellular kinase domain that contains a regulatory sequence on C- and N-terminal and possesses the actual enzymatic activity, but diverse extracellular domains for conveying ligand specificity, and a single transmembrane hydrophobic helix domain. Binding of

extracellular ligand to the receptor leads to receptor clustering and changes receptor conformation, subsequently phosphorylating tyrosine residues in the kinase intracellular domain and C-terminal regions. C-terminal residues are key signaling mediator between receptors and downstream kinase (15, 43).

RTKs are a large family that includes EGFR family (EGFR, Her2, Her3, and Her), INSR and insulin-like growth factor R (IGF1R), platelet-drive growth factor (PDGFR), hepatocyte growth factor receptor MET and RON receptors. Activation of these RTKs upon exogenous ligands binding ultimately lead to cell proliferation, differentiation, invasion, angiogenesis, embryogenesis, and many other functions through triggering signals transduction (44). Overall, under normal conditions RTKs maintain human early development as well tissue homeostasis by regulating cellular growth and death (45).

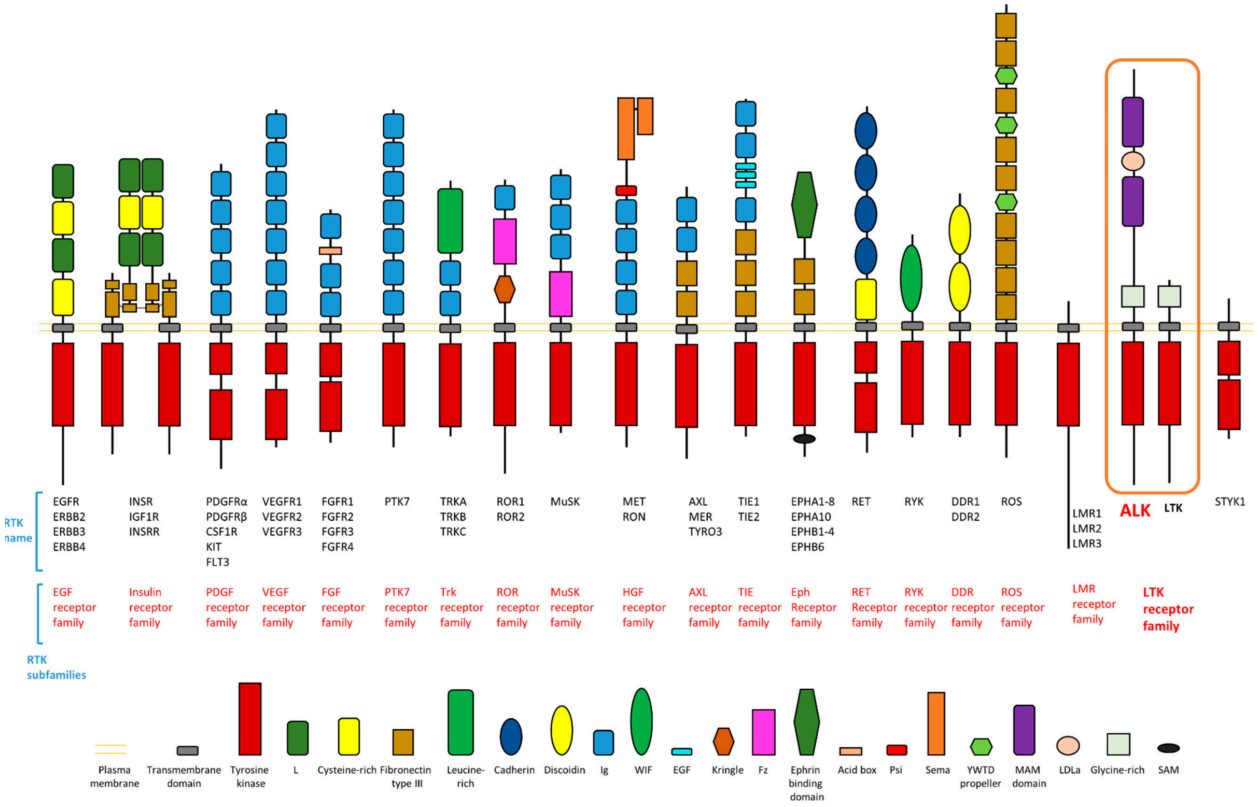

Figure 1.3 Receptor tyrosine kinase families. Reprinted from "Anaplastic Lymphoma Kinase (ALK) Receptor Tyrosine Kinase: A Catalytic Receptor with Many Faces". Copyright © 2018, *International Journal of Molecular Sciences*. No special permission is required to reuse all or part of article published by the journal.

1.2.3.2 Non-receptor tyrosine kinases (NRTKs)

Non-receptor tyrosine kinases (NRTKs) is a family of cytoplasmic proteins that exhibit structural variability and indirectly interacting with extracellular ligands in order to transduce signaling within the cell, for example SRC, ABL, JAK, AND FAK kinases. NRTKs play a fundamental role in regulating gene expression, immune response, cellular growth, proliferation, invasion, angiogenesis and so on, and have been critically involved in cancer biology. The 32 known NRTKs are classified based on the kinase domain sequence and function into 10 subfamilies (Figure 1.4).

As an example, the SRC family contains (SRC, YES, FYN, LYN, LCK, BLK, HCK, FGR, and YRK), ABL family contains ABL and ARG, while the focal adhesion FAK family consists of one member FAK (46, 47) . NRTKs function as subunits of RTKs with or without intrinsic protein kinase catalytic activity and mediate several signaling or protein-protein interaction signal transduction through phosphorylation cascades. Thus, NRTKs play a critical role in cancer biology and immune system through coherent crosstalk with RTKs as part of cell signaling process (46). Unlike RTKs, NRTKs lack the receptor-like and transmembrane-like features. Most of NRTKs are cytoplasmic, but some are attached to the cellular membrane (46). In common, they share a similar core kinase domain structure possess SH3 domain (N-terminal), SH2 domain, and the kinase domain.

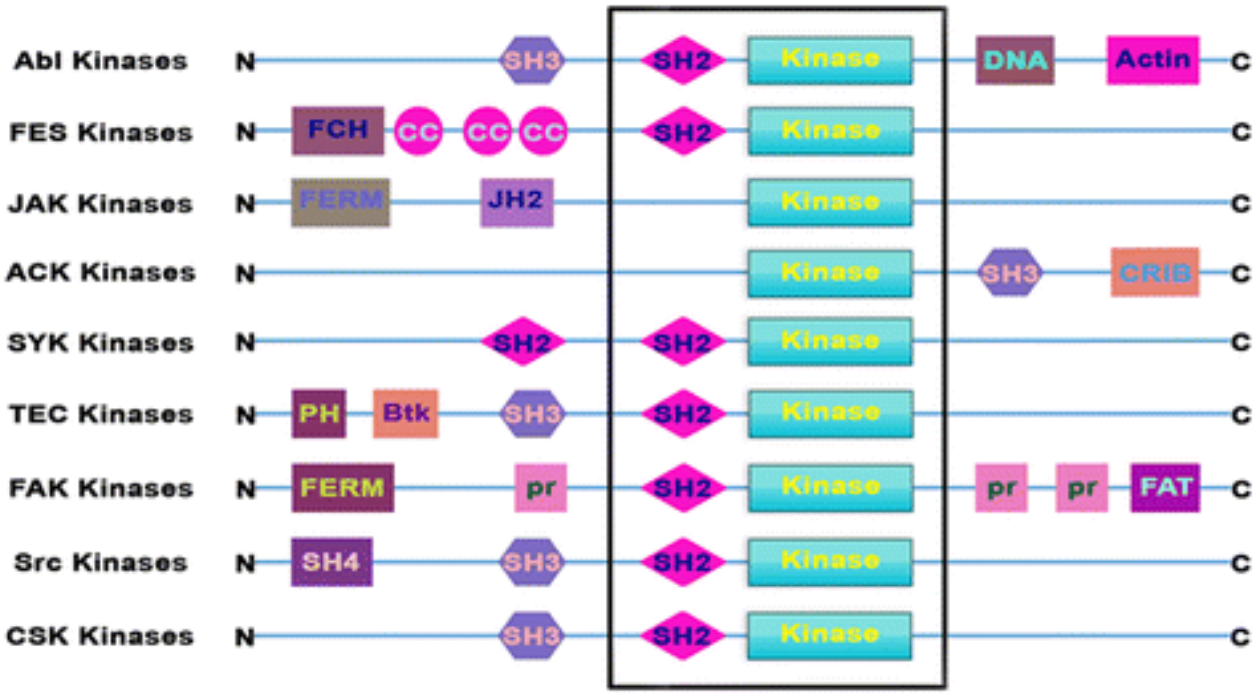

Figure 1.4 Main non-receptor tyrosine kinase families and illustration of shared domains: SH2 domains, SH3 domains, and the kinase domain. Reprinted from "Role of Non Receptor Tyrosine

Kinases in Hematological Malignances and its Targeting by Natural Products". Copyright © 2018, *Molecular Cancer*. No special permission is required to reuse all or part of article published by journal.

1.2.3.3 Activation of tyrosine kinases – an overview

Signaling transduction is a complex but well-coordinated process by which cellular components such as surface receptors, cytoplasmic and cytoskeletal proteins coherently engage in communication with extracellular medium, most commonly, through protein phosphorylation. Protein phosphorylation is the chemical process of transferring a terminus γ-phosphate group from adenosine triphosphate (ATP) to a tyrosine, serine, or threonine residues on the target protein, which in turn changes its conformation and modify substrate's activity (26, 48). ATP are considered the source of cellular free energy among all eukaryotic cells, mostly in an ester form, and it hydrolyzes to adenosine diphosphate (ADP) upon energy transfer reaction between substrate proteins (6, 16) (Figure 1.5). Tyrosine kinases phosphorylate tyrosine residues in substrate they are binding to, and triggers a series of molecular events between extracellular and intracellular components.

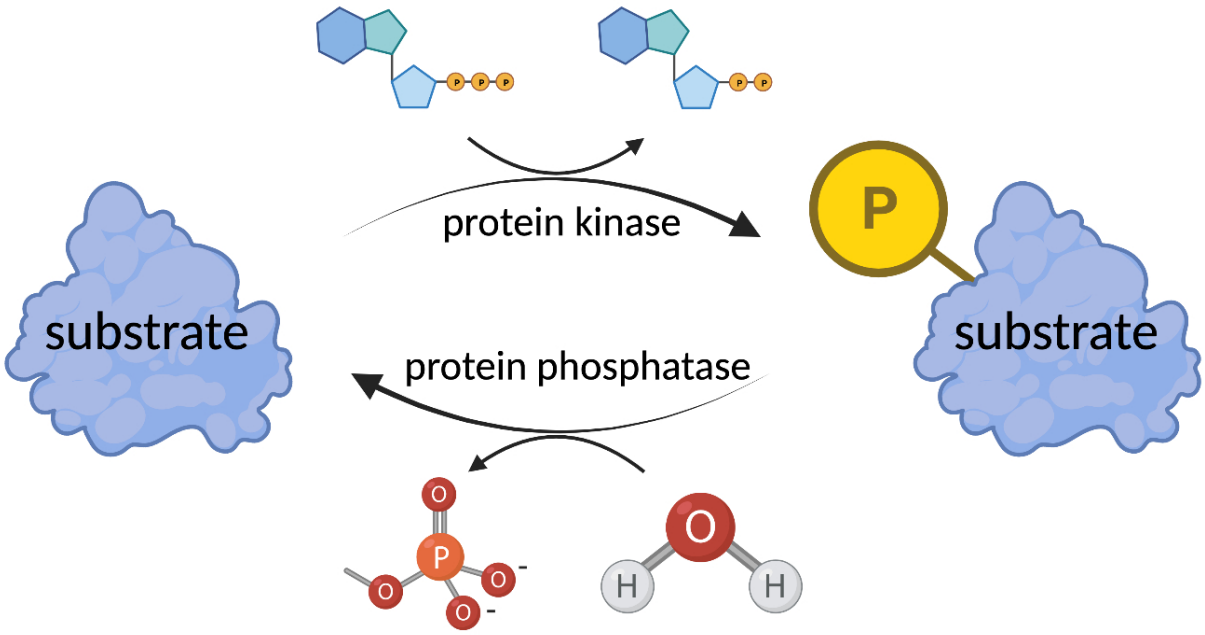

Figure 1.5 Illustration of phosphorylation cycle carried on the substrate protein.

Upon cellular demand, receptor tyrosine kinases are selectively activated by receptor-specific ligands that bind to the extracellular domain and deliver the intended signal. For example, epidermal growth factor (EGF) (39) and hepatocyte growth factor (HGF) ligands bind to their specific receptors EGFR and MET, respectively, and induce receptor dimerization and/or oligomerization which consequently changes the kinase conformation (45, 49). Ligand-receptor complex formation occurs in different ways by which the complex adopt a stable confirmation, that is, some ligands bind to two receptor molecules (e.g. growth hormone and the growth hormone receptor (GHR)), while in other cases two ligands bind to two receptor molecules (e.g. VEGF and VEGFR) which consequently stabilizes formed dimer and activates the kinase. For most RTKs, the resultant conformation facilitates *trans*-autophosphorylation of the kinase domain and disturb the *cis*-autoinhibition (43). The latter RTK autophosphorylation activates downstream kinases that contain phosphortyrosin binding domains (SH2 homology), and initiate downstream mediators

activation (50). Receptor dimerization lead to tyrosine residue phosphorylation, which in turn causes activation loop to adopt on-conformation that allows ATP transfer to the substrate protein. NRTKs which are located in the cytoplasm are recruited in signals transduction after the activation of upstream RTKs. In a similar manner to NRTKs, RTKs are regulated mainly by the phosphorylation process that is either independent (autophosphorylation) or dependant on other activators' binding such as inhibitors or other kinases. The latter process occasionally lead to proteins translocation to the nucleus where major transcription processes are undertaken.

It is well understood now that under normal physiological conditions tyrosine kinases regulate various signaling pathways via phosphorylation. However, mutated tyrosine kinases in cancer trigger uncontrolled signaling cascades and consequently uncontrolled cell growth. The latter findings and collected knowledge paved the way towards understanding the significance of tyrosine kinases, and led to establish new directions in cancer therapy, that is a new class of drugs called "tyrosine kinase inhibitors". Since then, researchers are studying and targeting tyrosine kinases, and plenty of papers targeting have been reported (51).

1.2.4 Tyrosine protein kinase ABL1 (Abl): the first targeted NRTK with proven clinical activity

Abl family is a cytoplasmic protein kinases that consist of two kinases ABL1 and ABL2. ABL1 (or Abl) is one of the extensively studied kinases over the last two decades upon the discovery of the Bcr-Abl mutation in chronic myelogenous leukemia (CML). Due to the vital role of Bcr-Abl mutation in conferring resistance to apoptosis in CML cells, it is the first targeted NRTK that

translated into effective clinical activity. Here we discuss the structure, function, and targeting of Bcr-Abl fusion protein.

1.2.4.1 Structure and function of Abl and fusion protein Bcr-Abl

The core of Abl protein has similar homology to that of the SRC family kinases. That is, Abl kinase contains SH2 and SH3 domains, SH2 linker, bilobal kinase domain (Figure 1.6). The core is surrounded by N- and C-terminal regions which regulate the kinase activity, while C-terminal region regulates the actin cytoskeleton, the kinase nuclear-cytoplasmic translocation, and most importantly the interaction between Abl and other SH3-containing proteins (52-54). Abl kinase activity is regulated by many intramolecular interactions that trigger the autoinhibition of Abl kinase domain. Both of SH2 and SH3 domains mediate Abl kinase autoinhibition, which is achieved when SH3 domain interaction with SH2 linker occurs which causes the linker to sandwich itself (off-mode) between the SH3 domain and the N-terminus tail. When the latter interaction complex is disturbed, Abl kinase is activated (on-mode) (55, 56). The N-terminal region contains myristic acid group that binds to the hydrophobic pocket in the C-terminal and induces the C-lobe to bend allowing SH2 domain to dock itself onto the C-lobe of the kinase domain (57). That explains the significant role of myristoylation signal in maintain the off-mode state. The N-terminal tail further regulating Abl kinase through SH2 and SH3 domains, that is, the Serine69 (Ser69) in the N-terminal region is phosphorylated and approaching the linker between SH2 and SH2 domains. Hence, Mutated Serine69 also contribute to Abl increased activation (58). Binding between residues 65-80 in N-terminal region and SH2 domain further support the observation that the N-terminal region indeed hold the SH2 and SH3 domains at the back of the kinase domain.

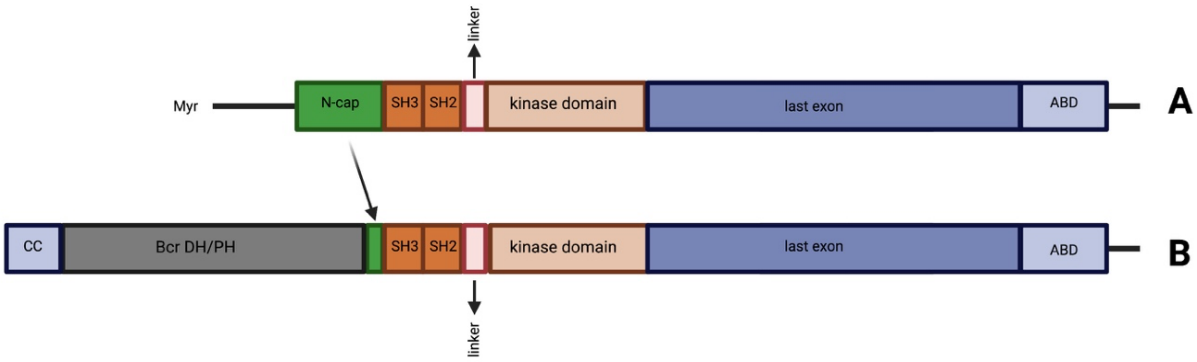

Figure 1.6 Domain composition of **a)** Abl-1b tyrosine kinase isoform and **b)** the fusion protein Bcr-Abl illustrating the DH/PH tandem domain by which the sequences discard most of the N-cap, leaving the remaining of Abl intact. Abbreviations: Myr, myristoyl group, N-cap, N-cap region, SH3 and SH2 domains, ABD, C-terminal actin-binding domain, CC, N-terminal coiled-coil oligomerization domain, Bcr DH/PH, DH and PH domains of oncogenic Bcr-Abl domains.

Disruption of the autoinhibition regulatory lead to oncogenic activation of the kinase. Bcr-Abl fusion protein. Unlike normal state, the fusion of Bcr-Abl genes in disease state (CML) encodes a constitutively active kinase (Figure 1.6). The latter abnormal activation causes CML cells to irregularly proliferate (15). Detailed analysis of crystal structure of Bcr-Abl fusion protein displays a bilobal architecture: N-lobe and C- lobe facing each other. The N-lobe consist of one α-helix and five β-sheets (β1 to β5) whereas C-lobe adopt a helical shape along the catalytic core. G-loop (also known as Wolker, phosphate-binding, or P-loop) located between β1 and β2 sheets of N-lobe is glycine rich and is highly flexible, thus it provides a suitable base for γ- and β- phosphate groups of ATP molecule to bind to it. Latter binding promotes a phosphoric anhydride bond breakage following attack from Asp363 of catalytic loop (59). The γ-phosphate group also binds to the catalytic lobe of the C-terminus allowing phosphate group transfer and catalysis to occur. Upon

ATP binding into the kinase domain, two hydrogen atoms from adenine also form hydrogen bonding with the hinge region that links the two lobes. Furthermore, Thr315 (also known as the gatekeeper) interacts with ATP which promote higher selectivity to some Bcr-Abl inhibitors. The back of binding pocket near N-lobe is essential to define an inhibitor specificity. That is, the gatekeeper's region of Abl kinase which has Th315 is replaced by isoleucine (T315I) in mutated form of the kinase (60-62).

The bcr-abl fusion in most CML cases is developed by a chromosomal translocation between chromosome 9 and 22 and is named "Philadelphia chromosome". The latter abnormality produces a permanently active bcr-abl kinase which in turn causes abnormal cells growth and proliferation in CML (61, 63, 64). Switching the catalytic domain on and off is controlled by the catalytic loop, which is stabilized in an open conformation upon tyrosine residue phosphorylation. Consequently, this offers β-strand a base for substrate binding. Due to activation loop flexibility usually it can alter its conformation to active or inactive to allow or to blocks substate binding, respectively. The activation loop consist of three key parts: Tyrosine393 residue (Tyr393), DFG motif (Asp-Phe-Gly) at N-terminus, and the peptide-substrate binding C-terminus. Tyr393 is the main site of phosphorylation in the activation loop within Abl kinase. When activation loop is folded into the active site Tyr393 forms a hydrogen bonding with (aspartic acid 363) Asp363, a highly conserved side chain significant for catalysis. Asp382 in peptide-substrate binding C-terminus coordinate during activation phase with Mg^{+2} ions, a crucial catalysis cofactors, and contains the substrate to be phosphorylated. Upon phosphorylation, Tyr393 residue leads to loop extension which facilitate kinase to adopt active conformation (59, 65).

1.2.4.2 Inhibition of tyrosine kinases activity: BCR-ABL tyrosine kinase

The discovery and understanding of tyrosine kinases and their role in cancer biology not only led to expand the discovery of more oncogenic kinase inhibitors but also initiated "personalized medicine" era. Despite imatinib selectivity, various resistance mechanisms to imatinib have been reported and led to expand the discovery and development for more effective kinase inhibitors targeting other mutant forms. Bosutinib, dasatinib, nilotinib, and ponatinib kinase inhibitors were designed and developed to overcome resistant forms of the kinase (66). For example, T315I a mutation caused by replacing threonine with isoleucine in position 315 of bcr-abl. Imatinib is the first targeted kinase inhibitor developed by Lyndon and his team (4) in the late 1990s as part of their search for protein kinase C inhibitors using drug screening approach. Upon identification of Bcr-Abl mutation namely Philadelphia chromosome mutation in CML patients, lead molecules library were screened against latter fusion protein and identified 2 lead compounds with phenylamino pyrimidine scaffold with a promising inhibitory potential against Bcr-Abl kinase as well other kinases. Further structural chemical development was carried out and lead to first to introducing a pyrimidine to the 3′-position which led to enhancing the biological activity of imatinib (Figure 1.7). Additional substituents were introduced to the phenyl ring and it was found that the amide group enhanced the molecule activity against Abl kinase. *In silico* study were performed led to adding a methyl group to the ortho position of the diaminophenyl ring but that decreased the oral bioavailability of the inhibitor which was overcame by replacing the latter functional group with N-methylpiperazine with improved water solubility and bioavailability. However, it was determined that N-methylpiperazine group may metabolize to aniline, thus was replaced with a benzamide group to give STI571 (later named Imatinib; Gleevec®) with enhanced

selectivity against Bcr-Abl as well as other kinases (4, 67, 68). Imatinib was clinically approved in 2001 after almost a decade from its discovery and development (68, 69).

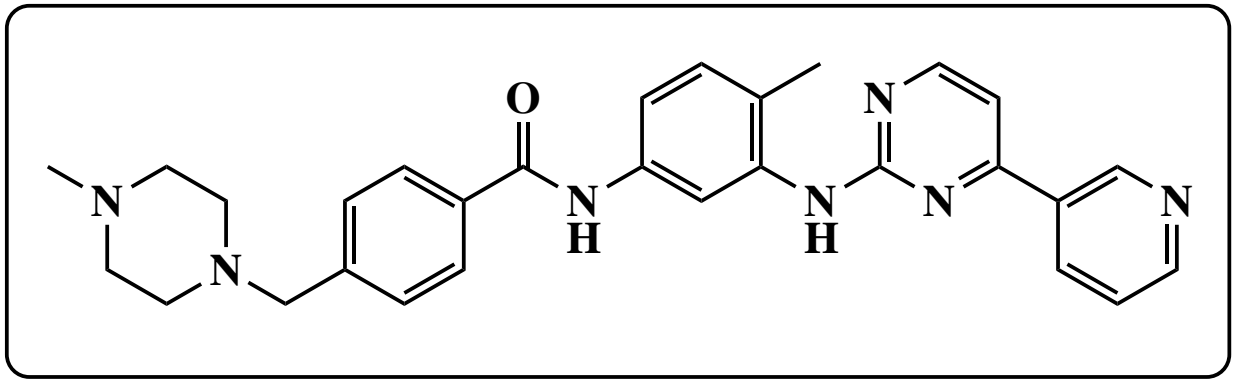

Figure 1.7 Chemical structure of imatinib the first tyrosine kinase inhibitor of Bcr-Abl in CML.

Imatinib is one of the first generation kinase inhibitors used for the treatment of CML in patients with bcr-abl fusion and successfully led to a complete hematological response. Imatinib typically bind at the ATP binding pocket of catalytic domain with high affinity and very high specificity to the active form of the kinase. Imatinib is bound into the binding pocket of kinase domain between C- and N-lobes whereas the pyridine part is locked into the binding site where adenine binds, while the remaining part of the molecule is bound into the hydrophobic region of the kinase domain. Normally, the adenine of ATP forms two hydrogen bonds with the backbone atoms of the peptide linking C- and N-lobes of the kinase domain (70). The first hydrogen donated by the amino group of ATP to the carbonyl oxygen of Glu316 corresponding residue, while the second hydrogen bond is donated from Met318 residue to the nitrogen atom of purine ring of ATP. Imatinib, just like most small molecules kinase inhibitors, anchors itself to the kinase domain in a similar manner and forms bonding similar to those between adenine of ATP and the kinase domain. However, the latter two hydrogen bonds are missing in case of imatinib (and similar kinase inhibitors) and is

replaced with water-mediated hydrogen bond (71). The overall binding hinders kinase mobility and prevent its activation. The Asp363 residue gets protonated after each phosphorylating step leading the kinase to adopt inactive conformation. Imatinib is known to attack the inactive conformation of the kinase, which is constitutively phosphorylated, during these transient off-conformation moments on Asp363 residue protonation.

A long term clinical study on the efficacy of imatinib for CML (n=553 patients) reported that the estimated overall survival rate was 83% at ten years, with complete cytogenetic response in 82% of the patients. Nevertheless, severe adverse events were also reported in 11.3% of the patients such as a second neoplasm (benign or malignant) (72). Resistance to imatinib has been increased remarkably (69), due to a primary or secondary (acquired) resistance, which alters the kinase conformation and consequently hinders the inhibitor binding (73), or due to bcr-abl independent resistance such as constitutive efflux of the drug or activation of alternative signaling pathways (69, 74). Various efforts have been undertaken to develop other TKIs to overcome imatinib resistance, which led to the second generation inhibitors targeting the mutated forms of the bcr-abl, as well as targeting downstream signalling pathways of bcr-abl. For example, dasatinib, bosutinib, and nilotinib are three TKIs rationally designed based on the mechanism of action of imatinib, and approved for clinical use for resistant CML to imatinib. Clinical study on newly diagnosed CML patients (n=300, 1.5 years) was conducted to compare the efficacy of dasatinib and nilotinib in comparison to imatinib. The study stated that patients who were treated with dasatinib or nilotinib have exhibited overall better response rate by 0.5, 1, and 1.5 years, with a complete hematological response in 94% and 82% of the patients at 0.5 and 1 year, respectively. It is worth mentioning that most of the second generation bcr-abl TKIs were potent against the

resistant forms except for T3151 mutation. This led to the development of the third generation of inhibitors (75). Ponatinib is a third generation bcr-abl TKI approved to date, and it showed a dual ability to inhibit both SRC and ABL. The development of the latter inhibitor was mainly intended to target the vital mutation T3151 (76). Indeed, a clinical study on patient in chronic phase of CML (n=90/128) ponatinib have demonstrated better clinical in CML patients with T3151 mutation. Thus, ponatinib is an alternative TKI for patients with T315I-positive chronic phase CML (77). More inhibitors such as tozasertib, danusertib, rebastinib, HG-7-85-01, and GNF-2 are developed to treat CML patients resistant to the previous TKIs, and are in clinical trial and may be approved in the near future (78-82). Among them, asciminib which is a third generation TKI that has been approved recently by the FDA for the treatment of CML harboring the T315I mutation (83).

1.2.5 The epidermal growth factor receptor (EGFR) protein

Epidermal growth factor protein (EGFR, or ERBB) is a family of tyrosine proteins located on the cellular membrane and is composed of EGFR (Her1 or ERBB1) and its three analogs Her2, Her3, and Her4 (or ERBB2, ERBB3, and ERBB4, respectively). They belong to the receptor tyrosine kinases family and share some structural features with other RTKs. ERBB kinases play an important role in neuronal, epithelial, and other functions in human development and homeostasis. In cancer state, ERBB kinases dysregulation lead to cancer progression by various mechanisms caused by mutations such as amplification and overexpression which drive cells proliferation, migration, survival, and differentiation. Classical chemotherapy, hormonal therapy, and radiotherapy have been failed occasionally to treat EGFR-overexpressing tumours, and chemoresistance due to intrinsic or acquired mutations have been reported extensively (84-86). Thus, EGFR proteins have been extensively studied and targeted with small molecules inhibitors

in recent decades (87). Since EGFR (ERBB1) has a major role in the context of this thesis, we will be elaborating on this target in the next section.

1.2.5.1 Structure and function of EGFR

EGFR protein kinase is transmembrane glycoproteins consist of three domains: extracellular domain that is leucin- and cysteine-rich, a hydrophobic transmembrane domain, and intracellular kinase domain with a cytoplasmic tail (C-terminal), which contains specific tyrosine sequence (Figure 1.8). The latter tail is linking the receptor with downstream signaling. The kinase domain consist of two lobes, the N-terminal lobe which consists of five β-sheets and one α-helix, and C-terminal lobe consists mostly of α-helices. The cleft between the two lobes consists of a hinge, a catalytic site, an activation lobe, and the kinase binding pocket for ATP binding. The interaction between the ATP molecule (or EGFR inhibitor) and the methionine backbone (NH) in the hinge is critical for binding to the ATP binding site. This general structural features are also shared with all ERBB analogs Her1, Her2, Her3, and Her4 while encoding genes are located at different chromosomes. As illustrated in Figure 1.8, the extracellular domain of EGFR could adopt open or closed conformation depending on the activation state. Binding of the ligand triggers the dimerization of two homodimers that could be in a form of homo- or hetero-dimerization. enabling the tyrosine phosphorylation to occur at the carboxy terminal region. The latter dimerization is responsible for the various signaling or amplification. Activation of EGFR receptor occurs by >10 growth factor ligands that bind to the receptor in various specificity, each ligand is composed of a small domain containing three disulfide bonds (42). Resultant activation forms a homo- or hetero-dimer complex capable to phosphorylating downstream cytoplasmic signaling pathways such as PI3K, mTOR, and Ras pathways. EGFR ligands are classified into three groups based on their

function: EGF which transform the growth factor α (TGFα), Amphiregulin (AR), and epidermal growth factor (39) bind specifically to EGFR, while betacellulin (BTC), epiregulin (EPR), and heparin-binding EGF (HB-EGF) bind to EGFR and ERBB4. Neurogulin-1 and -2 ligands (NRG-1 and NRG-2) recognize both ERBB3 and ERBB4 receptors, but NRG-3 and NRG-4 are special ligands to ERBB4. There is no identified receptor of ERBB2 and this is attributed to the incompatible structure of the extracellular domain.

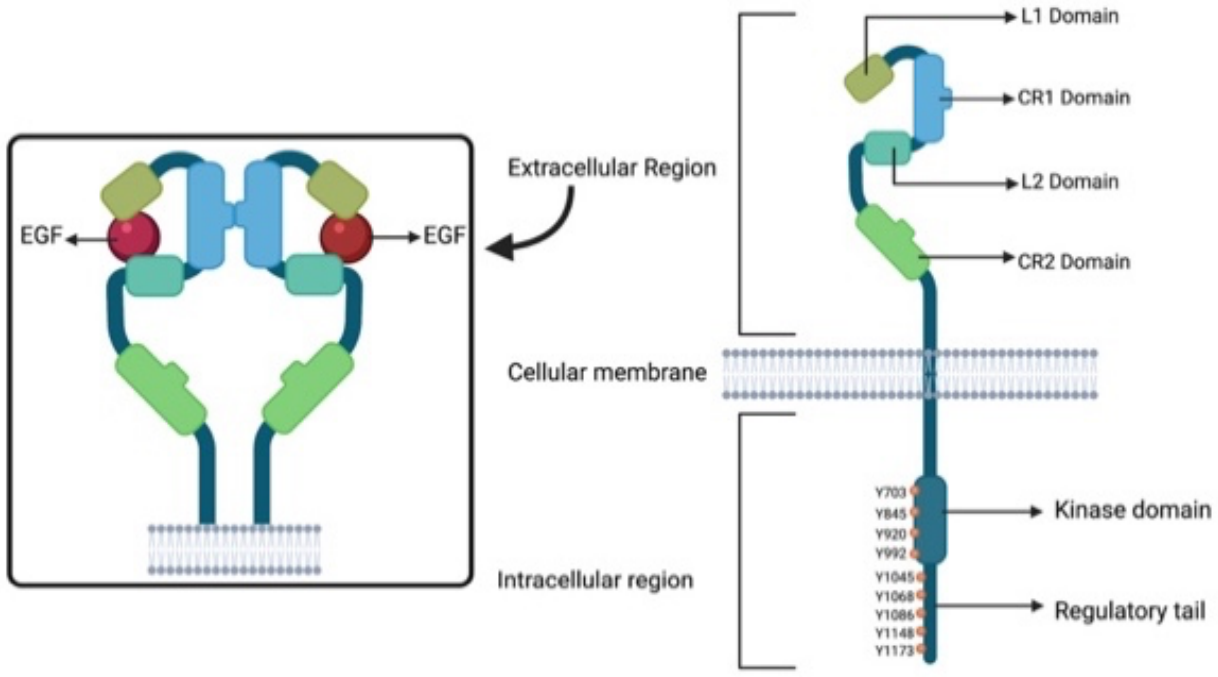

Figure 1.8 The structure of EGFR Receptor (right) and ligand-receptor complex (left).

EGFR dimerization and ligand binding induce the autophosphorylation of tyrosine resides, which serves as a binding site for kinases with SH2 domain in different downstream proteins. Phosphorylated EGFR transduce the signal to other kinases such as PI3K and Src, which ultimately lead to direct translocation of the activated proteins to the nucleus where gene transcription occurs. Overexpression of EGFR in some tumours is attributed to the gene amplification and transcription

activation (88, 89). These mutations are the primary cause of elevate EGFR levels in many cancers (90, 91). Another phenomenon of EGFR abnormal activity is the overproduction of EGFR ligands which consequently increase the expression of EGFR in cancer cells leading to autocrine or paracrine activation.

1.2.5.2 Targeted inhibition of EGFR tyrosine kinases activity

More than a hundred of EGFR-targeting small molecules have been developed and evaluated to treat tumours with irregular EGFR activity. EGFR is overexpressed in a various human tumours such as colorectal, kidney, breast, neck and head (92). Small molecules EGFR TKIs compete reversibly with adenosine of ATP to EGFR kinase domain and inhibit its phosphorylation (93). Gefitinib which was the first EGFR TKI developed in 2002 (Figure 1.9) to overcome resistance to traditional chemotherapies, and has showed an encouraging results in patients with non-small cell lung cancer (NSCLC) (94). It was reported that NSCLC patients who remarkably responded to gefitinib carried mutations in the EGFR kinase domain: delE746-A750 and L858R (95). Similarly, Erlotinib TKI used in the clinic for NSCLC carrying the same mutations. Although gefitinib and erlotinib have same effect, however, erlotinib have shown better safety profile, thus, it has been combined with gemcitabine as a first line treatment for metastatic pancreatic cancer (96). The discovery of T790 mutation, which is common among NSCLC patients (50–60% of patients) (97, 98), led to the development of second and third generations of EGFR inhibitors, which were rationally designed to target such mutation. Afatinib and dacomitinib inhibitors are second generation TKIs which were developed to further increase the inhibition potency. Both TKIs bind irreversibly to the ATP pocket of EGFR. Despite being designed to overcome T790 acquired resistance, preclinical studies showed limited efficacy in NSCLC patients (99-101). Hence, the

emergence of EGFR T790M resistance mutation led to further drug development to overcome this mutation. The third generation EGFR TKIs such as AZD9291 (osimertinib) (Figure 1.9) and HM61713 (olmutinib) both overcome activation and resistance mutations, and have exhibited a less adverse effects than early EGFR TKIs (102). Although the first and second generation TKIs are still the standard front-line treatment for advanced EGFR-mutant NSCLC, recent findings demonstrated that osimertinib has improved the overall survival in metastatic NSCLC in comparison with gefitinib or erlotinib (103). A recent clinical trial (n=556) demonstrated that overall survival with osimertinib in patients with EGFR-mutated advanced NSCLC was three years and two and a half years in the group who received gefitinib or erlotinib (103).

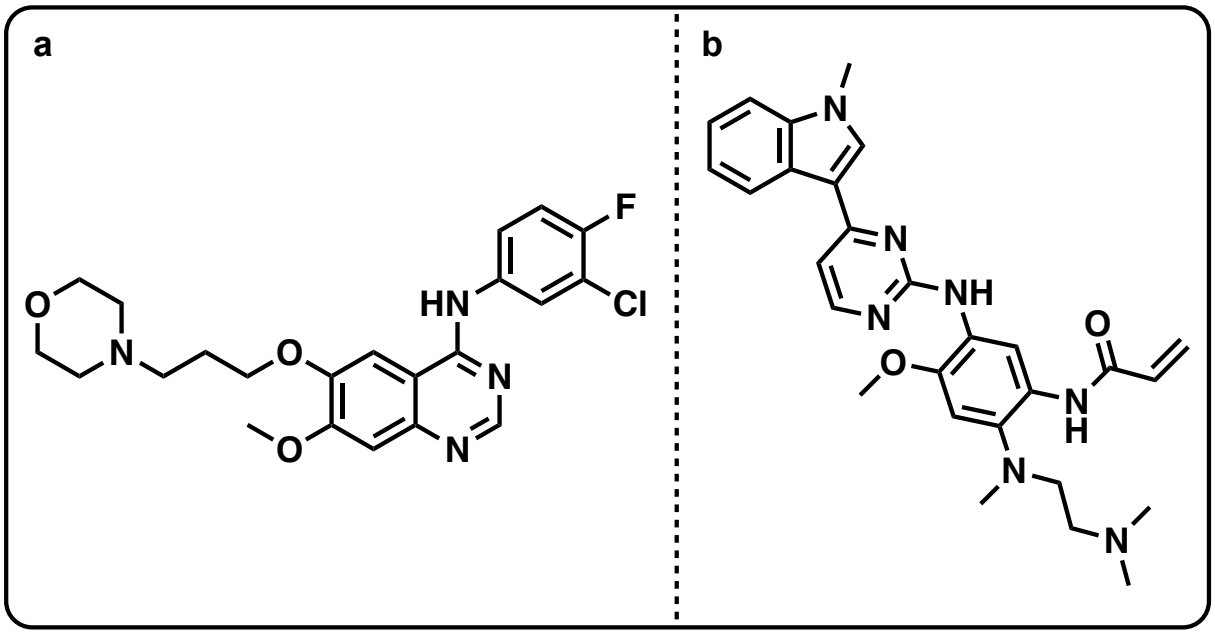

Figure 1.9 Chemical structure of EGFR-targeting tyrosine kinase inhibitors a) gefitinib and b) osimertinib.

1.2.6 Hepatocyte growth factor receptor

The mesenchymal-epithelial transition factor (MET) is a receptor tyrosine kinase that belongs to the MET family, along with Ron, and is expressed in different epithelial cells. MET has one known ligand hepatocyte growth factor (HGF) (104, 105). MET play a key role in mediating embryogenesis, wound healing, tissue regeneration, and nerve and muscle formation (106-108). However, under disease conditions, MET abnormal activation promote tumour progression in various cancer such liver, breast, prostate, and ovarian (109-112). The next two sections will discuss the structure of MET kinase and Met-targeted inhibitors.

1.2.6.1 MET structure and function

The mesenchymal-epithelial transition factor (c-MET) is a protein tyrosine kinase that belongs to MET family, beside Ron, and is located on the cellular membrane of different epithelial cells (Figure 1.10). It has one known ligand, the hepatocyte growth factor (HGF, also known as HGF/SF) (104, 105), a soluble cytokine secreted by mesenchymal, fibroblasts, and smooth muscle cells, and activates c-MET signaling through a paracrine mechanism as response to a biological demand (113). Under normal physiological state, MET kinase play a critical role in normal biological functions in human such as embryogenesis, wound healing, organ regeneration, tissue remodeling, and muscle formation (106-108). However, under disease state, MET activation promote cancer progression and development, such as in lung, gastric, prostate, breast, and liver cancers.

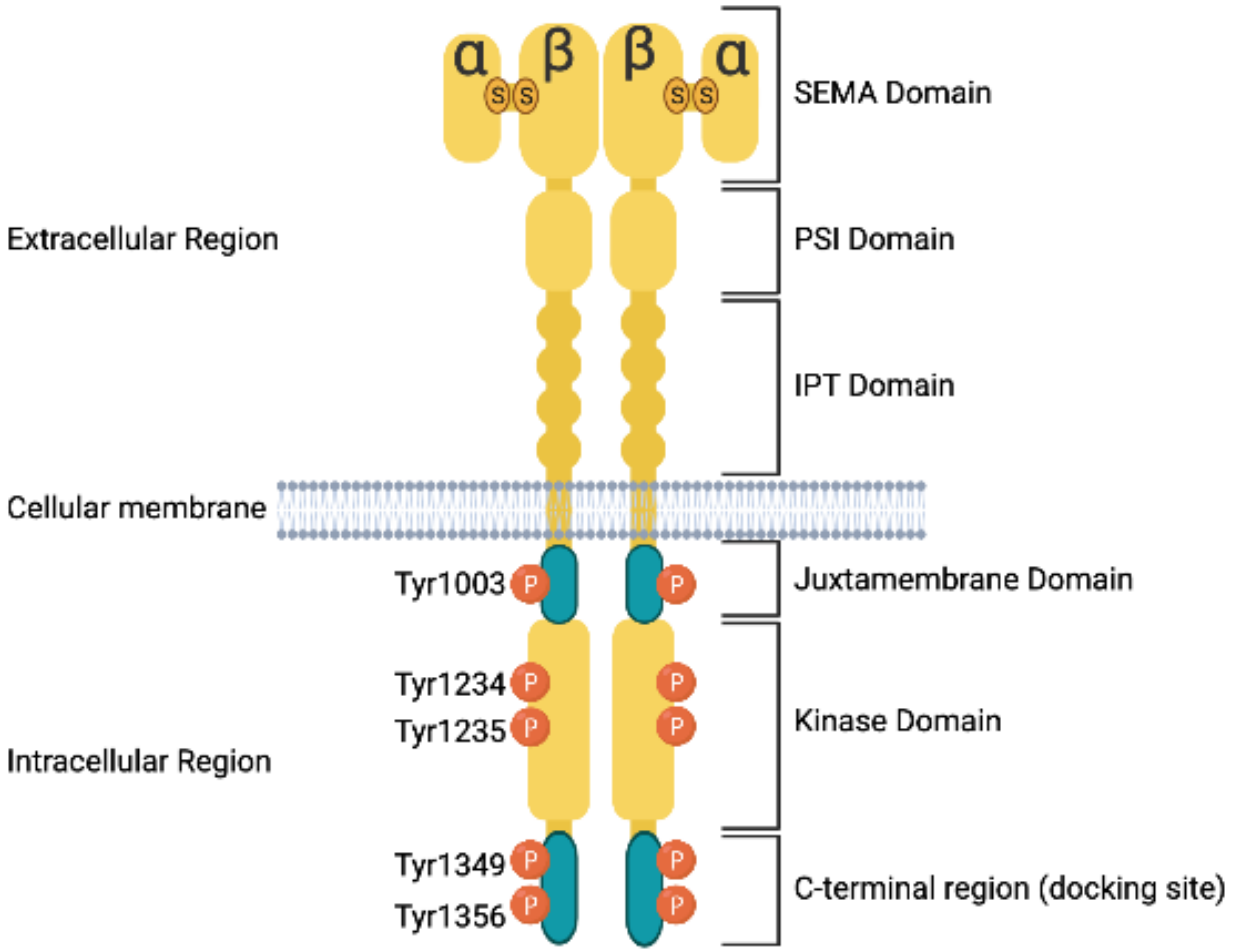

Figure 1.10 The structure of MET receptor

The signaling pathway of HGF/MET can crosstalk with other tyrosine kinases and activate different signaling pathways in tumours (Figure 1.11), which in turn lead to tumour proliferation, invasion, metastasis, and angiogenesis (114-116). For example , HGF/MET activation of SRC, JAK/STAT, Ras/MAPK, PI3K/AKT, and Wnt/β-catenin signaling pathways (109, 117-119). Activated HGF/MET pathway in many tumours is attributed to MET abnormalities such as gene mutation, amplification or overexpression (120, 121). The detection of high levels of MET in cancer patients is strong indication of poor prognosis. Indeed, numerous studies have revealed that abnormal activation of MET is involved in developing resistance to targeted therapies such as

tyrosine kinase inhibitors. Hence, dysregulated MET activity is highly associated with treatment failure in cancer therapy, and thus it became an attractive target for researchers.

Figure 1.11 c-MET receptor tyrosine kinase and its interacting downstream signaling pathways . Reprinted from "Role of the HGF/c-MET tyrosine kinase inhibitors in metastasic melanoma".

MET protein is encoded by its gene MET located on human chromosome 7 to yield a protein with a molecular weight of 120 KDa (122). MET protein is a heterodimer linked by α chain (extracellular) and β chain (transmembrane), in which β chain and is composed of six domains and a tail: SEMA domain, PSI domain, four IPT domains, transmembrane domain, juxtamembrane domain, tyrosine kinase domain, and c-termina tail that serves as a docking site. SEMA domain serves as a binding site for HGF ligand, whereas PSI domain sustain the latter binding in place. The juxtamembrane domain contains two critical residues for the negative regulation of the kinase (Serine976 and Tyrosine1003) (114, 120, 123). Upon HGF ligand binding to MET, Tyr1234 and Tyr1235 residues in the kinase domain undergo autophosphorylation, which in turn phosphorylate Tyr1349 and Tyr1356 residues in the C-terminal tail. A series of downstream signaling pathways activation occur upon the activation of MET. Such as PI3K and SRC pathways (124, 125). Dysregulation of MET in cancer occurs by different mechanisms such as gene amplification overexpression, and mutation. MET overexpression in tumours is controlled by a number of epigenic mechanisms including tumour hypoxia, growth factor secretion in tumours, and other oncogenic activation (126-128). Gene amplification of MET and the resulting overexpression is largely observed in many tumours, particularly, in colorectal and gastric cancers (129, 130).

1.2.6.2 Targeted inhibition of MET tyrosine kinases activity

Crizotinib and cabozantinib are among the early MET-targeting small molecules inhibitors developed to treat NSCLC (EML4-ALK fusion) and thyroid cancer, respectively. Crizotinib is an

ATP competitive TKI by which it targets the TK domain of the kinase and force the kinase to adopt conformational changes interfering with the ATP binding site (Figure 1.12) (131). Another TKI, cabozantinib that inhibits MET as well as other kinases (such as KIT and VEGFR) (132). Other MET TKIs are being developed such as Tivantinib, a non-ATP competitive inhibitor being evaluated in clinical trials alone or in combination with other chemotherapeutic agents for the treatment of hepatocellular carcinoma, NSCLC, and esophageal cancers (133-135).

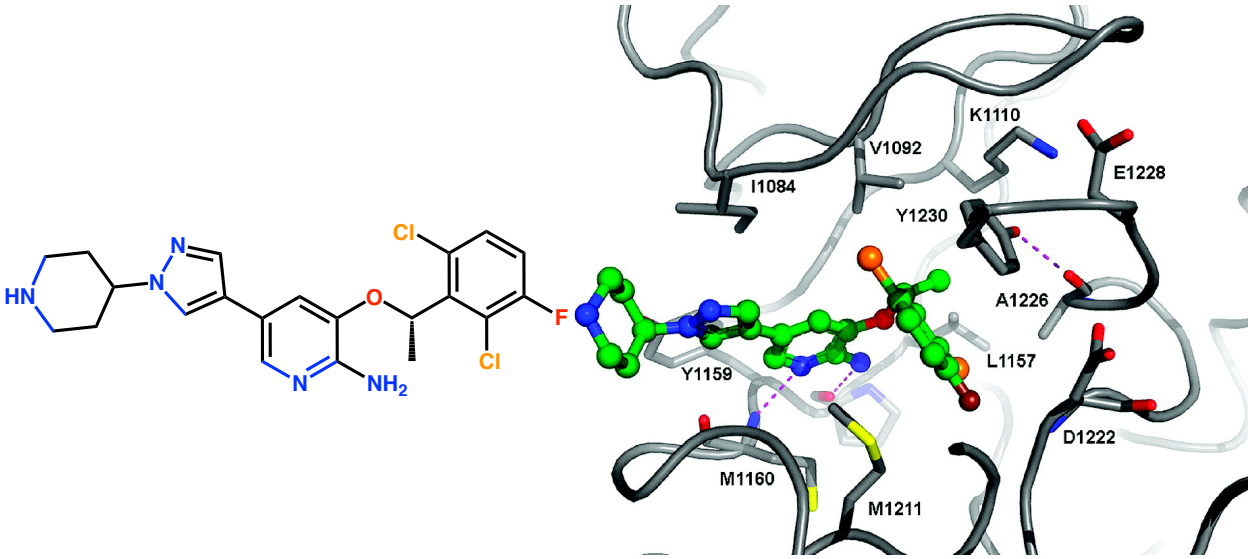

Figure 1.12 Chemical structure of crizotinib (left) and the cocrystal structure of crizotinib bound to c-MET kinase domain (right). Reprinted from "Structure based drug design of crizotinib (PF-02341066), a potent and selective dual inhibitor of mesenchymal–epithelial transition factor (c-MET) kinase and anaplastic lymphoma kinase (ALK)". copyright © 2011 *American chemical society*. No special permission is required to reuse all or part of article published by ACS.

1.3 CROSSTALK BETWEEN MET AND EGFR TYROSINE KINASE

In many cases, cancer cells use alternative receptors to transduce growth signaling when one receptor is inhibited. A typical example is that of the receptors insulin-like growth factor receptor 1 (IGF1R), MET and EGFR. The literature is replete with examples of resistance mediated through alternative receptors (9, 10). Ueda *et al.* (136), investigated the correlation between EGFR and IGF1R using immunohistochemistry in pancreatic carcinoma tissues. They found that both of EGFR and IGF1R are frequently overexpressed in both the primary and metastatic sites in the tissues being studied, which conclude that the crosstalk between differentially localized targets is determinant of aggressiveness of pancreatic cancer (136). Another example, in some cases despite the presence of PTEN do not downregulate MAPK pathway due to the activation of the latter receptor tyrosine kinase by IGF-1R (a receptor activated by HGF). Wang *et al.* (137), have reported that the resistance to vemurafenib treatment in metastatic melanoma is attributed to the hyperactivation of BRAF which induces IGF1R expression, as well as to the PTEN crosstalk and IGF1R in the same cancer type. Most importantly within the contest of this thesis is the crosstalk between MET and EGFR has been found to be vitally involved in therapeutic resistance in triple negative breast cancer (TNBC) as well as other cancers when used as single agents, which justify the need for dual inhibition of MET and EGFR in order to block the crosstalk signaling (Figure 1.13). Linklater and co-workers have proven the efficacy of using glesatinib and/or crizotinib (MET-TKIs) in combination with erlotinib (EGFR-TKI) against TNBC progression in metastatic tumourgraft (138).

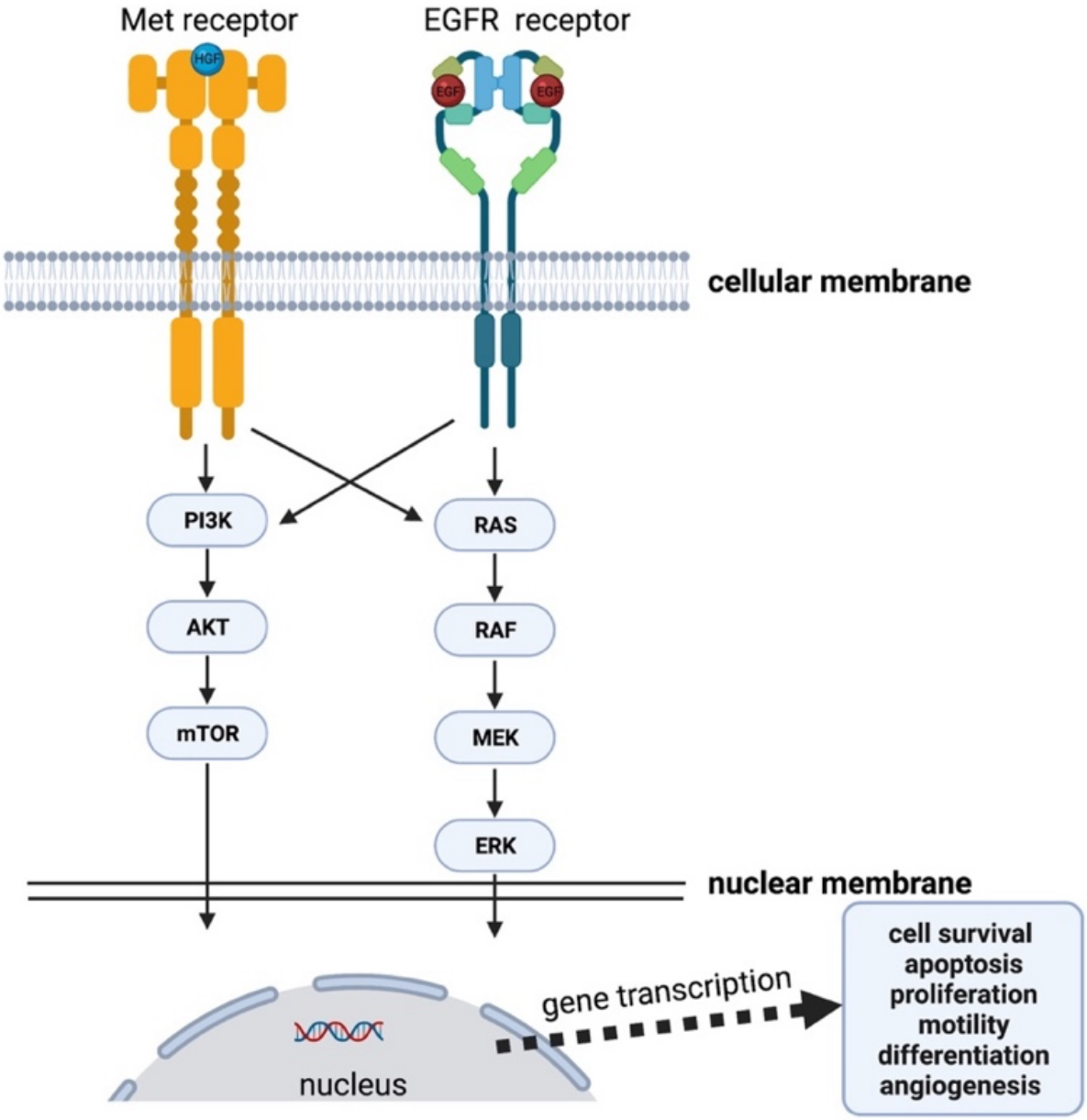

Figure 1.13 Schematic representation of the crosstalk between MET and EGFR receptor tyrosine kinases and downstream pathways.

1.4 Receptor tyrosine kinases trafficking (EGFR and MET)

Overexpression of receptors is one of the most common disorders targeted by modern cancer therapeutics. However, the process by which these receptors populated in the membrane is a

controlled process that is still under investigation. It is only very recently, around a decade ago, the debate about the transport and presence of receptor EGFR to the nucleus has been initiated (139-141). Protein synthesis occurs in the rough endoplasmic reticulum (ER) where ribosomes are anchored to carry the process of synthesis using free amino acids. These proteins are transferred to Golgi apparatus through the formation of vesicles that fuse with the cisternae of the Golgi and subsequently with corresponding enzymes are modified to contain signal sequence that tagged them for delivery to their specific destination. In case of receptor synthesis, they are destined to be localized in the membrane. Interestingly, following activation and signal transduction, these receptors take the return road where they can be either engulfed by lysosomes or recycled to the membrane. Although this process appeared to be simple, it is involved in complex number of specific enzymes acting on a wide variety of different proteins and that must be tagged for specific delivery and should their function be compromised, they will eliminated through lysosomes (142, 143).

In cancer, some unusual protein localization as a response to stress have been reported. The trafficking of EGFR which is well-known to proceed through endocytosis lysosome degradation or plasma membrane recycling has been recently reported to include mitochondrial transport as well as nuclear transport. In hepatocytes full length form of cell surface EGFR has been show to translocate to the nucleus where it has been shown to involve in transcription regulation and DNA repair. Interestingly, even ligands to EGFR such as EGF pro-transforming growth factor alpha (TGF-α) and pro-heparin like binding growth factor (HB-EGF) have been reported to be localized in the nucleus. More interestingly, recent evidence suggests that EGFR can undergo retrograde trafficking processed by which it can transported from Golgi to ER in the context of regulating the

nuclear transport of cell surface EGFR. It has been shown that upon treatment with EGF, full length EGFR can anchor to the membrane of the Golgi and ER in a configuration where c-terminus is exposed to the cytoplasm, and the N-terminus pointed toward the interior of Golgi and ER lumen. Coat proteins such as coat protein complex protein I (COPI) that mediate the Golgi-to-ER and COPII that is known to act on ER-to-Golgi (anterograde transport) are believed to be key players in this process.

Mechanisms involved in EGFR trafficking to the mitochondria have been under investigation for the past decade. Full length EGFR associates with cytochrome c oxidase subunit II, which is a key component of the oxidative phosphorylation cascade of the mitochondria. It is suggested that clathrin-mediate endocytosis and Src-signaling are believed to be involved in EGFR translocation to the mitochondria. Such translocation is also associated with the modulation of cytochrome c oxidase subunit II function and to cell survival. Importantly in the context of diseases such as glioblastoma it has been also reported the EGFRvIII variant can also located to the mitochondria and is associated to drug resistance.

EGFR trafficking to the nucleus is mediated by a nuclear localization signals (NLS) that is found in all EGFR family members. The presence of the NLS and that of importin β have been associated with EGFR translocation to the nucleus. EGFR and importin beta form a complex that is believed to be critical to the translocation to the nucleus. For exiting the nucleus, the nuclear protein termed exportin (CRM1) is believed to be involved in the nuclear export of EGFR, ERBB2, and ERBB3.

1.4.1 EGFR trafficking

Over the past decade, an emerging trend that received significant attention is the mitochondrial translocation of EGFR. The biology of EGFR in cancer cells is marked by its ability to escape lysosome-mediated degradation and to recycle to the plasma membrane. It has been shown that EGFR could translocated into cellular organelles such as ER, nuclei, and mitochondria.. Mitochondrial and nuclear EGFR appeared as full length when translocated in the organelles (E.g. mitochondria and nucleus) protein in the mitochondria and the nuclear. Despite significant advances over the past decade, the true function and role of nuclear and mitochondrial localization of EGFR remain unknow. However, it is important to mention that nuclear EGFR has been shown to be involved in DNA repair (144). Recent attempt to elucidate the function of mitochondrial re-localization showed that EGF induced translocation is associated with upregulation of ATP production. Interestingly, Che and co-workers suggested that these process enhanced motility *in vivo* and *in vitro* regulate mitochondria dynamics by interacting with MFN1 and disturbing MFN1 polymerization. To challenge this mechanism, they overexpressed MFN1 and this reversed the EGFR mitochondria translocation activity. Chen *et al.* (145). concluded that in addition to known role of EGFR as a receptor TK, the mitochondrial trafficking of EGFR may augment cancer progression by promoting invasion and metastasis.

1.4.2 MET trafficking

The MET protein is initially synthesized as 170 KDa single chain precursor that is glycosylated and cleaved in the Golgi apparatus into a disulfide linked alpha chain (50 KDa) and beta chain (140 KDa) (146). Trafficking of MET starts trough the Golgi apparatus to the plasma membrane where its level remain constant. Upon ligand binding MET can be internalized like other tyrosine

kinase receptors EGFR and VEGFR, however, its extracellular domain can be cleaved by a disintegrins and metalloprotease (ADAM) family of proteases and shed in the plasma (147). Recent study suggest that palmitoylation facilitate its trafficking and stability. Inhibition in palmitoylation decreases the stability of MET induced its accumulation in the Golgi apparatus (148). Overall, HGF binding triggers MET dimerization and phosphorylation, as well as recruitment into clathrin-coated pits leading to binding of ubiquitin ligase c to MET via Grb2 to ubiquitination of MET. Ultimately, MET is localized in the peripheral endosome and the perinuclear endosome from where it can be degraded. A proportion of MET may recycle to the plasma membrane through interaction with the Golgi apparatus (149).

1.5 FLUORESCENT MICROSCOPIC PROBING OF EGFR AND MET LOCALIZATION WITH THEIR FLUORESCENCE-LABELED INHIBITORS

Over the past decade, fluorescence imaging has been developed for visualizing specific proteins in the cell. The technology largely relies on the availability of specific antibodies that can be used to stain the protein of interest. Specific proteins can be visualized as fusion with green fluorescent protein (GFP) to avoid the need for fixation. However, this requires complex genetic manipulation that make them incompatible with the clinical samples. While for cell biological studies staining agents require high specificity, the need for pharmacological imaging is often directed at visualizing the distribution of small molecules with a strong therapeutic effect but often presenting multiple intracellular targets. In the past, radiolabeling of small molecules was used to localize their distribution in the cell, however, with the advance of fluorescent dyes, the past decade has seen a significant increase in the use of the approach to visualize small molecules. The most important class of molecules known for the target multiplicity are kinase inhibitors. They have a

canonical target that is believed to be the primary binding site, however, their off target effect is now well documented (150-152).

1.5.1 Fluorescence imaging and target multiplicity of EGFR inhibitors

EGFR tyrosine kinase inhibitors are commonly used in the clinical management of lung, breast, brain, and other cancers. However, while they are significantly block EGFR as the primary target, it has been demonstrated through various approaches, including kinases assays and chemical proteomics, that EGFR inhibitors bind to many targets including AXL, CDK1, and EPHA3. This indicates that fluorescent labeled small molecules can produce images that resulted from their target binding profile inside the cells. The first fluoresce microscopic study of the subcellular distribution of an EGFR inhibitor was reported by Jean-Claude's group (153). They demonstrated that a fluorescent labeled quinazoline inhibitor of EGFR was primarily distributed in the perinuclear region. This was believed to be due to the localization of nascent EGFR in the perinuclear region. Following Jean-Claude's publication there have been a few reports discussing the distribution by imaging of the EGFR in the perinuclear region. The debate around the perinuclear distribution of EGFR started as early as 1997 by Wikstrand and his team (154) who showed that the subcellular localization of EGFR and its corresponding EGFRvIII were membranal and perinuclear. The Golgi region was considered the preferred locus of distribution. Interestingly, twenty years later Boncompain *et al.* (155) identified two potent EGFR inhibitors as agents that can disrupt Golgi apparatus. They believed that EGFR inhibitors exert anti-Golgi function by binding to the *cis*-Golgi ARF GEF GBF1. However, the effect of these inhibitors was reversible, disappearing following washout of the compounds.

Lapatinib is a dual inhibitor of EGFR and Her2 used in the treatment of breast cancer, it belongs to quinazoline of ERBB inhibitors, with the exception that it fluoresces in the green due to its furane ring. Wilson *et al.* (156) showed using confocal microscopy that the green fluorescence associated with lapatinib was primarily localized intracellularly, with no detectable levels of distribution in the membrane. This distribution of lapatinib appeared perinuclear.

Zhang *et al.* (157) recently showed that quinazoline-based EGFR inhibitors with the IC_{50} of the range 0.71-2.30 μM accumulated in the mitochondria of A549 cells. Their proposed mechanism is that this may trigger apoptosis in these cells via mitochondrial pathway. A few months after Zhang *et al.* (157), Ilmi *et al.* (158), specifically designed mitochondrial targeting conjugate that carries two quinazoline-like moieties targeting EGFR. This conjugate carried a ruthenium complex acting as a fluorophore through a TEG derived linker. The conjugate retain significant EGFR binding property and was used for live imaging of AU87 malignant glioma cells. The result showed that the fluorescent was co-localized with that of mitochondrial agent indicating that it could capture the presence of EGFR in the mitochondria in these cells. Given the potential of target of quinazoline, the color may be also associated with other targets in the mitochondria such as ATP transporters and other. While this representing a theranostic approach, the size of these molecules may conclude their use as a therapeutic agents (158). Significant attention has been given to EGFR inhibitors for live imaging due to the significant of EGFR as a target for therapeutic intervention in many cancers including lung, brain, breast, and many others, However, a few small molecules-based imaging studies have been reported, such as SRC and PI3K (159). Vetter *et al.* (160) demonstrated using a potent inhibitor of SRC (dasatinib and saracatinib) that the localization of c-SRC and corresponding target could be visualized using a BODIPY as a fluorophore. While the

conjugation with saracatinib was not successful, the dasatinib BODIPY showed biological activity and could be used to track the localization of SRC withing fixed and live cells fluoresce microscopy.

In the context of developing small molecules for live imaging of EGFR, Golabi and Larroque developed a new quinazoline-based probe that contained an EGFR targeting scaffold optimized in house, and linked to a p-nitrobenzoxadiazole (NBD), and the resulting probe retained significant affinity for EGFR and was used to visualize EGFR in an isogenic panel of NIH3T3 cells transfected with EGFR and HER2. Imaging with the confocal microscopy showed that the probe was able to penetrating multilayer aggregates and inhibit EGFR auto-phosphorylation (161).

Small molecule imaging of EGFR was also demonstrated in the context of the combination targeting principle developed in our laboratory that seeks to design molecules capable of targeting EGFR while being programmed to be hydrolyze and generate a DNA damaging agent in order to accelerate apoptosis in the cells. Investigation into the mechanism of action of type of these molecules led to the design of AL236 molecule containing quinazoline moiety, a triazene chain designed to be hydrolyzed into alkyl diazoumin labeled moiety with a green fluoresce dansyl moiety designed to alkylate DNA. Hydrolysis of the chain was also generate a blue fluorescent called FD105. The question asked whether the entire combimolecule was primarily localized in the cell prior to generate the FD105 and dansyl diazonium alkylating moiety. Fluorescence microscopic studied showed that both the green color associated with DNA alkylating moiety and the blue color associated with the free quinazoline FD105 were co-localized in the perinuclear region of the cell. Importantly, the subcellular distribution of the fluorescent was diffused in

cytoplasmic NIH3T3-wt cells but discreetly distributed in the perinuclear region of NIH-3T3-EGFR transfected cells. The results suggested that the intact combimolecule primarily localized in the perinuclear region where it is subsequently hydrolyzed into its two moieties. Importantly, it was shown that DNA damage was selectively stronger in the cells that overexpress EGFR than in wild type counterpart, which suggest that the discrete subcellular distribution played a role in the intensity of the damage. It was proposed in the paper that the perinuclear distribution of the intact molecule placed in the closed vicinity of the nucleus and this accelerate the delivery of DNA species to the nucleus (162).

1.5.2 Fluorescence imaging and target multiplicity of MET inhibitors

The sequence homology of the hinge region in the ATP pocket of many kinases make it difficult to design highly specific kinase inhibitor. Therefore, most kinase inhibitors can bind to multiple kinases. If a kinase inhibitor is fluorescent labeled, one should expect that live imaging will reflect not a single but multiple binding to multiple macromolecules. This issue has been recently addressed by Kim *et al.* (163) who had the opportunity to study a fluorescent labeled probe with a highly specific MET inhibitor PF-04217903, and one with multitargeted MET inhibitor (foretinib). PF-04217903 exhibited 1000 fold selectivity in kinase profiling assay with 150 kinases (164). By contrast foretinib has been found to bind to both RON, ROS, MET, VEGFR and etc. (164). Imaging study with these two inhibitors showed PF to be predominantly localized in the membrane, by contrast foretinib is was also found to be localized in the perinuclear region. Whether this intracellular localization was due its multikinase binding property was not explained by the authors. However, it does present a pattern wherein multiple kinase inhibitors can have

preferential localization in the perinuclear regions whereas the highly specific ones have preferential binding in the membrane (164).

1.7 PROTEOMICS MOLECULAR DIAGNOSTICS

1.7.1 Definition

Molecular diagnosis is a group of molecular biology techniques utilized to detect and study variants in the human genome or proteome in order to predict and improve disease response to therapy. This powerful tool provides researchers and clinicians with preliminary information about mechanisms of disease to assist towards precise and tailored therapeutic regimen, and consequently a proper disease management. Genomics technologies as well as molecular biology advances have promoted molecular diagnostics research revolution over recent decades. Molecular diagnostics has become clinically important in many biomedical fields including cancer, oncology, pharmacogenomics, and infectious diseases (165-168). Traditional high throughput methods, such as next generation sequencing, enabled scientists to understand the mechanisms of human disease and identify disease biomarkers using multiple-variant-detection platform.

1.7.2 Classical Molecular Diagnostics

The term “molecular disease” was first used by Pauling and his team (169) upon their discovery in 1949 of a single variant at β-globin chain of sickle cell anemia, a biomarker for blood vessel blockage. Biomarker is a medical term that refer to a broad spectrum of medical signs that can be detected and measured in patients and as used an indication of a medical state (170). Although the molecular diagnostics revolution was initiated years afterward the latter discovery, Pauling and his

coworkers (171) have established the basics of molecular diagnostics. A few years later, DNA cloning and sequencing were valuable technologies to obtain preliminary information about sequence of genes, however, these tools provided insufficient understanding on the primary sequence of a gene. Further technological advances led to the development of DNA probes: a tool that spots allele variations within genomic regions via southern blotting (165, 167, 168, 172). Thereafter, Kan and colleagues (169) carried out a parental testing for thalassemia, and reported for the first time the detection and analysis of a DNA polymorphism in the β-thalassemia gene using hybridization of isolated DNA from fetal fibroblast. They used a restricted enzyme endonuclease that cuts DNA at specific short sequences, unlike previous tests that rely on whole DNA sequencing. Kan and his team (173) suggested that this tool could be used as a diagnostic tool for parental diagnosis of β-thalassemia from fetus, and utilized the same tools to detect variable alleles in sickle cells (174). Other genetic diseases were characterized soon afterward using RFLP approach, such as polymorphisms detection in phenylketourea (175) and cystic fibrosis diseases (176). Furthermore, multiple hemoglobin subunit beta (HBB) sequence variations were detected by Orkin and his team (177), and it was attributed to the exon mutation. Thereafter, the term “molecular diagnostics” were used widely in research laboratories (178, 179), and more molecular diagnostic approaches have been developed thenforth (175, 176, 180, 181). Molecular diagnosis research was further pursued afterward and aided by molecular biology methods e.g. electrophoresis, western blot, and southern blot (182-184). Despite advances of previously mentioned methodologies, molecular diagnostic was still inadequate for robust detection of variations due to many factors including the cost and complexity of analysis, until upon the invention and optimization of polymerase chain reaction (PCR) by Mullis and Saiki in 1985 (171, 185). Multiple PCR-based genetic tests became available allowing for detection of a few genomic

variants, via two methods: genetic screening or genetic scanning for detecting particular genomic variant(s) or the whole genomic variant within the studied DNA fragment, respectively. Indeed, PCR facilitated the laboratory identification of known and unknown mutations for various genetic services such as parental diagnosis and genetic screening, and have been used thenceforth. Early DNA sequencing and variants detection approaches are indeed feasible and highly accurate for molecular diagnosis, however, these approaches are low-throughput, costly, in addition to other factors that limit their use in clinical laboratories.

1.7.3 Modern Molecular Diagnostics

The term "omics" refers to the study of various biological disciplines that ends with the suffix "omics" in order to identify, describe, and quantify biological molecules of interest. For example, genomics, transcriptomics, metabolomics, proteomics, genomics refer to the study of the genome: its structure, function, evolution, and interactions between genes and with the environment. Likewise, transcriptomics refers to the study of transcriptome (mRNA) produced by genome, while metabolomics refers to the study of metabolites and metabolic response of a living system to pathophysiological stimuli. Proteomics is the study of the proteome; its expression, structure, functions, post-translation modification, and interactions. It is usually used to refer to the large-scale study of proteins using technologies to identify and quantify proteins from cells, tissues, or organism. Proteomics have remarkably aided cancer research mainly in early cancer diagnosis as well as prognosis, that is detecting and identifying biomarkers and monitoring cancer progression (186). Mass spectrometry (LC-MS-MS) and MALDI are among technologies widely used nowadays to investigate proteins interactions and post-translation modifications. Despite the cost

and complexity of proteomics technologies compared to earlier existing technologies, its role and significance in various research disciplines is undoubtable.

There are two approaches in proteomics: the top-down and bottom-up proteomics. As depicted in Figure 1.14, top-bottom proteomics consist of preparation of cell lysate subjected to a gel separation followed by MS analysis of collected fractions, purified protein analysis can be enzymically digested for MS/MS analysis. Data generated from top-down method represents intact protein ions and is used to identify and study protein of interest. Bottom-up proteomics consist of isolating the lysis and subjected directly to digestion and subsequent MS/MS analysis.

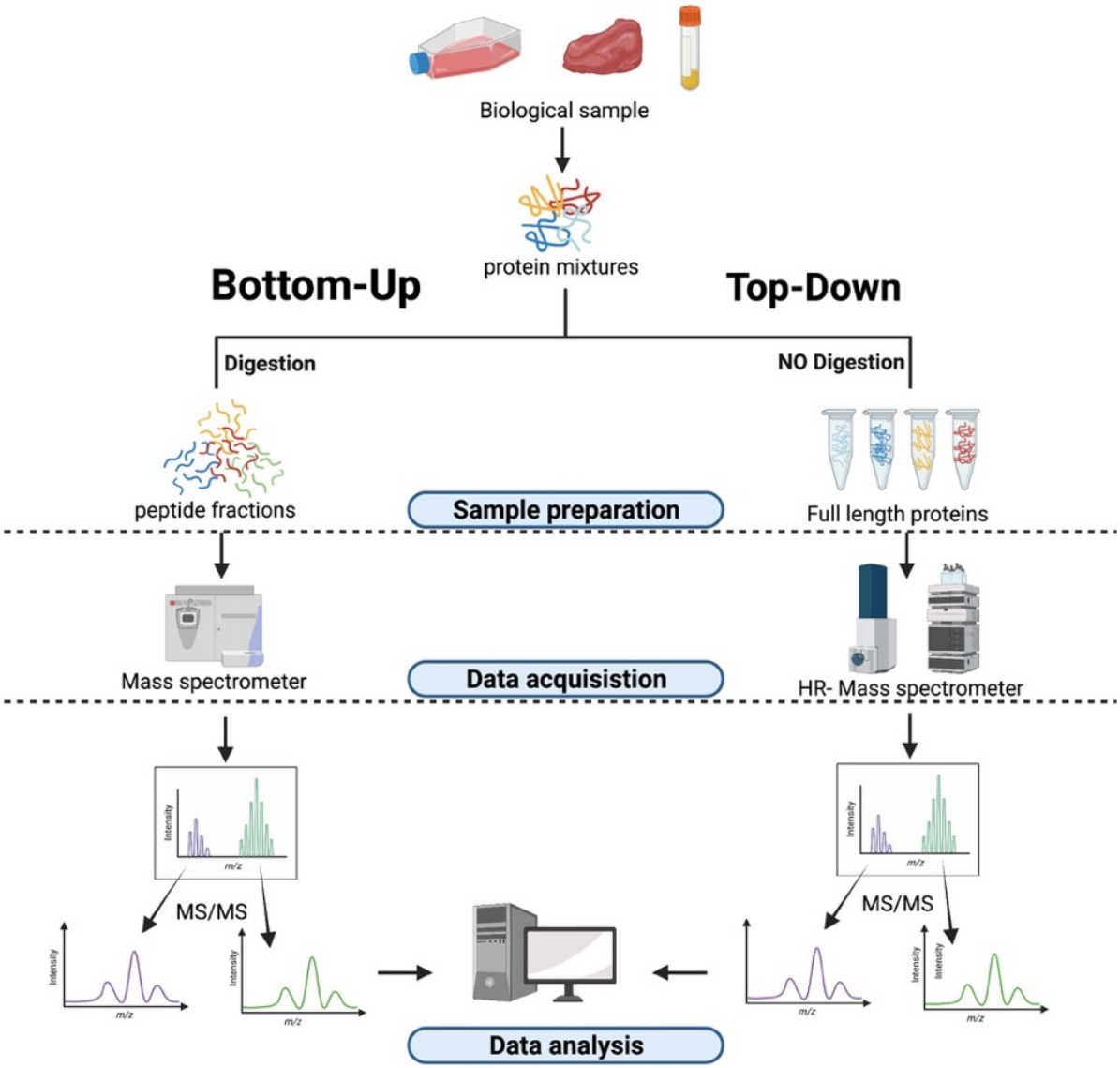

Figure 1.14 The typical workflow in bottom-up and top-down proteomic experiments.

1.7.3.1 Mass spectrometry: the instrument of proteomics

Mass spectrometry is one of the widely used tools to identify, characterize, and quantify proteins and their corresponding posttranslational modifications. Chromatography is a chemistry technique widely used to separate and purify substances, and it has been utilized to purify biological molecules such as proteins. For example, affinity, ion-exchange, and size exclusion

chromatography, which purify proteins based on the partition coefficient between mobile and stationary phases of the chromatography column (187-189). Classical techniques such as ELISA and western blot are still widely used and useful for selective protein analysis, however, they are unable to measure protein expression level (190, 191). More complex proteins are frequently separated with different techniques such SDS-PAGE, 2D electrophoresis, and 2D-DIG electrophoresis (192-194). Although protein microarrays have facilitated high throughput analysis, it is difficult to carry out the complete genome with the latter technology (195). On the other hand, mass-spectrometry-based proteomics is a powerful technique that has enabled a comprehensive and large-scale analysis of proteome with higher sensitivity. Proteomics offer a significant genomics and transcriptomics information for understanding the complexity of biochemical processes at molecular level. Protein abundance and function could be altered due to gene expression and posttranslational modifications (PTMs), which explains proteomics complexity over the corresponding genomics and transcriptomics. The latter complexity is usually simplified with the high throughput (HTP) strategies which ultimately increase the analyzed proteome coverage.

MS measures mass to charge ratio of ionized peptides and present them as a mass spectrum. Quantitative MS development was aided by the Edman degradation method, in which a particular amino acid residues are labeled and cleaved without disturbing the peptide bonds between other amino acid residues (196, 197). Currently, there are various proteomics quantitative methods depending on the research objective: labeled SILAC, ICAT, iTRAQ, MRM, and SWATH, in addition to the label-free methods (198-201). It became achievable nowadays to process a huge volume of proteomics data with high throughput techniques. Data generated from top-down

method represent intact protein ions and are used to identify and study protein of interest. Intact proteins are complex in terms of molecular structure, molecular weight, charge state. On the other hand, protein in bottom-up method is digested chemically (e.g. HCl) or enzymatically (e.g. trypsin) to peptides prior to LC separation (202). Eluted peptide fractions from the LC column are then subjected to an electrospray to ionize the fragments (203) that pass them to the mass analyzer which measures peptides mass in two steps using tandem mass spectrometer (202). The first step (MS1) is recording the number of molecular ions for different *m*/*z* (mass-to-charge ratio) values of the entire peptide, followed by measuring *m*/*z* of fragment ions detected from MS1 of the same peptide ions that is MS2. The two steps mass measuring (MS 1 and MS2) provide high confident of peptides presence in the sample. Each peptide sequence is further identified and matched to the original protein or protein mixture, while the intensity of peptides of fragment ions indicate the relative abundance among the original sample. Protein quantification usually performed in two mass-spectrometry-based approached: label-free and label-based approaches. Both approached will be discussed in detail hereinafter.

1.7.4.1 Quantitative proteomics: label-free proteomics

In principle, label-free approach relies on measuring relative amount of protein(s) in a biological sample based on the MS1 signal collected from tryptic digestion without a covalent peptide modification. The workflow includes running various digested samples continuously within the same experiment (204), which generate an elution profile of monoisotopic peptides. The MS1 signals of each peptide is uniquely combined over processing time and integrated. Since peptides are not labeled, they are distinguished from the chemical noise based on their isotopic pattern. The computer then calculates the area under the curve that represents the total number of ions of each

peptide individually. The MS1 signals are used as a quantitative reference of the main peptide concentration. Yet the area under the curve (peptide ratios) of each peptide does not read the relative amount of that peptide in the sample. Nevertheless, a peptide's amount can be relatively quantified within the same experiment from a another sample containing peptide of interest (205, 206). Combined areas under the curve (peptides ratios) gives a relative ratio of proteins, and it can be achieved by different algorithm-based means (207). For example, using signal intensity to calculate the average of peptides ratios, or using the median of peptide ratios (208). It is noteworthy that spectra generated from MS2 identify peptides in the protein sample but their signals are not used for protein quantification purpose. Label-free protein quantification approach has many advantages over the corresponding label-based approach. For example, label-free methodologies are generally simple, cost-effective, and requires less sample preparation. Contrarily, robust analysis of multiple samples is not achievable as instrument running time is long. Also, the median protein coefficients of variations between replicates is relatively high (20%), thus lower precision (206). Moreover, less abundant proteins reveal larger variability between replicates which lead to a poor reproducibility of the data. Another major drawback is the missing value problem whereas a significant fraction of a peptide in every sample will be missed during the MS detection (209) Various MS technologies and statistical methods are being developed to overcome these drawbacks (206, 208-213).

1.7.4.2 Quantitative proteomics: label-based proteomics

Label-based or so called stable isotope labelling with amino acid (SILAC) is unlike label-free proteomics, whereas heavy isotopes are used to chemically or metabolically label peptides of interest. In this approach, each sample is first processed separately in a label-free experiment to

profile peptide signals. Quantifying peptides of interest can be achieved *in vivo* (metabolic) or *in vitro* (chemically), in which a heavy amino acids is added to tissue culture medium (214) or to digested protein (215), respectively. Heavy and light isotopes have the exact chemistry (except for deuterium) and consequently they elute in a similar manner from LC column to the mass spectrometer where they are characterized based on their *m*/z ratios. It is achievable with this approach to label samples individually with different isotopes, then combining all samples for the same MS run. Thus, protein quantification is performed within the same experiment which allows for better reproducibility (216). The latter advantage leads to a higher precision as well as offers a high throughput analysis. However, there are various limitations of label-based approach, for example, the cost of the isotopic labeling materials are expensive. Moreover, complexity of MS1 spectrum increases as the number of samples increases. This it is recommended that the number of samples should not exceed the maximum number of labeling mixtures (216). A major limitation of SILAC is the modest ion statistics due to limited number of ion accumulated in most high-resolution analyzer used such as the Orbitrap. Thus, low abundant peptides ions will be insufficient to detect when eluted at the same time with another peptide with higher abundance. However, the latter drawback can be overcome with some analytical techniques such as ion-mobility spectrometry where ionized molecules or proteins are separated and identified based on their mobility in the carrier gas (217-219).

1.8 CHEMICAL PROTEOMICS

1.8.1 Definition

Chemical proteomics is a large-scale study of proteins interaction with small molecules in biological systems in order to identify targets and study a mechanism of action. It is a combination

of medicinal chemistry, cell biology, and biochemistry disciplines together. Development of quantitative proteomics methods and technologies in recent years have driven chemoproteomics research to grow rapidly towards drug discovery and development. Proteomics-based study of a drug interaction with biomolecules using classical methods is based on full-length or fragments of purified protein or enzyme of interest. This classical methods does not reflect accurately the activity of the target in its physiological context, consequently, generated data are not sufficient to study target-drug interaction in an *in vitro* or *in vivo* systems. On the other hand, chemoproteomics techniques allows to study an intact protein from cell extracts or fractions while maintaining its folding, integrity, and post-translation modifications and without disturbing the protein interaction with other proteins. Chemoproteomics approaches are classified into approaches, amongst them is the shotgun chemoproteomics by which the proteome is screened to evaluate a particular response to small molecules, and targeted chemoproteomics by which engineered chemoprobes are used to capture known or unknown potential targets from the proteome (220-224).

1.8.2 Shotgun approach - Chemical Proteomics

Shotgun proteomics is also known as global proteomics, and it involves exposing cells or animals to the treatment followed by cell- or organ-wide proteome analysis. This technique is widely used due to its simplicity and feasibility, and samples are typically analyzed with modern instruments which enable the identification of 1000-10000 proteins from a digested sample (225-232). Starting with peptides instead of intact protein in shotgun analysis is advantageous over starting with an intact protein. This is attributed to the unicity and less complexity of peptides over intact protein, which translates into a rapid LC separation, homogenous ionization, complete fragmentation, and easier data interpretation (233). With shotgun proteomics, proteins are identified and quantified

based on their abundance in a given sample, which could be proteins unrelated to the signaling pathways studied.

1.8.3 Experimental Workflow for Chemical Proteomics

Sample from serum or lysate are typically processed to separate protein from the whole sample, followed by a chemical modification (reduction and alkylation) that breaks sulfide bonds between cystein, and finally the linearize protein is digested into smaller peptides. Peptides are subsequently loaded onto a C18 column and washed to remove salts and buffers used for sample preparation. Eluted peptide fractions pass through LC-MS system which fractionate peptides for enhanced MS/MS detection. There are various types of chromatography columns that can separate complex peptide mixtures and can be used separately or in combination with other columns. For example, reversed phase, ion-exchange, size exclusion, and affinity columns. Upon de-complexing peptide mixtures, fractions are sprayed into the electrospray ionizer that further polish peptide fractions by eliminating chemicals such (e.g. salts) that may supress adducts formation. The ionized fractions then travel into the mass spectrometer with enough resolution and the *m/z* are detected accordingly. The final step is data processing, where data of *m/z* obtained from whole peptide mass (MS1) and peptides fragmentations masses (MS2) are screened with a sequence database to find peptide matching sequence to its corresponding protein. The data including MS and MS/MS are analyzed algorithmically where the search for peptides sequences in undertaken through a rich database that matches each detected spectra to its corresponding protein.

1.8.4 Chemical proteomics approaches

Over the past decade proteomics data from chemical proteomics analysis were primarily lysate-based. The usual process us to analyze the target multiplicity of a given small molecules e.g. kinase by growing the target cells e.g. tumor cells, lysing them and capturing the targets on weather immobilized beads or using specific chemoprobes. Cell lysate offers a broad range of targets from the proteome and particularly in case of cancer allow to carputer proteins that maybe involved in cancer progression. Many approaches have been developed to immobilize drugs on beads that are exposed to the lysates and the resulting binding proteins are considered to be either its primary target or off-target effect. Following the immobilization the beads or probes are washed and digestion can be on beads or the protein competitively removed by exposure to large concentration of the primary target inhibitor. The digested proteins are further analyzed by MS usually using orbitrap technology. There are three major approaches that will be discussed in the context of this thesis: **A)** immobilization approach/kinobeads **B)** chemoprobe approach **C)** bioorthogonal approach.

1.8.4.1 Immobilization approach/kinobeads

The kinobeads approach utilizes sepharose beads which contain reactive functional group that can be used through chemical reactions primarily with an amino group from the corresponding inhibitor to be immobilized. The reaction with amino group side chain are performed on epoxy sepharose. As an example, compound such as BGT-226 is immobilized through a hydroxy succinimide (NHS-activate sepharose) through covalent linkage with the primary amine. Brhemer *et al.* (159) used epoxy sepharose to react with a quinazoline amine.

While many studies used the approach of this immobilization it was only in 2007 Bantscheff introduced the term kinobeads to describe the creation of beads to immobilize seven kinase inhibitors which together were capable of enriching over 269 human kinases through the immobilized from tissues and cell lysates (234). Typically the kinobeads workflow includes three major components for processing the cell lysate 1. The beads are exposed to a lysate which is called vehicle control 2. The beads are exposed to a solution of lysates pre-treated with an increased conc dose range of the inhibitors. The pull-down corresponding to step usually show the diversity of the targeted and off-target proteins. Enrichment of the off-target proteins can be performed by increasing the dose of free inhibitor. Like in an ELISA assay, the resulting curve can be used to calculate the IC_{50} and this can be converted into a dissociation constant by calculations as described by (234-236). It should be noted that in the case of TKIs the observed data related to ATP-competitive binding affinity therefore this is no appropriate for allosteric inhibitors. It is important to mention that binding data obtained from dose-response of the free-inhibitor are not sufficient to conclusively demonstrate the strength of binding in the cell. Therefore, the binding profile is usually hypothesis generator that has been verified by biological experiments. As an example, Brehmer *et al* (159) immobilized gefitinib-like inhibitor (Figure 1.15) and from the resulting pull-down they identified among many kinases RICK and GAK. However, to confirm that strength of binding with free gefitinib in an independent kinase assay had to be performed where they found that RICK, BRK and GAK for IC_{50} binding between 49-90 nM, which is considered extremely potent binding given that the IC_{50} for binding for the canonical target EGFR 14 nM in the assay.

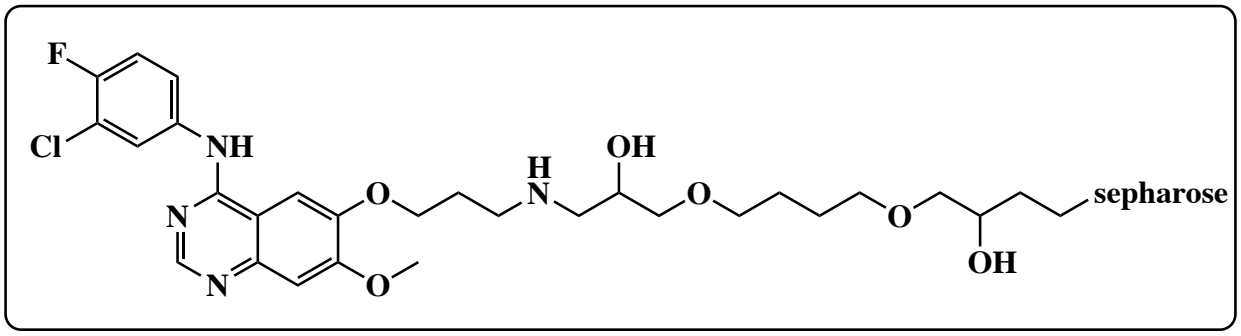

Figure 1.15 Immobilization of AX14596 on sepharose beads through a reaction with epoxy activated sepharose.

Furthermore, the RICK and GAK inhibitory potency was confirmed by western blotting. These data has given evidence that the approach cant only report on the diversity of targets binding profile of the inhibitor but also could lead to target of targets with strong affinity for the inhibitor in the study (159). Furthermore biochemical assays and growth inhibition assay with corresponding inhibitors may translate their potential impact as novel anticancer therapeutics. Following EGFR cellular targets study, an important broad spectrum study was performed using the kinobeads with imatinib as a kinase inhibitor, which was the first approved kinase inhibitor drug in the clinic following a 90% response against CML. The study utilized kinobeads that immobilized seven kinase inhibitors including three BCR-ABL TKI imatinib, bosutinib, and dasatinib. Proteins detached from the beads were analyzed by MS using iTRAQ for quantitation of the captured proteins. Using such approach that consist of competitivity challenge the binding with does-range of imatinib, they demonstrated that imatinib can bind to 192 number of tyrosine kinases, and more importantly, they identified an important kinase Discoidin Domain Receptor Tyrosine Kinase 1 (DDR1) and N-Ribosyldihydronicotinamide:quinone deductase 2 (NQO2) as novel targets of imatinib. This was validated by biochemical assays in cells exposed to imatinib. As an example,

western blot analysis showed a dose-dependent inhibition of DDR1 and complete inhibitor of the receptor was seen in the nano molar range. Further confirming the strong binding property of imatinib to DDR1 (234).

1.8.4.2 Activity-based probe approach

The term activity-based probe is derived from activity based proteomics which is a new subdivision of proteomics recently developed to analyze protein activity and monitor the regulation of enzymes in situation of complex proteomics. The probes designed for activity based purposes are generally divided into three compartments 1) the tag 2) linker and 3) the warhead. The warhead is the substrate of the enzyme while this model is refer to structure activity of the probe, many probes for proteomics contain warhead that is not designed for enzyme-active site covalent binding, e.g. kinase inhibitor, however, contain the same structure i.e. a tag, a linker, and a warhead. The warhead is deigned to specifically to bind to the active site of the enzyme. The function of the linker is to distance the functional group from the tag, which is designed to be captured by a labeled partner (e.g. streptavidin in case of biotin), or to be intrinsically fluorescent. The linker or spacer can be a chain of polyethylene glycol (237), or a peptide in cases where protein mimicry is needed. The linker can be designed to be cleavable which can be an advantage when pull-down of proteins involved in protein interaction, need to be captured intact. In this case mild reductive condition is required for cleavage of the linker, which are usually carry a diazo benzene moiety. As an example of a cleavable and non-cleavable probe, we will discuss DCG-04 an activity-based probe targeted to serine proteases and a cleavable specifically designed probe for non-denaturing chemical proteomics. DCG-04 was designed with a biotin tag, an alkyl linker, peptide-like linker, and an epoxy ester that mimic the structure of E-64 which is a substrate for

cathepsin, This probe has been used to profile enzyme in a complex cell lysate using the catalytic activity as a bait. DCG-04 was designed with a stable non hydrolyzable linker (238).

In situations where the pull-down d of the proteins require mild condition to avoid disruption of protein-protein interaction, chemical probing and proteomics are considered a tremendous challenge. Budin *et al.* (239) designed a specific probe to target DNA gyrase with its interactive protein undisrupted. They utilized a linker containing the 2-(4'-hydroxy-2'-alkoxy phenylazo)benzoic acid (120) moiety designed to be cleaved under mild condition with sodium dithionite. This spacer was placed between a aminocoumarin novobiocin as the warhead and biotin as a tag, which was used to capture the bound proteins on streptavidin magnetic beads. Their results showed that the cleavable linker approach could lead to the pull-down of functionally active gyrase protein (239).

1.8.4.3 Bioorthogonal approach

It is important to mention that chemical proteomics primarily utilizes cell lysate which is a milieu where proteins distribution is decompartmentalized in cells proteins are distributed in specific organelle and complexation different binding partners that are required for the proper function. Therefore, true strategy to capture protein in their native conformation should involve a minimally invasive approach .i.e. probing with cell permeable probes. This situation is also similar to the *in vivo* context when plasma must be collected prior to probing. Strategy to probe in situ would be the most suitable to reflect the reliability of the protein milieu. The click chemistry has been optimized in a such way that it can be successful at the temperature and condition of the intracellular milieu and *in vivo*. Therefore, there have been many successful attempts to probe with

a click acceptor or donor that can either diffuse into the cell or be available *in vivo*. This is designed to be two steps strategy where the click acceptor or donor is given first and the crossers ponding donor or acceptor is given in a second step to form a probe in situ. Shi *et al.* (240) demonstrated using a cell permeable dasatinib probe termed DA-2. DA-2 contained two compartments, one which is dasatinib warhead, and the second is the click acceptor moiety which also contains alkyl diazirine. The strategy was to administer the probe DA-2 to cell where it could bind to the protein under native state and the cells will be subsequently lysed and irradiated for creating covalent linkage. This would be compared to the traditional affinity matrix whereby the probe is immobilized and then subsequently subjected to pull-down. The in situ approach led to the capture of more kinases for dasatinib than the traditional method. In addition to the canonical ABL and SRC family TKs, new unknown targeted were identified PCTK3, STK25, eIF-2A, PIM-3, PKA C-α, and PKN2. The ability of dasatinib to block was validated by immunoblotting experiment that confirmed the binding affinity of dasatinib for the new targets developed through the bioorthogonal approach. Recently, these bioorthogonal in situ app was used by Wagner's group (241) in Strasbourg to demonstrated the visibility of altering the pharmacodynamic of a drug by administering it in a first step the click acceptor and in a second step a click donor to enhance water solubility and clearance. The proof of concept of this application was made with warfarin a common anticoagulant used in the clinic. Briefly, warfarin analog carrying an alkyne acceptor was administered to the animal and anticoagulation activity was confirmed. This activity was turned off by administering a water soluble PEG linker that accelerated clearance (Figure 1.16). To confirm the formation of the click reaction *in vivo*, the click product was separately synthesized. Indeed , it was shown that formation of the water soluble probe was responsible for the acceleration of clearance.

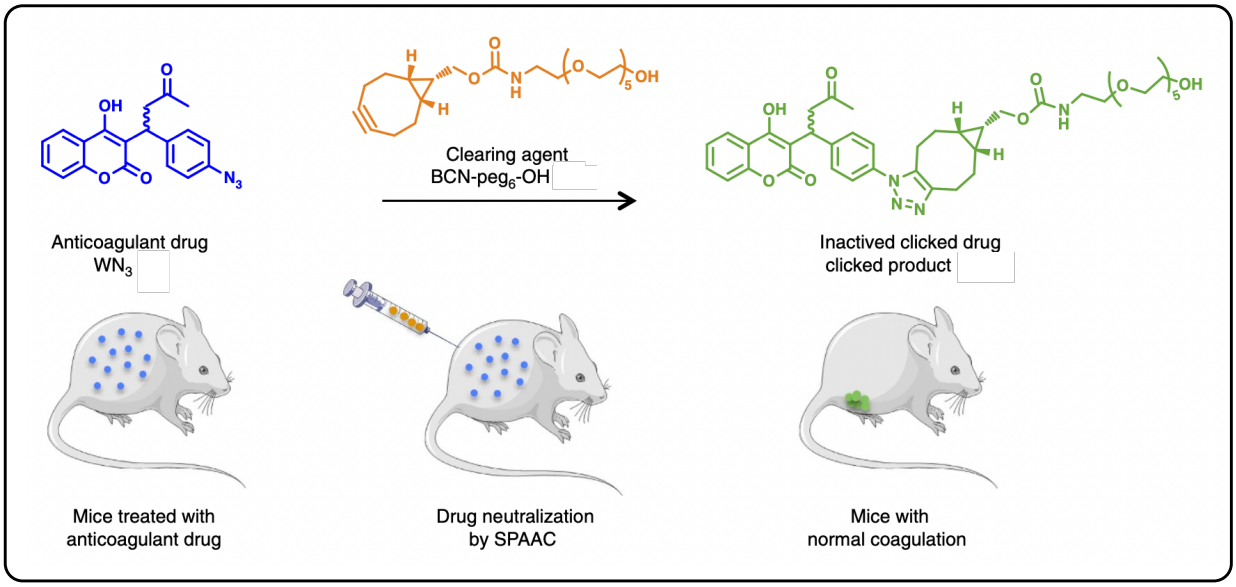

Figure 1.16 Enhancement of the kinetics elimination of the anti-coagulating agent warfarin through a bioorthogonal reaction with a water soluble linker. Reprinted with modification with permission from "An *in vivo* strategy to counteract post-administration anticoagulant activity of azido-Warfarin". Copyright © 2017, *Nature Communications*. No special permission is required to reuse all or part of article published by the journal.

1.9 KINOBEADS IMPACT ON MECHANISTIC STUDIES

Ku *et al.* (242) profiled the selectivity of two fibroblast growth factor receptors (FGFRs) inhibitors dovitinib and orantinib, and quantified their off-targets using kinobeads immobilized inhibitors from cancer cell lysate or human placenta tissue. They were able to capture a number of off-targets in addition to all members of the FGFRs such as AURKA, FLT4-VEGFR3, IKBKE, and PRGFRβ (242). The development of immobilization of clinical kinobeads have significantly contributed not only to target identification but to elucidation to the mechanisms of resistance to

TKIs. As an example, in a pull-down strategy by Koch *et al.* (243) have identified EPHA2 as biomarker for resistance to an gefitinib (an EGFR inhibitor) in lung cancer. In this special study they used siRNA-mediated knock-down technology to assess the role of EPHA2 in the resistance gefitinib. They concluded that EPHA2 is a promising target and could be considered for drug combination therapies (243). A similar work was undertaken by Bantscheff and co-workers (234) where profiled the interaction of three TKIs with purine-binding proteins in addition to protein kinases in cell lysates of HeLa and CML K562 cells. The TKIs dasatinib, bosutinib, and imatinib were immobilized for proteins enrichment. They quantified the proteins by mass spectrometry (iTRAQ), and were able to analyze signaling pathways involved with these target kinases by monitoring changes in drug-induced phosphorylate state. This study concluded that SRC and ABL family kinases are among the targets of the latter inhibitors, in addition to identifying DDR1 and NQO2 as two novel targets of imatinib (234). Glycogen synthase kinase 3 (GSK3) is associated with neurological diseases and is being investigated as a target for many drugs.

1.10 RESEARCH OBJECTIVES

The primary objective of this thesis was to develop new tools for interrogating biological fluids through fluorescence imaging and the pull-down of actionable targets that can be used to either design new drugs or new target-based drug combinations. There are more than 500 Kinases in the kinome and each of these kinases are involved in complex signalling network that characterize tumour progression and sensitivity to cancer therapeutics. Because kinase inhibitors can bind to multiple kinases, we believe that a chemoprobe carrying a kinase inhibitor warhead will pull-down sets of kinases that can be used to characterize biological fluids (cell lysates and human plasma). Likewise, we believe that if the tag is replaced with a fluorescent label, one could image the

distribution or localization in the cells of the kinase warhead using live cell imaging. Thus, our objective can be summarized into two specific ones that exploit the target multiplicity of kinase inhibitors. **a)** to develop tools to read kinase signatures and evaluate their significance in chemotherapeutic drug response and **b)** tagging the inhibitor with fluorescent label in order to visualize their distribution and localization of their target kinases.

Work under the specific objective of the thesis has been executed over the past years is presented herein within five chapters and met the following specific aims.

1) To synthesize a novel chemoprobe containing a quinazoline warhead designed to bind to the ATP pocket of EGFR, and study its chemical proteomics in cell lysates (chapter 2).
2) To synthesize a novel chemoprobe containing a crizotinib warhead designed to bind to the ATP pocket of MET, and study its chemical proteomics in cell lysates as well as validate its potential as a tool to provide rationale for enhancing the potency of paclitaxel, an antitubulin used in the chemotherapy of prostate cancer (chapter 3).
3) To synthesize a fluorescent molecules containing an EGFR- or MET-targeted moiety, and a fluorescent tag designed to be cell permeable for live imaging (chapter 4).
4) To demonstrate the visibility of using the chemoprobes to capture molecular signature in patients who have received therapy with a MET inhibitor (crizotinib) (chapter 5).

We have discussed the contribution to knowledge achieved through the above objectives in chapter 6.

2. CONNECTING TEXT

The past two decades have seen a significant development in the field of bioorthogonal chemistry, which is defined as the art of designing reactions that can be performed in the biological milieu without interference with the biological process. For example, live cells imaging can be performed by making molecules that can bind to its intracellular target in a first step and in a second introducing a tag that can react with the target-bound molecule *in situ*. A fluorescence tag will allow to localize the target by live cell imaging. The best known chemical reaction that lends itself to biological conditions is the click reaction. Click chemistry involves reaction of an azide with an alkyne to give a triazole *in situ*. Another type of ligation that is often used to capture the bound molecule is called "tetrazine ligation". Tetrazine ligation is based on the reaction of a *trans*-cyclooctene and an s-tetrazine in Diels-Alder reaction that followed by retro Diels-Alder reaction to lose N_2 gas. Click chemistry is the most dominant type of reaction used in bioorthogonal chemistry, and more importantly it is often used to create biological probes *ex vivo*. In this case, when the molecule is too large to penetrate the cell, the biological target is captured following lysing of the cell or fixation to allow it to enter the cell. While the term bioorthogonal is restricted to an *in vivo* achievable one, synthesis of a probe *ex vivo* in order to capture targets from cell lysate is often referred to as bioorthogonal chemistry. In this thesis, the approach that we chose to study is to synthesize the chemoprobes using click chemistry for ligation and cell lysis to capture the targets. The typical synthesis undertaken here with this strategy is discussed in the current chapter 2 . Based on the premise that kinases play a sign role in cancer drug sensitivity, we surmised that by capturing the kinase profile of a given drug, we only read its binding profile but also perhaps generate pull-down profiles that can characterize specific drug responses. Chapter 2 covers our effort to synthesize an EGFR targeted probe.

CHPATER 2

DESIGN AND SYNTHESIS OF A NOVEL EPIDERMAL GROWTH FACTOR RECEPTOR (EGFR)-TARGETED PROBE: AFFINITY PULL-DOWN FROM CANCER CELLS

Alaa Baryyan[1], Kurt Dejgaard[2], Karine Pasturaud[1], and Bertrand Jean-Claude[1]

[1]Cancer Drug Research Laboratory, Department of Medicine, The Research Institute of The McGill University Health Centre, 1001 Decarie Boulevard, Montreal, Quebec, H3A 3J1, Canada

[2] Department of Biochemistry, McGill University, Montréal, Québec, Canada.

2.1 ABSTRACT

The anilinoquinazoline are the largest class of EGFR inhibitors that bind to the ATP pocket through formation of hydrogen bonding with the quinazoline and anchorage of the phenylaniline into the hydrophobic pocket. Molecular design by our group led to the synthesis of an anilinoquinazoline scaffold carrying an N-methylphenyl benzamide moiety that confers a strong EGFR inhibitory activity through hydrogen bonding with Asp776 of the ATP site of the EGFR. Here, in order to explore the kinase binding profile of such a new scaffold for probing biological fluids, we designed a chemoprobe AB31 that kept the N-methylphenyl benzamide intact and was expanded toward a biotin tag through a pegylated linker, elongated by click chemistry. To validate the ability of the this probe to capture EGFR and other potential binding partners to the quinazoline warhead, we used cell lysate from the human epidermoid carcinoma A431 cells that overexpress EGFR and performed a magnetic pull-down for proteomics analysis. The results showed that this probe could pull-down full length EGFR and other proteins from the A431 cell lysate, and the study was expanded to other cell types including normal and cancer prostate cells (RWPE1, PC3, DU145, 22RV1, and LNCaP). The pull-down profiles was cell-specific and include proteins from two major classes: kinases and mitochondrial proteins. In contrast to other reported pull-down profiles with other EGFR kinase inhibitors, AB31 pulled down very few kinases , the most common ones being EGFR, CDK1, CDK2, PDXK, and mTOR kinases. Importantly, competitive experiment with pre-exposure to gefitinib suppressed its ability to pull-down a large number of mitochondrial proteins (e.g. ATPA and ATPB) suggesting that it can either directly bind to EGFR which is in cluster with other mitochondrial proteins, or has affinity to the ATP transporters of the mitochondria.

2.2 INTRODUCTION

The quinazoline are considered to be the largest class of inhibitors of epidermal growth factor receptor (EGFR) with more than 3 drugs approved by the FDA for the treatment of lung cancer including tarceva, afatinib, and erlotinib (1-4). Despite the significant number of analysis of the kinase profile of the latter drugs, only one study reported on the immobilization of the quinazoline inhibitor for defining their binding profile. Indeed, Brehmer *et al.* (5) immobilized AX14596 as ana along of gefitinib to mimic it binding profile using epoxy sepharose beads in order to mimic the binding profile of gefitinib on sepharose beads (Figure 1.15, Chapter 1). The study that was the first one describing a receptor tyrosine kinase inhibitor profiling showed that inhibitors carrying a scaffold similar to that of gefitinib could bind and allow to identify new potential targets of gefitinib including AURKA and B, CSK, and EPHB4. A later study using the same approach was conducted by Augustin *et al.* (6) who immobilized gefitinib and identified its potential targets along with other inhibitors. The search for kinase profiling of these inhibitor was inspired by the actionable role of many kinases in proliferation, invasion, and resistance. For example, co-expression of EGFR and MET confers resistance to clinically approved EGFR inhibitors (7). Recently, Koch *et al.* (8) using proteomics for kinase profiling identified EPHA2 as a novel kinase that confers resistance to EGFR inhibitors in the clinic, indicating that identifying kinases that bind to an inhibitor may help discover novel targets for therapeutic intervention against refractory tumours. Here, based upon previous studies by our group that showed a new structure activity relationship in the quinazoline series involving hydrogen bonds at the Asp776 of the ATP site of EGFR, we sought to investigate the binding profiles of the new warhead with the purpose of discovering potentially new targets for therapeutic intervention. Indeed, Barchechath *et al.* (9) showed through molecular modelling that this potency was mediated by the binding of N-benzyl

nitrogen to Asp776 located at the entrance of the binding cleft. The latter study has inspired the design of new inhibitors by Lu *et al.* (10).This unique and unusual binding mode of the scaffold suggests that it may generate a different profile than the one observed for gefitinib immobilized on epoxy sepharose beads. Immobilization of gefitinib was performed through a reaction of its closest analog (AX14596) with the epoxy sepharose to yield a product in which the linker is rather short. Here, we designed and synthesized AB31 with a longer spacer and instead of immobilizing on beads, utilized a peg linker to enhance the distance between the quinazoline warhead and the tag. Recent work by Golabi *et al.* (11) who used the scaffold to build a fluorescent probe (AL906) (Figure 2.1) showed an IC_{50} for EGFR inhibition in the nano-molar range (12 nM) (11). Based upon the strong binding of the quinazoline N-methylphenyl benzamide, we expected a versatile kinase pull-down in human tumour cells. Our ultimate goal was to determine pull-down profile could be different from that of the gefitinib scaffold, and to verify whether the profile will vary from cells to cells. it was used to generate a pull-down profile of proteins and kinases of human tumour cells. Thus, the study was performed with a human carcinoma vulva cells A431 that overexpress EGFR for validating its ability to pull-down EGFR (12), and to further study the differential pull-down profile in prostate cancer cells expressing varied levels of EGFR. Overexpression of EGFR in prostate cancer is associated with tumour progression and drug resistance (13-15). Thus, we surmised that probing cell lysates obtained from prostate normal (RWPE1) and cancer cells (PC3, DU145, 22RV1, and LNCaP) might reveal new targets for therapeutic intervention with EGFR in prostate cancer.

Figure 2.1 Design of the chemoprobe AB31 based upon the structure activity relationship of the EGFR-binding N-methylamino benzamide scaffold of SB163 and AL906 discovered in our laboratory. AB22 was synthesized as a control probe deprived of the scaffold.

2.3 MATERIALS AND METHODS

2.3.1 Cell culture

Human epidermoid carcinoma cells A431, prostate LNCap, DU145, 22RV1, and PC3 cancer cells were maintained in DMEM or RPMI 1640 containing 10% FBS and supplemented with 10 mM

HEPES buffer, gentamycin, ciprofloxacin, and fungisone. Cells were incubated at 37°C in a humidified environment of 5% CO_2, 95% air. All reagents were purchased from Wisent.

2.3.2 Affinity pull-down of EGFR-targeted chemoprobes in human cancer cells

Magnetic beads (Pierce streptavidin magnetic beads) were washed twice with a washing buffer on a magnetic stand. Concentrations of 5 and 2.5 μM of AB31 and AB22, respectively, were added to the beads and incubated for 2 h at room temperature on a shaker. Beads were collected and washed with a washing buffer twice. Cell cultures harvested with a trypsin–EDTA solution and lysed with HEPES-acetate buffer supplemented with 1mM PMSF. Cell cultures harvested similarly, and protein concentration adjusted to 1.5-2 mg/ml and lysate used freshly. Functionalized beads were incubated with lysate at 5° C for 2 h. Beads were washed three times with a washing buffer, and bound proteins were digested on-beads overnight with MS-grade trypsin (Promega), beads were washed with MS-grade acetonitrile and peptides fractions collected and for LC-MS/MS analysis.

2.3.3 Synthesis of chemoprobes

All starting materials were commercially purchased from Broadpharm, Sigma Aldrich, or Ark Pharm. Anhydrous solvents were purchased from Sigma Aldrich. NMR spectra were obtained using Bruker 400 spectrometers.

2.3.3.1 Synthesis of EGFR-targeted chemoprobe AB31 and control probe AB22

The synthesis of **1**, **2** and **3** was proceeded according to a previously published work from our laboratory. Briefly, compound **1** was stirred in tetrahydrofuran (THF) and pyridine at 0º C, and 4-

(chloromethyl)benzoyl chloride was added to the mixture and stirred for 1 h at 0º C overnight. The solid was filtered and washed with aqueous HCl (1M), aqueous K_2CO_3 10%, dichloromethane and ethylacetate, then with water to yield **2**. To synthesize **3**, product **2** was dissolved with potassium iodide (KI) in DMF under argon and mixture stirred for 3 h at 70º C. Solvent was removed and product was collected with column chromatography to yield product **3**. To synthesize **4**, a solution of **3** in DMF and stirred with 4-azidobutanoic acid dissolved in DMF with hydroxybenzotriazole (HOBt), 4-dimethylaminopyridine (DMAP), and 1-Ethyl-3-(3-dimethylaminopropyl)carbodiimide (EDCI). After reaction completion, solvent was evaporated and product **4** was collected with column chromatography (Scheme 2.1)

To synthesize the biotin tag, a solution of N-(20-amino-3,6,9,12,15,18-hexaoxaicosyl)-5-((3aS,4S,6aR)-2-oxohexahydro-1H-thieno(3,4-d)imidazol-4-yl)pentanamide in diMethylformamide a N,N-Diisopropylethylamine (DIEA) and ((1R,8S,9s)-bicyclo(6.1.0)non-4-yn-9-yl)Methyl (4-nitrophenyl) carbonate were added and the mixture was stirred at room temperature overnight. The product was extracted in DCM and washed with water. The crude extract was purified by column chromatography to yield the product **5** (Scheme 2.2). ^{1}H NMR (DMSO-d_6, 400 MHz, 298 K) δ 7.82 (t, J = 6.2 Hz, 1H), 7.08 (t, J = 4.4 Hz, 1H), 6.40 (s, 1H), 6.34 (s, 1H), 4.30 (dd, J = 7.8, 4.9 Hz, 1H), 4.12 (ddd, J = 5.8, 4.4, 1.8 Hz, 1H), 4.03 (d, J = 8.2 Hz, 2H), 3.50 (s, 12H), 3.42 – 3.42 (m, 1H), 3.39 (t, J = 5.9 Hz, 3H), 3.17 (dt, J = 6.0, 3.8 Hz, 2H), 3.11 (dd, J = 11.9, 6.0 Hz, 3H), 2.82 (dd, J = 12.4, 5.1 Hz, 1H), 2.57 (d, J = 12.2 Hz, 1H), 2.28 – 2.09 (m, 5H), 2.06 (dd, J = 11.0, 3.8 Hz, 2H), 1.65 – 1.40 (m, 6H), 1.34 – 1.25 (m, 3H) ppm. ES-MS (ESI) *m/z* (%): 749. 39 (100) $(M + Na)^+$.

For the probe ligation, solution of **4** in DMF was added to biotin tag **6** in DMF. The reaction was stirred at 90°C over oil bath and monitored over 3 days with MS and TLC. Upon reaction completion, solvent was evaporated and the residual compound was recovered and purified on preparative TLC to yield **AB31** (Scheme 2.1).

To synthesize the mock probe, a solution of azidocyclohexane in DMF was added to compound **6** in DMF. The reaction was stirred at 75°C over an oil bath and monitored over 2 days with MS and TLC. Upon reaction completion, solvent was evaporated and the residual compound was recovered and purified on preparative TLC to yield compound **AB22** (Scheme 2.2). ^{1}H NMR (DMSO-d_6, 400 MHz, 298 K) δ 7.82 (t, J = 5.6 Hz, 1H), 7.11 (t, J = 5.6 Hz, 1H), 6.38 (d, J = 24.4 Hz, 2H), 4.30 (dd, J = 7.6, 5.1 Hz, 1H), 4.27 – 4.17 (m, 1H), 4.16 – 4.09 (m, 1H), 4.05 (dd, J = 7.8, 3.6 Hz, 2H), 3.51 (s, 23H), 3.44 – 3.35 (m, 5H), 3.30 (s, 1H), 3.18 (q, J = 5.8 Hz, 2H), 3.14 – 3.04 (m, 3H), 3.02 – 2.95 (m, 1H), 2.94 (dd, J = 7.2, 3.7 Hz, 1H), 2.81 (dt, J = 8.0, 4.1 Hz, 1H), 2.78 – 2.69 (m, 1H), 2.58 (d, J = 12.4 Hz, 2H), 2.07 (dd, J = 12.8, 5.3 Hz, 3H), 1.96 – 1.88 (m, 2H), 1.87 – 1.76 (m, 4H), 1.55 (dddd, J = 29.3, 19.1, 17.1, 9.0 Hz, 10H), 1.34 (s, 1H), 1.33 – 1.26 (m, 2H), 1.18 – 1.05 (m, 1H), 0.92 (s, 2H) ppm. ES-MS (ESI) *m/z* (%): 874.5 (100) $(M + Na)^+$.

2.3.4 Mass spectrometry (LC-MS/MS): proteomics

For LC-MS analysis, a Q Exactive HF (Thermo Scientific) mass spectrometer was coupled on-line to an EASY-nLC 1000 HPLC system (Thermo Scientific). Rehydrated tryptic peptide fragments were separated on a 25 cm C18 column (Acclaim 75 μm inner diameter, 2 μm particles, Thermo Scientific) fitted upstream with a 2cm trapping column (Acclaim PepMap 100, Thermo Scientific) in a 100 min gradient from 3% to 38% in buffer B (99.9% acetonitrile, 0.1% formic

acid) at 350 nL/min, for a total run time of 120 minutes. Mass spectra were acquired in data-dependent mode. Briefly, each survey scan (range 375 to 1,400 m/z, resolution of 120,000 at m/z 200, maximum injection time 60 ms, AGC target of 5E6) was followed by high-energy collisional dissociation based fragmentation (HCD) of the 25 most abundant isotope patterns with a charge ≥ 2 (normalized collision energy of 25, an isolation window of 2.5 m/z, resolution of 15,000, maximum injection time 60 ms, AGC target value of 2E5). Dynamic exclusion of sequenced peptides was set to 3.5 s. All data were acquired using Xcalibur software (Thermo Scientific).

2.3.5 Data analysis of proteomic raw files

The acquired MS raw files were processed with the Mascot Distiller (version 2.5.1.0, Matrix Sciences). The Mascot search engine (Matrix Sciences, version 2.5) was used for peptide and protein identification at a Mascot p-value of less then 0.05. The human UniProtKB database (August 2017) was used as database. Trypsin was set as the enzyme specificity. And data were searched with a precursor ion mass accuracy of 6 ppm, MSMS mass accuracy was set to 50 mDa. Oxidized Methionine was allowed as a variable modification. Search data were imported to Scaffold for additional data validation (FDR < 5%). Comparative Label-free relative protein quantification was performed using the validated data spectral counts per protein across samples.

2.4 RESULTS

2.4.1 Chemistry of AB31

In order to target EGFR, we used structure activity relationship already established in our laboratory to design **AB31**. As shown in Figure 2.1, compound **3** has been shown in our laboratory

to behave as a potent EGFR inhibitor due to the additional binding role played by the N^1,N^2-dimethylethane chloromethylbenzoyl moiety. Briefly, **1**, **2** and **3** were obtained as previously described using a coupling reaction between chloromethyl benzoyl chloride and **2** (9, 16, 17). Alkylation of **2** in the presence of excess N^1,N^2-dimethylethane-1,2-diamine gave **3**, which was coupled 4-azidobutanoic acid to give **4**. In a parallel synthesis, biotin-PEG6-NH2 was treated with 4-nitrophenyl to give **5**. Click reaction between **4** and **5** gave probe **AB31** in good yield.

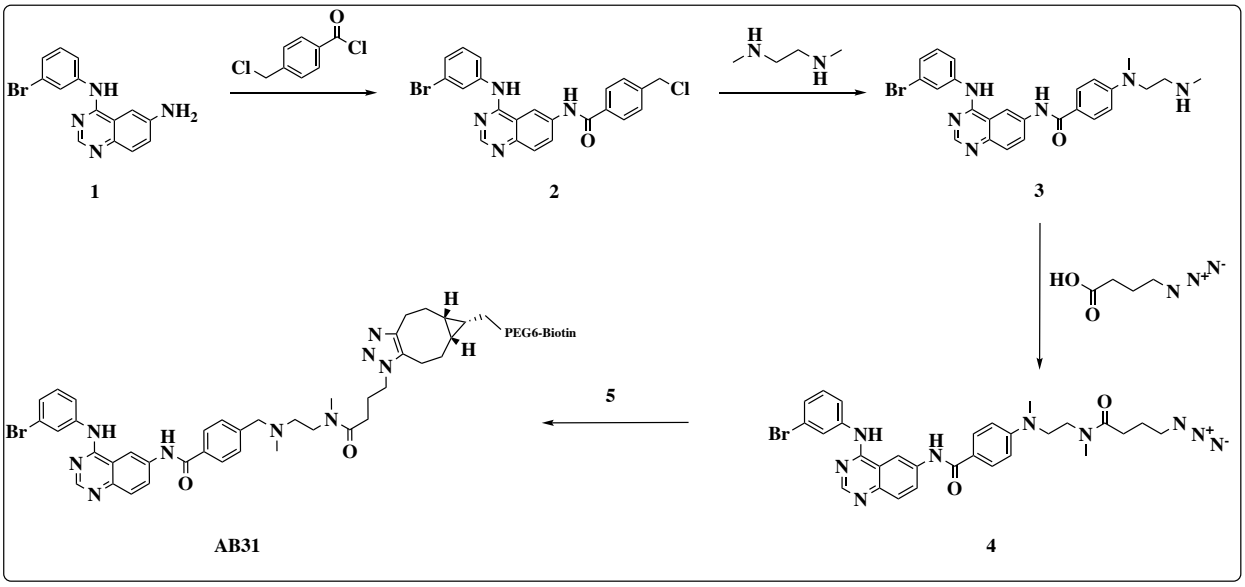

Scheme 2.1 Synthesis of AB31 using a click reaction between click donor 4 and an acceptor 5.

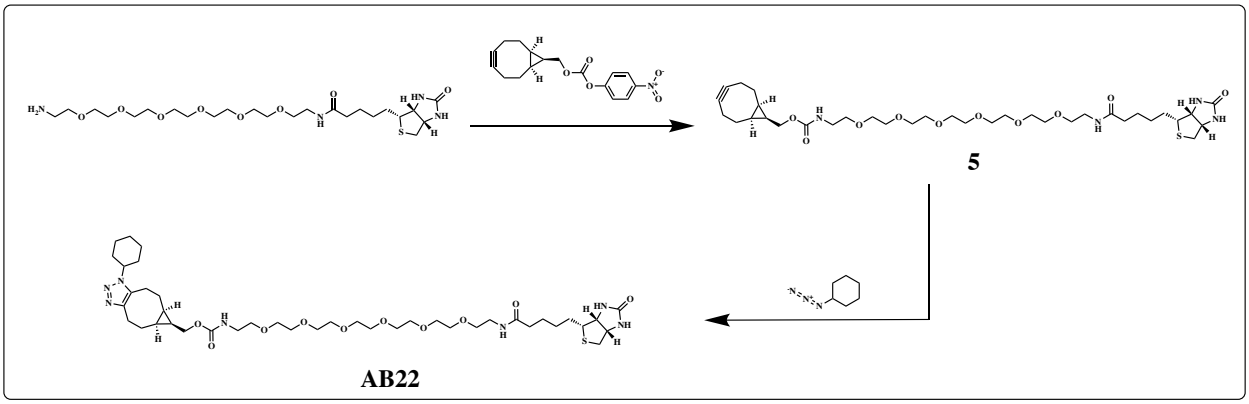

Scheme 2.2 Synthesis of AB22 using a cyclohexyl azide to replace the quinazoline scaffold.

Molecular modelling of the probe in the ATP binding site showed that the bromophenyl moiety was anchored in the binding site with interaction between N-methylbenzyl (protonated form) and Asp776 (Figure 2.2a-c), which suggests that it can bind optimally to the ATP binding site of the EGFR.

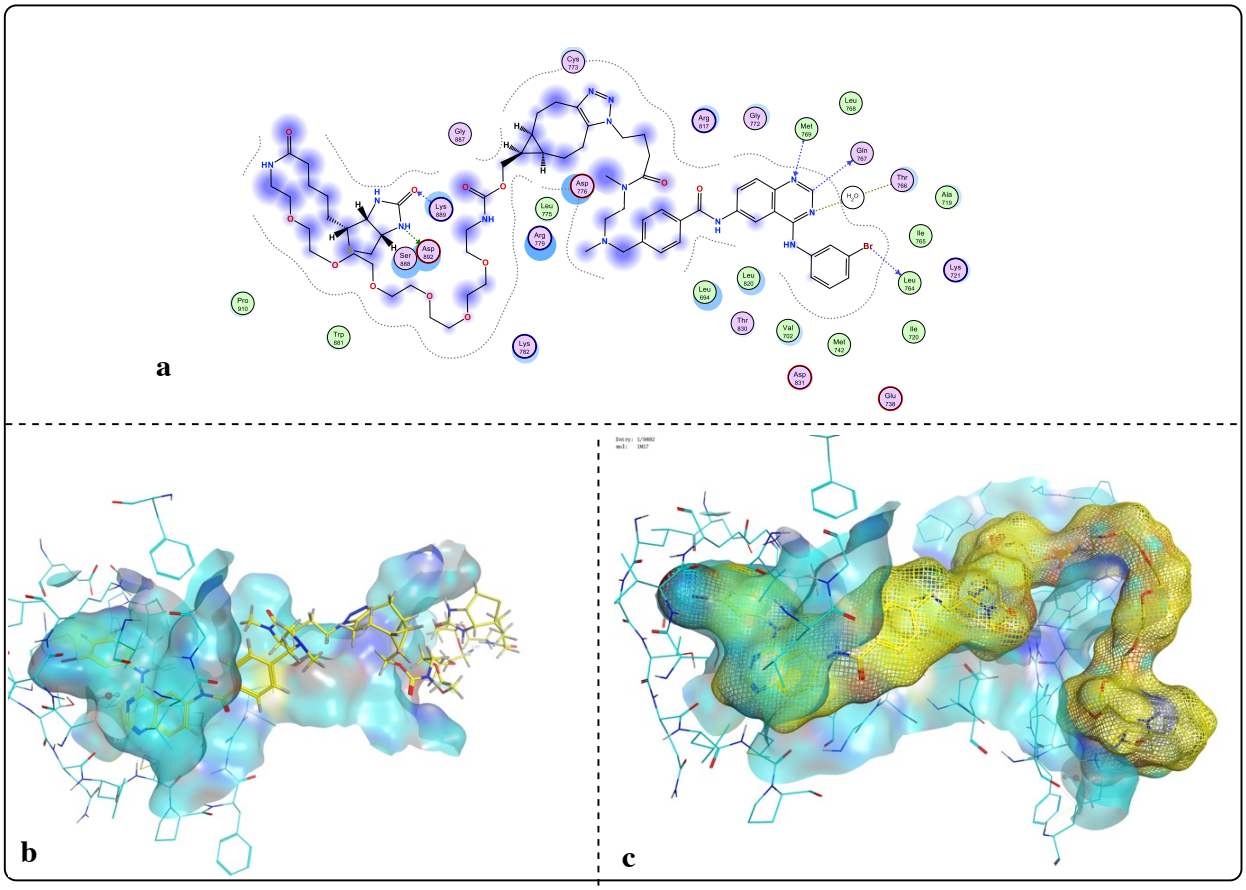

Figure 2.2 (a) Ligand interaction pose by AB31 showing the localization of the bromo aniline moiety in the hydrophobic pocket and the nitrogen of the quinazoline moiety forming hydrogen bonds with Met769, and Thr766. Surface pockets of the receptor **(b)** only the receptor and **(c)** ligand-receptor.

2.4.2 Pull-down

In order to validate the EGFR targeting potency of AB31, A431 cells were grown and lysed after 24 h. The lysates was probed with AB31, and the attached proteins captured using a streptavidin bound magnetic beads. The resulting proteins were digested with trypsin and subjected to proteomics analysis. The results showed that AB31 could capture its canonical target EGFR ($p=0.0051$) and other proteins. This result validate the ability of AB31 probe to bind and capture EGFR in cell lysate (Table 2.1).

2.4.2.1 Probing with prostate cancer cells

Following the validation of the probe in A431 cells, we attempted to test whether the pull-down profile will be similar in prostate cancer cells, one castrate resistance and androgen sensitive, and normal prostate cells. EGFR was pulled down from normal RWPE1 and cancer DU145 cells. Interestingly, it could not be captured from 22RV1 and PC3.

2.4.2.2 Probing drug treated and non-treated A431 cells

Since AB31 was consistently pulling down EGFR in all assays, we attempted to general pull-down profile in cells treated with the standard of care paclitaxel in comparison with vehicle. While in non-treated samples, EGFR could be pulled down along with PDXK. Treatment with paclitaxel appeared not to present any targets that could be captured by AB31, suggesting that an EGFR inhibitor with this scaffold should not be advice for combination with paclitaxel.

2.5 DISCUSSION

Recently, we reported the design of a fluorescent probe AL906 that carries an EGFR targeting scaffold similar to that of AB31 with an IC_{50} of 12 nM for EGFR inhibition (Figure 2.1). Unlike other inhibitors of EGFR (e.g. gefitinib and tarceva) that only binds through hydrogen bond of their quinazoline nitrogen, this scaffold contains an additional amino group that increases its binding strength to the ATP pocket by forming an additional hydrogen bond with Asp776. Other inhibitors capable of forming the latter interaction have subsequently being reported by other studies (10, 18, 19), and proven using X-ray crystallography (10). While immobilization of inhibitors containing the quinazoline warhead of gefitinib have already been shown to pull-down kinases from cell lysates, this work is the first attempt to identify the pull-down profiles of an inhibitor capable of forming the Asp776 hydrogen bond. Interestingly, as shown by proteomics analysis, AB31 could pull-down EGFR with other proteins that did not belong to the kinase family. Remarkably, this pull-down this did not generate a broad kinase targeting profile in A431 cells. Even when the study was expanded to other cell lines, the kinases profiling remine poor. The most common kinases pull-down were pyridoxal kinase (PDXK), mTOR, and CDK1, with only two tyrosine kinases being captured EGFR and EPHA2 (Table 2.1). Interestingly, the large proportion of the kinases observed do not correspond to the ones commonly pulled down by the kinobeads immobilization approach. This difference may be due to the additional aminomethyl benzamide moiety grafted on the quinazoline ring that confers a binding mode specific for EGFR. Importantly, AB31 appeared to pull-down a large number of mitochondrial proteins (Table 2.2). This perhaps reflect its ability to bind to ATP transporters in addition to perhaps bind to perinuclear localized EGFR. Indeed, previous work with AL906 a fluorescent probe containing the aminomethyl

benzamide scaffold showed that it was primarily localized in the perinuclear region (11). This indicates that perhaps these scaffold has binding targets localized in the perinuclear organelles.

It is noteworthy that pull-down pattern by AB31 was cell-specific. For instance, it captured EPHA2 from PC3 cells with highest level among kinases. In cell lysates from DU145, AB31 captured mTOR, eukaryotic translation initiation factor 2 alpha kinase 2 (E2AK2), deoxycytidine kinase (DCK). Unlike profiles from PC3 and DU145 cells, 22RV1 cells captured a larger number of proteins such as phosphoglycerate Kinase 1 (PGK1) and Nucleoside diphosphate kinase b (NDKB). In normal prostate cells RPWR1, the probe AB31 captured EGFR as well as CDK1 and PDXK. Overall, except for EPHA2 and EGFR, none of the kinases captured in these specific cell lines was of the tyrosine kinase family. As mentioned earlier, this may be due to the mode of binding of the aminomethyl benzamide scaffold.

Kinase	AB31						AX14596*
	A431	PC3	DU145	22RV1	LNCaP	RWPE1	HeLa
EGFR	+	+	+			+	+
PRKDC							
PFKAL				+	+		
NUCKS				+			
CD11B	+		+		+		
CDK1	+						
PDXK	+			+	+		
NDK8	+						
NOL9	+		+				
E2AK2	+	+	+	+			
PDK1L	+						
EPHA2		+	+				
M3K5		+					
NUAK		+					
ERBB4			+				
PRP4B			+		+		
BAZ1B			+				
CTRO			+				
STK24			+				
SMG1			+				
RIK1							
RIPK2			+				
mTOR			+		+		
DCK			+	+	+		
GSK3A			+				
PFKAM				+			
KAP2				+			
AGK				+	+		
PANK4				+			
KTHY				+			
ATM					+		
OXSR1				+	+		
PAK4					+		
MK01						+	
EPHA3				+			
ADK				+			
PAK2				+			
GSK3B				+			
CSK				+			+
CSK21				+			
SRPK2				+			
WNK1				+			
AURORA A							+
AURORA B							+
BLK							+
BUB1							+
BRK							+
CAMKII							+
CAMKIIA							+
CAMKIIB							+
CAMKIIG							+
CAMKIID							+
CK1D							+
CK1E							+
EPHB4							+
FYN							+
GAK							+
HCK							+
ILK							+
IKKE							+
JNK2							+
LYN							+
MET							+
P38A							+
RICK							+
TNK1							+
YES							+

* Daub et al., 2005, Cancer Research

Table 2.1 Comparison of the pull-down kinase profile of AB31 from lysates of A431 and normal and cancer prostate cells that ovrexpress EGFR with the pull-down pattern of AX14596 immoobilized on sepharose beads.

Mitochondrial Protein		ATP Proteins
ECHA	PCCA	ATPB
SQRD	PCCB	ATPA
ATP5I	CH60	ATP5I
ODO2	PRDX3	ATPG
ATPG	ATPB	ATPD
GLYM	GRP75	
STML2	ATPA	
ODBA	ODPX	
ODBB	ODPB	
QCR2	ODPA	
ATPD	CH10	
DUT	DHE3	
OPA1	TOP1	
ACAD9	AL1A3	
COX41	EFTU	
QCR1	LPPRC	
COX5B	MPCP	
ECHB	MDHM	
TRAP1	CISY	
PRDX5		

Table 2.2 List of mitochondrial and ATP proteins captured with AB31

2.6 REFERENCES

1. Dohle W, Jourdan FL, Menchon G, Prota AE, Foster PA, Mannion P, et al. Quinazolinone-Based Anticancer Agents: Synthesis, Antiproliferative SAR, Antitubulin Activity, and Tubulin Co-crystal Structure. J Med Chem. 2018;61(3):1031-44.

2. Herbst RS. Erlotinib (Tarceva): an update on the clinical trial program. Semin Oncol. 2003;30(3 Suppl 7):34-46.

3. Malhotra A, Bansal R, Halim CE, Yap CT, Sethi G, Kumar AP, et al. Novel amide analogues of quinazoline carboxylate display selective antiproliferative activity and potent EGFR inhibition. Medicinal Chemistry Research. 2020;29(12):2112-22.

4. Hekal MH, Abu El-Azm FS. New potential antitumor quinazolinones derived from dynamic 2-undecyl benzoxazinone: synthesis and cytotoxic evaluation. Synthetic Communications. 2018;48(18):2391-402.

5. Brehmer D, Greff Z, Godl K, Blencke S, Kurtenbach A, Weber M, et al. Cellular Targets of Gefitinib. Cancer Research. 2005;65(2):379.

6. Augustin A, Lamerz J, Meistermann H, Golling S, Scheiblich S, Hermann JC, et al. Quantitative Chemical Proteomics Profiling Differentiates Erlotinib from Gefitinib in EGFR Wild-Type Non–Small Cell Lung Carcinoma Cell Lines. Molecular cancer therapeutics. 2013;12(4):520-9.

7. Bardelli A, Corso S, Bertotti A, Hobor S, Valtorta E, Siravegna G, et al. Amplification of the MET receptor drives resistance to anti-EGFR therapies in colorectal cancer. Cancer discovery. 2013;3(6):658-73.

8. Koch H, Busto MEDC, Kramer K, Médard G, Kuster B. Chemical proteomics uncovers EPHA2 as a mechanism of acquired resistance to small molecule EGFR kinase inhibition. Journal of proteome research. 2015;14(6):2617-25.

9. Barchéchath S, Williams C, Saade K, Lauwagie S, Jean-Claude B. Rational design of multitargeted tyrosine kinase inhibitors: a novel approach. Chem Biol Drug Des. 2009;73(4):380-7.

10. Lü S, Zheng W, Ji L, Luo Q, Hao X, Li X, et al. Synthesis, characterization, screening and docking analysis of 4-anilinoquinazoline derivatives as tyrosine kinase inhibitors. Eur J Med Chem. 2013;61:84-94.

11. Golabi N, Larroque AL, Peyrard L, Williams C, Jean-Claude BJ. Subcellular distribution and mechanism of action of AL906, a novel and potent EGFR inhibitor rationally designed to be green fluorescent. Invest New Drugs. 2021;39(1):240-50.

12. Zhang F, Wang S, Yin L, Yang Y, Guan Y, Wang W, et al. Quantification of epidermal growth factor receptor expression level and binding kinetics on cell surfaces by surface plasmon resonance imaging. Anal Chem. 2015;87(19):9960-5.

13. de Muga S, Hernández S, Agell L, Salido M, Juanpere N, Lorenzo M, et al. Molecular alterations of EGFR and PTEN in prostate cancer: association with high-grade and advanced-stage carcinomas. Modern Pathology. 2010;23(5):703-12.

14. Day KC, Lorenzatti Hiles G, Kozminsky M, Dawsey SJ, Paul A, Broses LJ, et al. HER2 and EGFR Overexpression Support Metastatic Progression of Prostate Cancer to Bone. Cancer Res. 2017;77(1):74-85.

15. Schlomm T, Kirstein P, Iwers L, Daniel B, Steuber T, Walz J, et al. Clinical Significance of Epidermal Growth Factor Receptor Protein Overexpression and Gene Copy Number Gains in Prostate Cancer. Clinical Cancer Research. 2007;13(22):6579-84.

16. Larroque-Lombard AL, Ning N, Rao S, Lauwagie S, Halaoui R, Coudray L, et al. Biological Effects of AL622, a Molecule Rationally Designed to Release an EGFR and ac-Src Kinase Inhibitor. Chemical biology & drug design. 2012;80(6):981-91.

17. Domarkas J, Dudouit F, Williams C, Qiyu Q, Banerjee R, Brahimi F, et al. The combi-targeting concept: synthesis of stable nitrosoureas designed to inhibit the epidermal growth factor receptor (EGFR). Journal of medicinal chemistry. 2006;49(12):3544-52.

18. Rachid Z, Brahimi F, Qiu Q, Williams C, Hartley JM, Hartley JA, et al. Novel nitrogen mustard-armed combi-molecules for the selective targeting of epidermal growth factor receptor overexperessing solid tumors: Discovery of an unusual structure− activity relationship. Journal of medicinal chemistry. 2007;50(11):2605-8.

19. Rao S, Larroque-Lombard A-L, Peyrard L, Thauvin C, Rachid Z, Williams C, et al. Target modulation by a kinase inhibitor engineered to induce a tandem blockade of the epidermal growth factor receptor (EGFR) and c-Src: the concept of type III combi-targeting. PloS one. 2015;10(2):e0117215.

3. CONNECTING TEXT

In chapter 2, we demonstrated the feasibility of a chemoprobe containing an EGFR inhibitor warhead, and a linker attached to a biotin tag that could bind to and be pulled down with streptavidin magnetic beads. Our chemical strategy was to ligate the kinase warhead to the biotin moiety via a click reaction. We demonstrated that the synthesized probe AB31 could pull down EGFR in A431 cell lysates but did not generate a very broad affinity pull-down profile in each cell line. The hepatocyte growth factor receptor MET plays a significant role in cancer progression and through signaling redundancy with EGFR promotes resistance to kinase inhibitors. Its inhibitor crizotinib is known to have a very broad kinase targeting profiles. Therefore, we attempted to build a probe carrying a crizotinib warhead. Based on the premise that kinases play a significant role in cancer drug sensitivity, we surmised that by capturing the kinase profiles in cells treated with a given a cytotoxic drug, we could identify new targets for enhancing the potency of the latter drug. In chapter 3, we sought to make a proof-of-concept of the approach by synthesizing AB19, a MET-targeted probe, and studying pull-down profiles in prostate cancer cell lysates following treatment with paclitaxel, a cytotoxic drug used in the clinical management of prostate cancer in the advanced stages.

CHAPTER 3

DESIGN, SYNTHESIS, AND VALIDATION OF A MET-TARGETED CHEMOPROBE FOR IDENTIFYING KINASES TO BE TARGETED FOR SENSITIZING CELLS TO PACLITAXEL: A PROOF-OF-CONCEPT STUDY

Alaa Baryyan[1], Kurt Dejgaard[2], and Bertrand Jean-Claude[1]

[1]Cancer Drug Research Laboratory, Department of Medicine, The Research Institute of The McGill University Health Centre, 1001 Decarie Boulevard, Montreal, Quebec, H3A 3J1, Canada

[2] Department of Biochemistry, McGill University, Montréal, Québec, Canada.

3.1 ABSTRACT

Chemotherapy, through various signaling pathways changes the kinase distribution profiles in tumour cells. Here we posit that if a tool can be developed to identify binding partners to these kinases, novel and more efficacious combinations can be developed to not only enhance potency but also expand the use of kinase inhibitors in the advanced stages of solid tumours. The approach we chose to study was to design a chemoprobe carrying a kinase inhibitor warhead to capture and read the kinase binding profiles before and after treatment. Thus, we designed AB19 a chemoprobe carrying the scaffold of crizotinib, a MET inhibitors with broad kinase binding profile. The ability of AB19 to bind to MET was validated using KATO-II gastric cancer cells in which MET is amplified. The results showed that it pull down MET (its primary target) and many other kinases, including LCK, SRC, EPHA2, and FAK1 that play actionable role in cancer progression. Importantly, we found that the kinase pull-down profile by the chemoprobe is similar to that reported in kinase assays for free crizotinib, thereby validating the ability of the chemoprobe to simulate the free drug. In vitro studies with AB19 revealed the following: (a) the pull-down profiles vary with cell lines, with the presence or absence of some important oncoproteins, (b) under conditions where the cells were treated with paclitaxel, a standard of care drug used in the clinical management of advanced cancers, the pull-down profiles were well conserved between treated and non-treated cells. However, disappearance and appearance of key targets were observed. Based upon the detection of an increase in AURKA and mTOR spectral counts, we designed combinations under equieffective and sequential combinations. Of all the combinations and studies, the result showed that the AURKA inhibitor, namely alisertib was the most efficient in sensitizing cells to paclitaxel, suggesting that this chemical proteomics approach can be used to identify synergistic combinations.

3.2 INTRODUCTION

Over the past two decades, significant advances in the field of molecular biology and pharmacology led to the identification of protein kinases as targets for chemotherapeutic intervention against many cancers. Several receptor tyrosine kinases (RTK) have been identified that drive tumour progression and resistance to chemotherapy. Epidermal growth factor receptor tyrosine kinase (EGFR TK) and MET tyrosine kinases (MET TK) have been amongst the most targeted oncogenes products for therapeutic intervention against many cancers including lung, prostate, and gastric cancers (1-6). Advances in the development of drugs against the former receptors have been significantly hampered by the emergence of mutations that reduce binding to the ATP pocket of the receptors (7). Despite significant efforts toward engineering molecules to bind to the resistant mutant forms of EGFR, the resulting drugs do not efficiently block tumour progression in the advanced stages. As an example, despite the development of drugs that can specifically bind to the resistant forms of EGFR or the selective therapy of patients expressing EGFR inhibitor sensitive mutant, the survival rates in non-small cell lung cancers (NSCLC) remain approximately 1.5 year (8). This indicates that as the tumour progresses mechanism to evade the effects of modulating the targets become predominant and cytotoxic therapy with classical antitumour drugs becomes the only option. While cytotoxic therapy represents an important option in the advanced stages, the degree of target heterogeneity associated with tumour progression is a major deterrent for combination therapy with kinase inhibitors. Here we surmise that if kinase targets activated by treatment with chemotherapy could be identified, given the current availability of large numbers of clinical inhibitors, potential therapies could be developed that include one or two kinase inhibitors, leading perhaps to synergistic combination against refractory tumours.

Paclitaxel is one of the most commonly used cytotoxic agents in the clinical management of many tumours, including lung, gastric and prostate cancer (9-11). Its mechanism of action is based on binding to tubulins and stabilization of the microtubules and inhibition of tubulin depolymerization. Tubulin binding agents (TBAs) are known to activate stress response in tumour cells (12). Treatment of tumour cells with TBAs leads to activation of the JNK and the AKT/mTOR axis, indicating that it may alter the kinase distribution in the cells, thereby offering potential target for modulating sensitivity to antitubulins (13). We surmised that probing cells with a kinase affinity probe might reveal such kinases modulated by anti-tubulin treatment.

Over the past decade, the concept of affinity probes through chemical proteomics has emerged as an invaluable strategy for identifying kinase binding profiles within cells. It consists of immobilizing a given inhibitor through covalent linkage with sepharose beads, or through a functionalized linker to perform pull-down that allow to capture kinases identifiable by mass spectrometry using a proteomics approach (14). For example Daub *et al* (15), showed that a gefitinib analog (AX14596) immobilized through a reaction with epoxy sepharose could define the binding profile of gefitinib. Likewise, dasatinib probe showed kinase pull-down profiles similar to that obtained from kinase assays involving dasatinib alone (16). In the current study, we chose to design a probe that targets MET, a receptor tyrosine kinase, which is being investigated for the treatment of gastric cancer. To test the feasibility of the approach, we used one gastric cancer cell line and a panel of prostate cancer cells, which are known to express varied levels of MET. The choice of MET targeting was inspired by the very broad kinase profiling reported for crizotinib. Indeed, its kinase profile includes functionally important kinases such as Ros, FAK, IRAK, EPHA2, etc. In the context of this work, we designed and synthesized a novel chemoprobe

AB19, built for a magnetic pull-down approach. As shown in Figure 3.1, it contains a biotin warhead spaced from crizotinib moiety through a polyethylene glycol (PEG) linker elongated through click chemistry. Our goal was to use this probe to generate pull-down patterns from lysates of cells expressing varied levels of MET that can be correlated to drug response *in vitro*. We chose to study cell response to paclitaxel, which is a chemotherapeutic drug used in the clinical management of many cancers in the advanced stages, including gastric and prostate. We wished to identify kinases that appeared or disappeared from drug treatment, and that could possibly be targeted to modulate drug response in the future. Paclitaxel is being able to arrest cells in G2M phase (12), we probed the cells immediately after treatment and 24 h later in order to verify whether the probe could report on the kinase distribution before and after treatment. It was found that pull-down profiles did not vary significantly, but their abundance was altered. Importantly, inhibitors of two kinases pulled down following paclitaxel treatment were tested in combination under equieffective and sequential exposure.

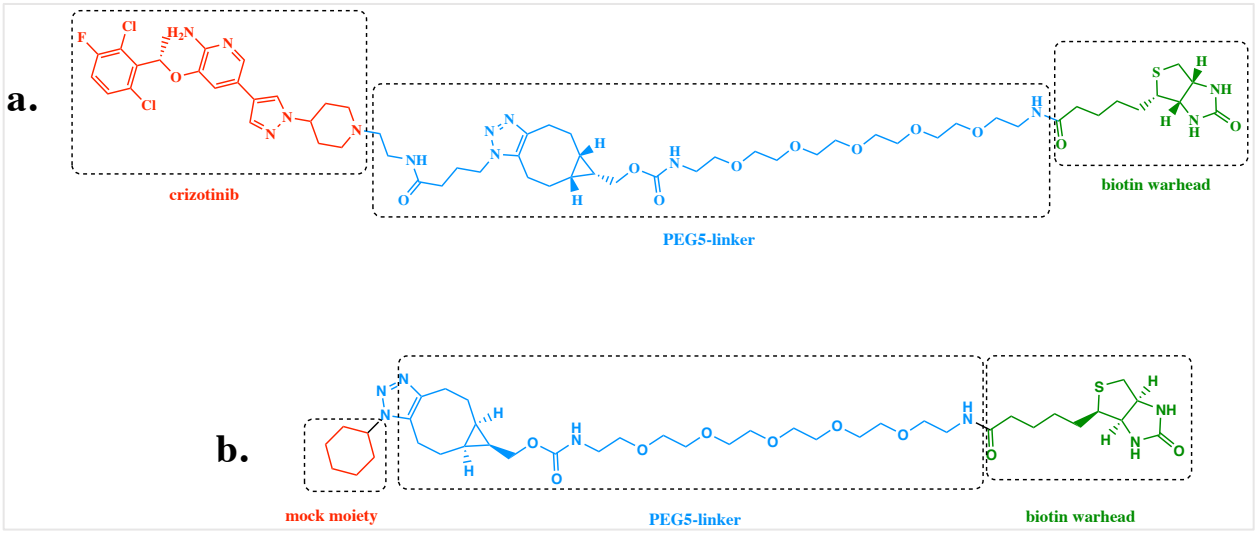

Figure 3.1 The structural composition of **a)** MET-targeted probe (AB19) and **b)** mock probe that carries a mock moiety (AB22).

3.3 MATERIALS AND METHODS

3.3.1 Cell culture

Human gastric cancer cells KATO-II, prostate LNCap, DU145, 22RV1, and PC3 cancer cells were maintained in RPMI 1640 containing 10% FBS and supplemented with 10 mM HEPES buffer, gentamycin, ciprofloxacin, and fungisone. Cells were incubated at 37°C in a humidified environment of 5% CO_2, 95% air. All reagents are purchased from Wisent.

3.3.2 Growth inhibition assay

Growth inhibition was determined using the sulforhodamine B (SRB) assay as described by Skehan (17). Briefly, cells were allowed to attach for 24 h in 96-weel plates after which a dose range of drugs was added in triplicates. Five days later, the medium was removed and the cells fixed with 50% trichloroacetic acid (TCA) for 2 h, after which the plates were rinsed with tap water and allowed to dry overnight. A solution of SRB (0.4%) was added to stain the cells for 2 h, followed by washing with 1% acetic acid and the plates were left to dry overnight. A solution of 10 mM Tris-base (200 μL) was added for colorimetric detection by UV. Growth percentages were calculated by T/C x 100 and IC_{50} determined using GraphPad prism. Combinations indices (CI) and plots were generated using Compusyn with data from the linear part of the sigmoids. CI values > 1 indicated antagonism, values < 1, synergism, and values = 1, additivity.

3.3.3 Cell cycle analysis

Cells were grown in 6-well plates and treated with 10 μM of paclitaxel, crizotinib, or drug-free medium for 2 and 24 h. Cells were trypsinized and centrifuged at 1000 rpm for 10 min, washed

twice with PBS. Cell pellets were fixed in ice-cold 70% ethanol with vortexing and stored in -20 °C overnight. Ethanol was removed 24 h later and cells washed with PBS twice prior to staining with PI/RNAse solution and incubated at 37 C for 30 minutes before flow cytometry analysis.

3.3.4 Chemistry

All starting materials were purchased from Broadpharm, Sigma Aldrich, or Ark Pharm. Anhydrous solvents were purchased from Sigma Aldrich. ^{1}H-NMR spectra were recorded at the ambient probe temperature using Bruker 400 spectrometers. Mass spectra were recorded using the Amazon spectrometer ES-MS instrument. Proteomics analysis was performed on Exactive instrument. Purification of the products was performed on column chromatography or silica gel plates.

3.3.4.1 Synthesis of tert-butyl (R)-(2-(4-(4-(6-amino-5-(1-(2,6-dichloro-3-fluorophenyl)ethoxy)pyridin-3-yl)-1H-pyrazol-1-yl)piperidin-1-yl)ethyl)carbamate (1). Compound **1** were synthesized by stirring crizotinib in dimethylformamide (DMF) and trimethylamine (TEA) with tert-butyl (2-bromoethyl)carbamate overnight at room temperature. The solvent was evaporated under reduced pressure, and the crude was extracted in DCM and washed with water/brine prior purification on a TLC plate to yield pure the product **1** (Scheme 1). ^{1}H NMR (DMSO-d6, 400 MHz, 298 K) δ 7.94 (s, 1H), 7.75 (d, J = 1.8 Hz, 1H), 7.57 (dd, J = 9.0, 5.0 Hz, 1H), 7.52 (s, 1H), 7.44 (t, J = 8.7 Hz, 1H), 6.89 (d, J = 1.7 Hz, 1H), 6.65 (t, J = 5.2 Hz, 1H), 6.08 (q, J = 6.6 Hz, 1H), 5.63 (s, 2H), 4.12 – 4.02 (m, 1H), 3.05 (dd, J = 12.5, 6.3 Hz, 2H), 2.93 (d, J = 11.5 Hz, 2H), 2.35 (t, J = 7.1 Hz, 3H), 2.12 (s, 1H), 2.07 (s, 1H), 2.01 – 1.84 (m, 5H), 1.80 (d, J = 6.6 Hz, 3H), 1.38 (s, 10H) ppm. ES-MS (ESI) *m/z* (%): 615.1987 (100) $(M + Na)^{+}$.

3.3.4.2 Synthesis of (R)-5-(1-(1-(2-aminoethyl)piperidin-4-yl)-1H-pyrazol-4-yl)-3-(1-(2,6-dichloro-3-fluorophenyl)ethoxy)pyridin-2-amine (2). A solution of 6M hydrochloric acid in methanol was added to compound **1** on ice bath and the mixture stirred for 5 h. The reaction mixture was concentrated under reduced pressure and dried under pump overnight to yield the product **2** which was used directly without further purification for the next step (Scheme 1). ^{1}H NMR (DMSO-d_6, 400 MHz, 298 K) δ 7.94 (s, 1H), 7.75 (d, J = 1.8 Hz, 1H), 7.57 (dd, J = 8.9, 5.0 Hz, 1H), 7.52 (s, 1H), 7.44 (t, J = 8.7 Hz, 1H), 6.89 (d, J = 1.7 Hz, 1H), 6.08 (q, J = 7.0 Hz, 1H), 5.64 (s, 2H), 4.17 – 3.99 (m, 2H), 2.92 (d, J = 12.2 Hz, 2H), 2.72 – 2.64 (m, 2H), 2.36 (t, J = 6.6 Hz, 2H), 2.16 – 2.03 (m, 3H), 2.02 – 1.88 (m, 5H), 1.80 (d, J = 6.6 Hz, 3H) ppm. ES-MS (ESI) *m/z* (%): 515.16 (100) $(M + Na)^+$.

3.3.4.3 Synthesis of compound (R)-N-(2-(4-(4-(6-amino-5-(1-(2,6-dichloro-3-fluorophenyl)ethoxy)pyridin-3-yl)-1H-pyrazol-1-yl)piperidin-1-yl)ethyl)-4-azidobutanamide (3). Compound **2** was dissolved in DMF and stirred with 4-azidobutanoic acid dissolved in DMF with hydroxybenzotriazole (HOBt), 4-dimethylaminopyridine (DMAP), and 1-Ethyl-3-(3-dimethylaminopropyl)carbodiimide (EDCI). After reaction completion, solvent was evaporated and product **3** which was collected with preparative TLC (Scheme 1). ^{1}H NMR (DMSO-d_6, 400 MHz, 298 K) δ 7.93 (s, 1H), 7.80 (t, J = 5.4 Hz, 1H), 7.75 (d, J = 1.7 Hz, 1H), 7.57 (dd, J = 9.0, 5.0 Hz, 1H), 7.52 (s, 1H), 7.44 (t, J = 8.7 Hz, 1H), 6.89 (d, J = 1.7 Hz, 1H), 6.08 (q, J = 6.7 Hz, 1H), 5.64 (s, 2H), 4.13 – 4.02 (m, 1H), 3.21 – 3.14 (m, 3H), 2.94 (d, J = 11.5 Hz, 2H), 2.38 (t, J = 6.8 Hz, 2H), 2.19 – 2.12 (m, 3H), 2.10 (dd, J = 9.7, 7.7 Hz, 3H), 2.02 – 1.84 (m,

5H), 1.79 (t, J = 5.0 Hz, 3H), 1.72 (dt, J = 21.9, 7.1 Hz, 4H) ppm. ES-MS (ESI) *m/z* (%): 604.19 (100) $(M + H)^+$.

3.3.4.4 Synthesis of the chemoprobe (AB19). Solution of the azide product **3** in DMF was added to Biotin-PEG5-BCN (a gift from Dr Alain Wagner, University of Strasbourg) in DMF. The reaction was stirred at 90°C on an oil bath and monitored over 3-4 days with MS and TLC. Upon reaction completion, solvent was evaporated and the residual compound was recovered and purified on preparative TLC to yield the chemoprobe **AB19** (Scheme 1). ^{1}H NMR (MeOH,d_4, 400 MHz, 298 K) δ 7.82 – 7.77 (m, 1H), 7.70 – 7.66 (m, 1H), 7.57 – 7.51 (m, 1H), 7.46 (ddd, J = 5.9, 4.9, 0.4 Hz, 1H), 7.28 – 7.20 (m, 1H), 6.97 – 6.89 (m, 1H), 6.25 – 6.12 (m, 1H), 4.52 – 4.45 (m, 1H), 4.39 – 4.33 (m, 2H), 4.32 – 4.26 (m, 1H), 4.15 (dd, J = 6.8, 0.5 Hz, 3H), 3.63 – 3.56 (m, 8H), 3.56 – 3.50 (m, 5H), 3.49 – 3.46 (m, 1H), 3.35 (t, J = 3.0 Hz, 17H), 3.26 (dd, J = 11.7, 6.2 Hz, 4H), 3.24 – 3.16 (m, 2H), 3.15 – 3.12 (m, 2H), 3.12 – 3.00 (m, 5H), 2.95 – 2.88 (m, 1H), 2.88 – 2.73 (m, 3H), 2.74 – 2.67 (m, 1H), 2.54 (td, J = 6.7, 0.5 Hz, 3H), 2.29 – 2.18 (m, 9H), 2.17 – 1.98 (m, 9H), 1.91 – 1.86 (m, 4H), 1.73 – 1.54 (m, 9H), 1.48 – 1.40 (m, 3H), 1.30 (s, 5H), 1.33 – 1.26 (m, 14H) ppm. ES-MS (ESI) *m/z* (%): 655.77 (100) $(2M + Na)^+$.

3.3.5 Affinity pull-down of MET-targeted chemoprobe AB19

Magnetic beads (Pierce streptavidin magnetic beads) were washed twice with a washing buffer on a magnetic stand. Concentrations of 2.5 μM of AB19 and AB22 were added to washed beads and incubated for 2 h at RT on a shaker. Beads were collected and washed with a Hepes acetate washing buffer twice. Cell cultures harvested with a trypsin–EDTA solution and lysed with HEPES-acetate buffer supplemented with 1mM PMSF. For cell treatment, adherent cells were treated with 10 μM

paclitaxel for 2 and 24 h and control samples treated with drug-free medium. Cell cultures harvested similarly, and protein concentration adjusted to 1.5-2 mg/ml and lysate used freshly. Functionalized beads were incubated with lysate at 5° C for 2 h. Beads were washed three times with a washing buffer, and bound proteins were digested on-beads overnight with MS-grade trypsin (Promega), beads were washed with MS-grade acetonitrile and peptides fractions collected and for LC-MS/MS analysis.

3.3.6 Mass spectrometry (LC-MS/MS)

For LC-MS analysis, a Q Exactive HF (Thermo Scientific) mass spectrometer was coupled on-line to an EASY-nLC 1000 HPLC system (Thermo Scientific). Rehydrated tryptic peptide fragments were separated on a 25 cm C18 column (Acclaim 75 μm inner diameter, 2 μm particles, Thermo Scientific) fitted upstream with a 2cm trapping column (Acclaim PepMap 100, Thermo Scientific) in a 100 min gradient from 3% to 38% in buffer B (99.9% acetonitrile, 0.1% formic acid) at 350 nL/min, for a total run time of 120 minutes. Mass spectra were acquired in data-dependent mode. Briefly, each survey scan (range 375 to 1,400 m/z, resolution of 120,000 at m/z 200, maximum injection time 60 ms, AGC target of 5E6) was followed by high-energy collisional dissociation based fragmentation (HCD) of the 25 most abundant isotope patterns with a charge ≥ 2 (normalized collision energy of 25, an isolation window of 2.5 m/z, resolution of 15,000, maximum injection time 60 ms, AGC target value of 2E5). Dynamic exclusion of sequenced peptides was set to 3.5 s. All data were acquired using Xcalibur software (Thermo Scientific).

3.3.7 Data analysis of proteomic raw files

The acquired MS raw files were processed with the Mascot Distiller (version 2.5.1.0, Matrix Sciences). The Mascot search engine (Matrix Sciences, version 2.5) was used for peptide and protein identification at a Mascot p-value of less then 0.05. The human UniProtKB database (August 2017) was used as database. Trypsin was set as the enzyme specificity. And data were searched with a precursor ion mass accuracy of 6 ppm, MSMS mass accuracy was set to 50 mDa. Oxidized methionine was allowed as a variable modification. Search data were imported to Scaffold for additional data validation (FDR < 5%). Comparative Label-free relative protein quantification was performed using the validated data spectral counts per protein across samples. Statistical significance for changes between 2 and 24h or control and treated samples for each captured protein (e.g. AURKA, mTOR, and RON) was determined using two-tailed unpaired t-test.

3.4 RESULTS

3.4.1 Design and Synthesis of the chemoprobes

The synthesis of MET-targeting probe **AB19** proceeded according to Scheme 1. Briefly, commercially available crizotinib was treated with tert-butyl(2-bromoethyl)carbamate to give **1**. The BOC protecting group of **1** was removed under acidic conditions to give aminoethylpiperidine **2**. Coupling of **2** with azidobutylcarboxylic acid led to azide **3**. The biotinylated probe (AB19) was obtained as in Scheme 1, using a click reaction between **3** and biotin-PEG5-BCN to give a glassy solid mixture, which was purified on a preparative TLC plate. The structure of the pure **AB19** was confirmed by ^{1}H NMR and mass spectrometry. The synthesis of the AB22 was described in chapter 2.

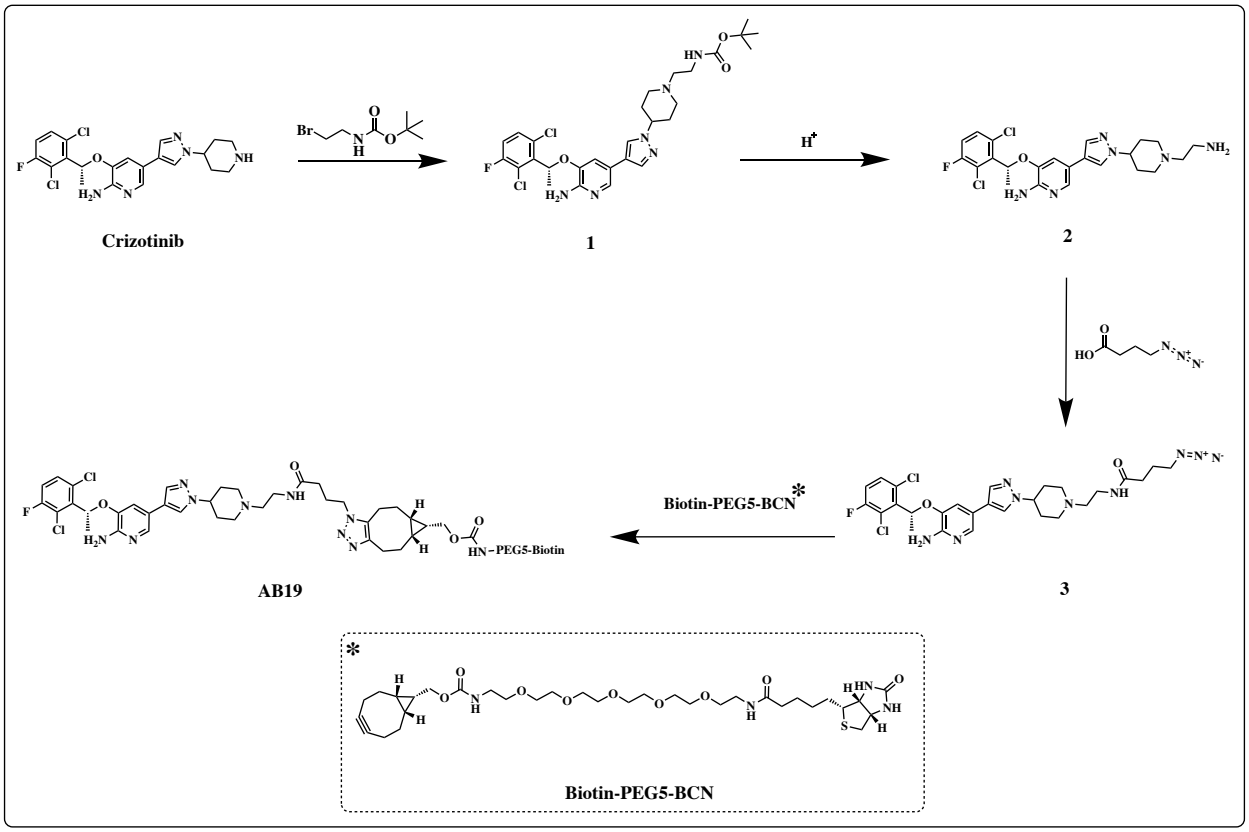

Scheme 3.1 Synthesis of the crizotinib-based probe (AB19)

AB19 was designed with a moiety that that straddled the structure of crizotinib and a lengthy linker that ends with a biotin tag (Figure 3.1). Molecular modelling of AB19 based upon crizotinib MET receptor co-crystallized structure available on the protein database (PDB code 2WGJ), showed that the crizotinib backbone occupies the ATP binding site of MET with the rest of the molecule localized in the solvent exposed area of the receptor and beyond (Figure 3.2a-b). This allows us to predict that AB19 could bind to and pull-down its canonical target MET.

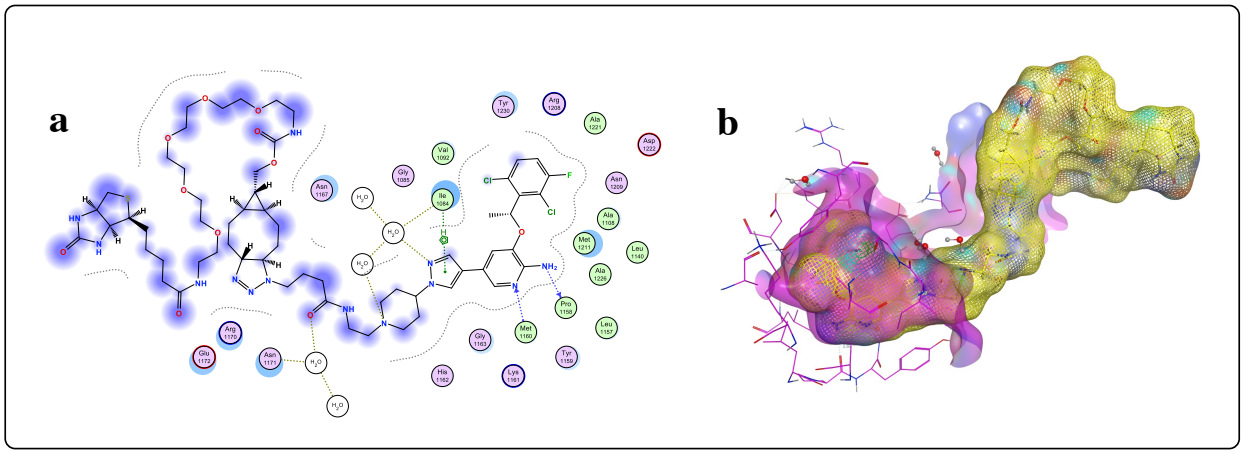

Figure 3.2 (a) Binding interaction of AB19 warhead into ATP pocket of MET kinase **b)** Surface binding of AB19 into the ATP binding pocket of MET

3.4.2 Pull-down proteomics

3.4.2.1 Proof of Principle

To test the ability of AB19 to pull-down MET or related targets, we first chose to perform an experiment with a lysate of a cell line in which MET is amplified. Since MET is being evaluated as a target for gastric cancer, the KATO-II cell line was chosen to perform our experiment. Indeed, the results showed that from the cell lysate, MET was the most abundant protein pulled down from the analysis, using streptavidin bound beads (Table 3.1). Importantly, as predicted, in addition to abundantly pulling down MET, other kinases appeared in the proteomics analysis, including, LCK, SRC, EPHA2, FAK1, AURKA, , and SLK. The ten kinases pulled down from the KATO-II cell line figured in a publicly available profile for crizotinib (18), further confirming the ability of AB19 to pull down targets associated with a crizotinib-like binding structure. The fact that the kinase pulldown profiles obtained with the probe AB19 overlap with the kinase profiles of free crizotinib suggests that AB19 can be considered an “immobilized” mimic of crizotinib.

3.4.2.2 Drug Response Proteomics

While many chemical proteomics studies use the affinity probe approach to define the kinase profiling of the probe warhead, our study sought to identify these profiles in systems perturbed by drug treatment. Here we planned to study the type of kinase profiling that could emerge following paclitaxel treatment As mentioned earlier, mechanism of action is based on binding to microtubules and arresting tumour cells in the mitotic (M) phase. Therefore, in order to determine whether drug treatment can lead to the appearance or loss of new targets, the cells were treated for 2 h and immediately probed with AB19, or for 24 h before probing. As shown in Figure 3.3, when the cells were treated with paclitaxel for 24 h, there was no apparent growth inhibition over the whole dose range. However, a dose dependent arrest in M was observed in all the cell lines (Figure 3.4).

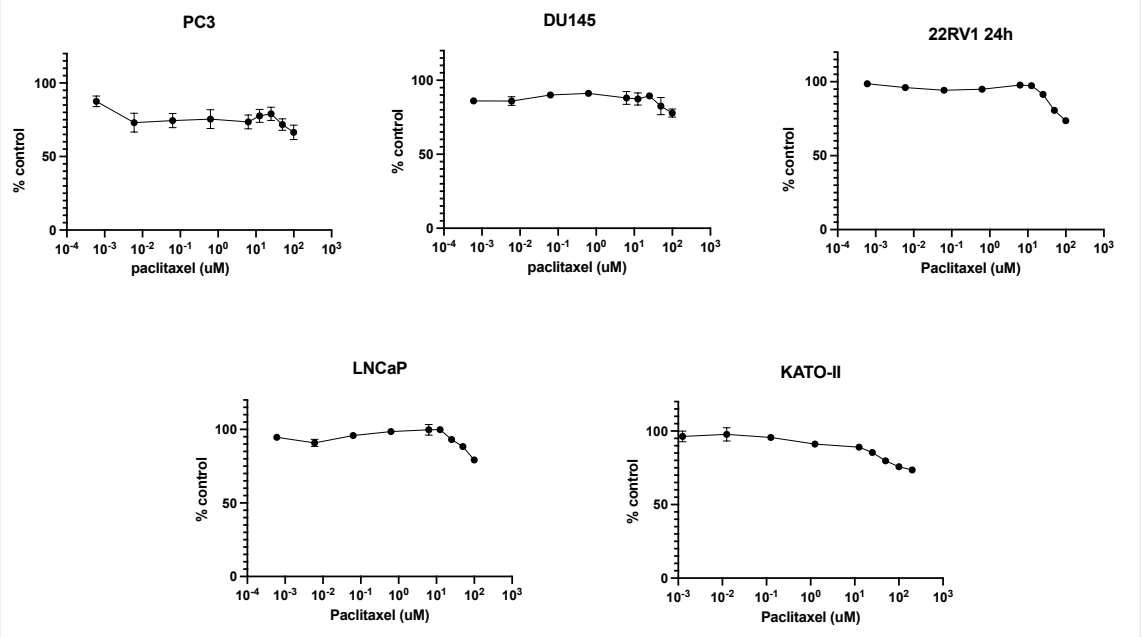

Figure 3.3 Growth inhibition of paclitaxel against gastric carcinoma and a panel of prostate cancer cells at 10 μM for 24 h.

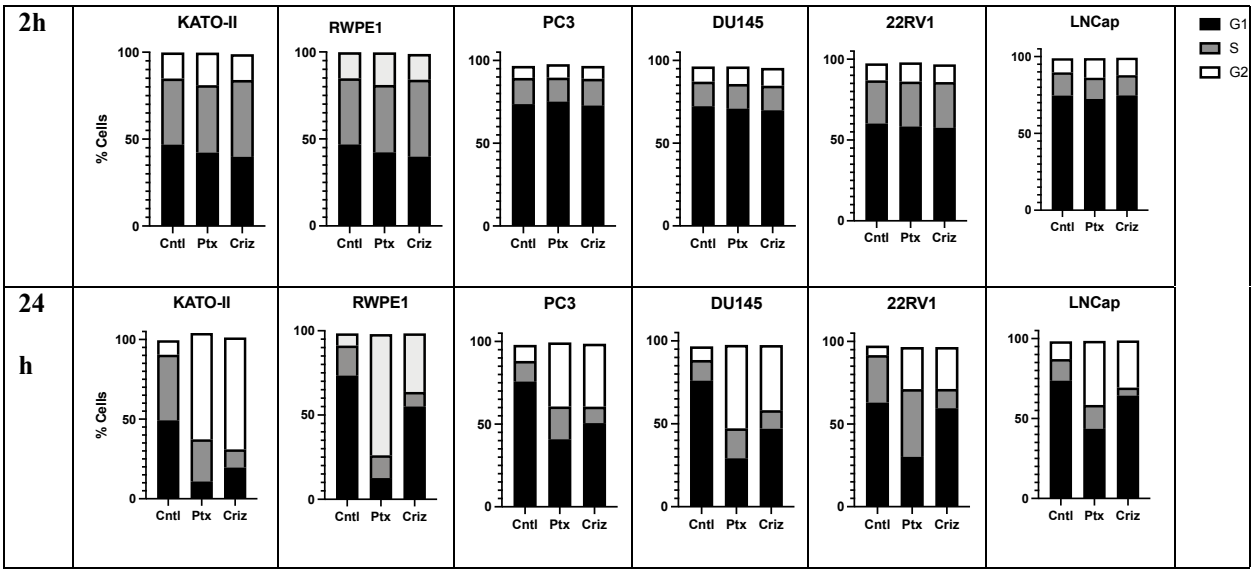

Figure 3.4 Cell cycle analysis of gastric and prostate cell lines following 2 and 24 h exposure to the cytotoxic drug (paclitaxel)

In addition to MET, the probe was able to pull-down a discrete number of kinases, with no distinct pattern between the cell lines. The pulled down proteins could be classified into cell surface receptors of the RTK class (e.g. EPHA2, RON, etc.) and cell cycle proteins (e.g. AURKA, AURKB, CDK, etc.). Importantly, the pulled down AURKA is involved in microtubules formation and cell cycle progression (18, 19), which are mechanisms related to those of paclitaxel. These results suggest that at basal levels, the chemoprobe can capture relevant anti-tumour targets. A large proportion of kinases captured by the probe in the cell lines corresponded to those previously reported in the kinase profile of crizotinib. As depicted in Table 3.1, many kinases are common to the overall captured profile of the cell lines and kinase profiles reported in the literature.

Protein	KATO-II	PC3	DU145	22RV1	LNCaP	RWPE1*
MET	+	+	+			+
EPHA2	+	+	+			+
LCK	+					
SRC	+					
MLKL	+					
FAK1	+	+	+	+	+	
AURKA	+	+	+		+	+
AURKB	+	+	+	+		
CDK1			+			
SLK	+					+
RIPK2	+	+		+		
TBK1			+			
RON		+	+			+
KAD1						+
UFO		+	+			+
IRAK3			+			
LBR			+			
M4K5		+	+			+
GSK3A		+	+			+
NOL9			+			
IRAK1				+		
ABL2		+				
M4K3		+				
TYK2		+	+			
NDKA				+		
PDXK						+
NAGK						+
YES				+		
PAK2						+
STK10						+
* n=1						

Table 3.1 List of pull-down kinases captured by AB19

Interestingly, conditions where cells were exposed to paclitaxel for 2 h and analyzed after 24 h did not show a significant number of new pulled down proteins. Changes appeared in the abundance of these proteins. As an example, Nuclear Casein Kinase (Nucks), where the protein abundance was doubled in the 24 h treatment (data not shown).

Treatment of cells with paclitaxel for 2 and 24 h revealed a significant cell cycle arrest in the M phase, indicating that crizotinib is added to a cell population synchronized in G2M (Figure 3.4). Therefore, it is expected that the kinase distribution profile of treated cells will be different from non-treated ones. Surprisingly, the pull-down pattern of untreated cells showed pull-down profiles similar to treated cells with minor differences in the nature of protein pull-down as shown in Table 3.2 Variations were seen in the total counts of this protein with e.g. MET and EPHA2 decreasing by 31-fold and 17-fold, respectively. Likewise, comparison between probing 2 h after treatment versus 24 h, showed changes in abundance of proteins but not in the nature of the pulled down proteins. Remarkably, a surge of AURKA and mTOR was seen in the DU145 and PC3 prostate cancer cell lines. Overall, statistical significance was primarily seen in the changes of AURKA from 2 to 24h (DU145, $p=0.0337$), and between control and treatment after 24h exposure to paclitaxel (DU145, $p=0.0064$). Statical significance was also seen with changes in the number of counts for RON (DU145, $p=0.0257$) between control and treatment after 24h exposure to paclitaxel. These observed changes inspired the design of the following combinations: a) paclitaxel + crizotinib, since the probe mimics crizotinib binding profile, b) paclitaxel + alisertib (AURKA inhibitor), and c) paclitaxel and torkinib (mTOR inhibitor).

Protein	Fold Change C24 > T24			Protein	Fold Change T2 > T24		
	KATO-II	PC3	DU145		KATO-II	PC3	DU145
MET	▼ 31	▼ 8.3	▼ 3.6	MET	▼	▼	▲ 1.8
AURKA	–	–	▲ 19	AURKA	▼	▲ 1.9	▲ 14.3
AURKB	–	▲ 1.7	▲ 1.6	AURKB	–	–	–
RIPK2	–	–	▲ 2	RIPK2	–	–	▲ 6
FAK1	–	–	▲ 1.4	FAK1	▼	–	▲ 2
EPHA2	▼ 17	▼ 1.6	–	EPHA2	▼	▲ 1.6	–
LCK	–			LCK	▼		
SRC	–			SLK	▼		
SLK	–			SRC	▼		
MLKL	–			MLKL	▼		
ABL2		–		ABL2		–	
M4K3		–		M4K3		–	
TBK1			▲1.8	TBK1			▲ 14
NOL9			–	NOL9			–
CDK1				CDK1			–
IRAK3			–	IRAK3			▲ 7
mTOR		▼ 31	▲ 1.2	mTOR			▲ 19
RON		–	▲ 19	RON		▼ 3.3	–
M4K5		▼ 2	▲ 1.2	M4K5		▼	
AXL (UFO)		▼ 5	▼ 3	AXL (UFO)		–	–
GSK3A		–	–	GSK3A		–	–
TYK2		–	–	TYK2		–	▲ 3
MERTK			–	MERTK			–

Table 3.2 Kinases captured by AB19 from gastric and prostate cancer cell lysates and changes appeared in their levels from 24 h untreated (left) and treated (right).

▲ increased score
▼ decreased score
– no change

3.4.3 Paclitaxel-kinase inhibitor combinations

Based upon on the results obtained from the pull-down analysis, we designed two schedules of administrations: one in which the drugs were concomitantly exposed to paclitaxel and the kinase inhibitor, and one in which the cells were pre-exposed to paclitaxel and one in which the kinase inhibitor, and one in which the cells were pre-exposed to paclitaxel followed by addition of the kinase inhibitors to block the targets induced by paclitaxel treatment. Combination indices (CI) were calculated using median effect plots as described by Chou and Talalay (20). The results

showed that paclitaxel alone was extremely potent in all the cell lines (IC_{50}, nM). Sequential administration that better reflects the probing schedules, showed paclitaxel effects to dominate the IC_{50}, with no apparent synergy, no additivity (data not shown).Concomitant administration led to synergy in some cases (e.g. mTOR or AURKA inhibitors), with the combinations of paclitaxel + the AURKA inhibitor alisertib being the most efficacious. It was found synergistic in a broad range of % effects/doses in the three prostate cancer cell lines studied (Figure 3.5).

3.5 DISCUSSION

The discovery of kinase inhibitors or/and their mode of action has marked the beginning of personalized medicine in cancer. Identification of patients expressing sensitive (EGFR) mutant, and specific biomarkers (ALK) for indicating drugs like gefitinib or crizotinib has provided significant clinical benefits. However, the duration of responses are short and patients progress to a more aggressive phenotype of the disease. In these advanced stages, potent chemotherapeutic drugs are used as therapeutic option. While targeted kinases at early phases of the disease remain the common dogma, it is important to know that in these advanced stages, they continue to play an important role in disease progression and drug sensitivity. Signaling redundancy and compensatory signaling in the advanced stages of the disease compromise apoptotic pathways and reduce sensitivity to cytotoxic therapy. Various pathways associated with stress response activate kinases that further deplete response to chemotherapeutic drugs.

Exposure of tumours to paclitaxel has been shown to activate oxidative stress (21), which in turn lead to further activation of various signaling pathways involving kinases (22). In this study, we surmised that a strategy designed to identify and block these kinases could lead to significant potentiating of cytotoxic therapy. Here we adopted a chemical proteomics approach to define the

kinase binding profiles in tumour cells before and after treatment with a cytotoxic drug. AB19, which was designed to carry the MET/ALK inhibitor (crizotinib), was successfully synthesized Its ability to pull down its primary target MET validated its kinase pull-down potential, and this was further exploited to detect other binding partners for ultimately reading a broad spectrum of kinases in cells. Indeed, in KATO-II cells, AB19 was able to pull down or read 30 kinases, many of them being actionable kinases, which as outlined in Table 3.1 can be involved in compensatory signaling and others in DNA repair. Importantly, in addition to exhibiting a strong capability to read a diverse array of kinases, the data produced by AB19 pull-down can give an insight into the scope of intracellular targets in which crizotinib can bind to as a free drug. Perhaps, its mechanism of action may not be solely based on interaction with MET, but also with other receptors responsible for activating adverse compensatory signaling. Importantly, the kinase footprint generated by AB19 appeared to vary from cell line to cell line, with very few kinases being common to the pull-down, indicating that the pull-down pattern could serve as a signature representing these cells.

Having demonstrated that AB19 could be used to define discrete kinase binding profiles, we subsequently tested its ability to distinguish between non treated and treated cells following exposure to paclitaxel, an extremely potent cytotoxic drug. Interestingly, little change was seen between the pull-down patterns of non-treated control cells and treated. The most noticeable change of all treatments appeared with inhibitors of AURKA kinase and mTOR, which were the only kinases that could appear from probing after treatment. The kinase changes observed seem to derive from cell cycle perturbation induced by paclitaxel. At the paclitaxel doses of the pull-down, significant cell cycle arrest in M phase was observed. Importantly, AURKA and B kinases are proteins expressed during M phase of the cell cycle. This could explain the observed increase in

their counts in the pull-down following drug treatment (23). Both AURKA and B, the receptor serine/threonine kinases, are key regulator for cells progression and mitosis, and found to be amplified and overexpressed in various cancers including leukemia (23). In particular, AURKA promotes the G2M transition through centrosome maturation as well as mitotic spindle processes, thereby promoting cell survival (24). There are a few ongoing preclinical studies to test some AURKA small molecules inhibitors, as well as some clinical trials to test AURKA inhibitors as monotherapies or in combination with other classical chemotherapeutic agents (24, 25).

Furthermore, induction of kinases in the mTOR axis may originate from stress responses associated with drug treatment. Likewise, the apparent increase of RON could emerge from the stress pathway or through compensatory signaling. The modulation of these four kinases indicates that their activation perhaps play a role in the response to paclitaxel. Thus, we surmised that their blockade could lead to sensitization to paclitaxel. Accordingly, we designed combination experiments to verify this hypothesis. Interestingly, modulation of some of the kinases captured by the probe led to sensitization to paclitaxel or to antagonistic effect. The probe being a mimic of crizotinib, we expected that when actionable kinases pulled down by the probe were blocked, a synergistic effect would be observed with paclitaxel. Thus, the first combination to be tested was crizotinib + paclitaxel as at increasing doses, we expected crizotinib to block AURKA, RON, UFO etc., which are part of its kinase pull-down profiles. Unfortunately, in three of the four cell lines tested, the combination of paclitaxel + crizotinib was antagonistic. However, in KATO-II that presents a uniquely broad kinase profile, the combination was synergistic at low doses. Given that mTOR and AURKA are known targets for chemotherapeutic intervention against refractory tumours, we thought it of interest to design combinations where these two targets are directly

blocked with their known inhibitors torkinib and alisertib, respectively. Crizotinib + paclitaxel and paclitaxel + torkinib combinations were additive or antagonistic in the three prostate cell lines. Strikingly, more synergistic effects were observed between the AURKA inhibitor alisertib and paclitaxel. While the reason for the antagonistic effect between crizotinib and paclitaxel was unclear, we believe that its synergistic effect on KATO-II may be due to the ability of crizotinib to block a larger number of actionable kinases activated by the paclitaxel treatment in the latter cell line. Given that mTOR plays significant role in cell survival, its antagonistic effect in combination with paclitaxel was unexpected. This may probably be due to the fact that the activity in the combination was largely dominated by cytotoxic mechanisms that are independent of mTOR. Importantly, alisertib appears to be the only drug to significantly add to the potency of paclitaxel. This can be explained by the unique role of AURKA in regulating microtubule formation and cell cycle progression. Accordingly, its inhibition in addition to the blockade of tubulin depolymerization by paclitaxel, may synergize to induce apoptosis in these cells. Interestingly, our observation was validated by the recent and successful clinical trial involving the combination of AURKA + paclitaxel against ovarian and breast cancers (Figure 3.5) (26-28)

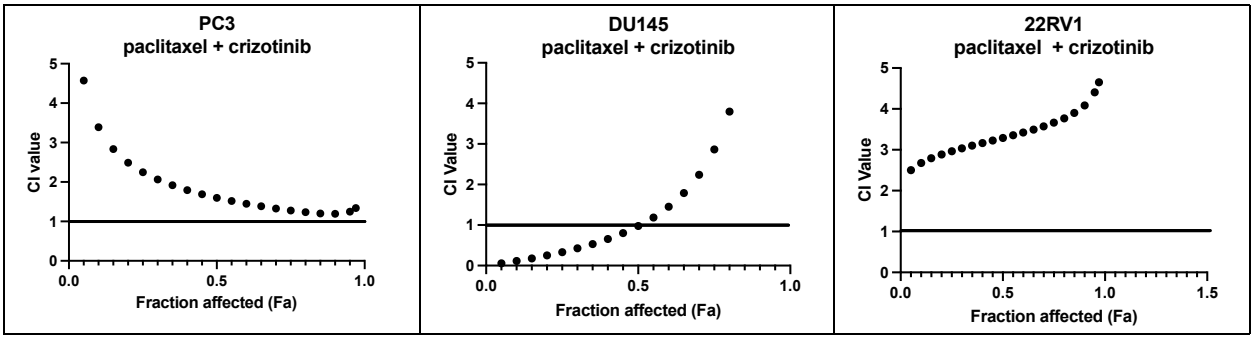

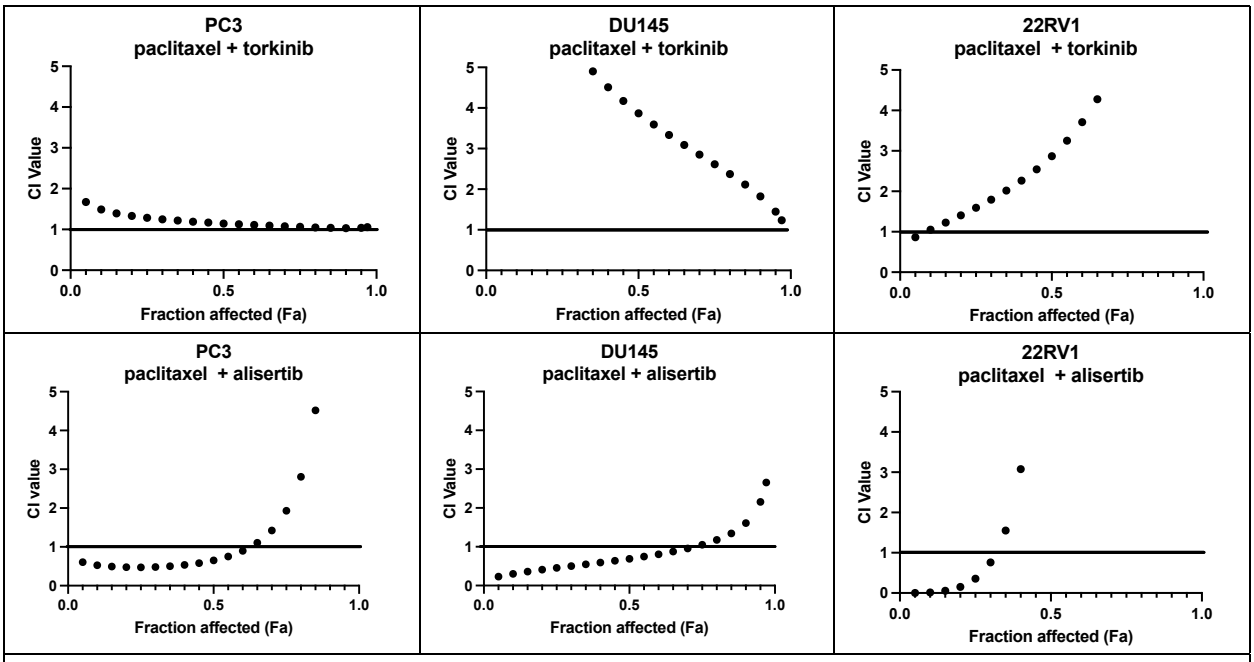

Figure 3.4 Chemical proteomics-based combination of kinase inhibitors with paclitaxel in human prostate cancer cells. CI and Fa values were calculated with Compusyn and graphs plotted with GraphPad Prism. CI values > 1 indicate antagonism, CI =1 additivity, and CI < 1 synergy. The formula used for determining the CI is: CI = (D)1 /(Dχ)1 + (D)2/(Dχ)2. (Dχ)1 and (Dχ)2 are concentrations of each drug alone, (D)1 and (D)2 are concentrations of drugs in combination.

3.6 REFERENCES

1. Salgia R. Role of c-MET in cancer: emphasis on lung cancer. Semin Oncol. 2009;36(2 Suppl 1):S52-S8.

2. Varkaris A, Corn PG, Gaur S, Dayyani F, Logothetis CJ, Gallick GE. The role of HGF/c-MET signaling in prostate cancer progression and c-MET inhibitors in clinical trials. Expert opinion on investigational drugs. 2011;20(12):1677-84.

3. Anestis A, Zoi I, Karamouzis MV. Current advances of targeting HGF/c-MET pathway in gastric cancer. Ann Transl Med. 2018;6(12):247-.

4. da Cunha Santos G, Shepherd FA, Tsao MS. EGFR mutations and lung cancer. Annu Rev Pathol. 2011;6:49-69.

5. Nastały P, Stoupiec S, Popęda M, Smentoch J, Schlomm T, Morrissey C, et al. EGFR as a stable marker of prostate cancer dissemination to bones. British Journal of Cancer. 2020;123(12):1767-74.

6. Arienti C, Pignatta S, Tesei A. Epidermal Growth Factor Receptor Family and its Role in Gastric Cancer. Frontiers in oncology. 2019;9:1308-.

7. Krishnamurty R, Maly DJ. Biochemical mechanisms of resistance to small-molecule protein kinase inhibitors. ACS chemical biology. 2010;5(1):121-38.

8. Barrón F, Zatarain-Barrón ZL, Cardona AF, Arrieta O. Extending the curve: survival of EGFR-mutated lung cancer patients in the 21(st) century. J Thorac Dis. 2018;10(3):1265-8.

9. Ramalingam S, Belani CP. Paclitaxel for non-small cell lung cancer. Expert Opin Pharmacother. 2004;5(8):1771-80.

10. Kelly WK, Curley T, Slovin S, Heller G, McCaffrey J, Bajorin D, et al. Paclitaxel, estramustine phosphate, and carboplatin in patients with advanced prostate cancer. Journal of clinical oncology. 2001;19(1):44-53.

11. Shimoyama R, Yasui H, Boku N, Onozawa Y, Hironaka S, Fukutomi A, et al. Weekly paclitaxel for heavily treated advanced or recurrent gastric cancer refractory to fluorouracil, irinotecan, and cisplatin. Gastric Cancer. 2009;12(4):206-11.

12. Weaver BA. How Taxol/paclitaxel kills cancer cells. Mol Biol Cell. 2014;25(18):2677-81.

13. Maloney SM, Hoover CA, Morejon-Lasso LV, Prosperi JR. Mechanisms of taxane resistance. Cancers. 2020;12(11):3323.

14. Wang Y, Ma H. Protein kinase profiling assays: a technology review. Drug Discovery Today: Technologies. 2015;18:1-8.

15. Brehmer D, Greff Z, Godl K, Blencke S, Kurtenbach A, Weber M, et al. Cellular Targets of Gefitinib. Cancer Research. 2005;65(2):379.

16. Shi H, Zhang CJ, Chen GY, Yao SQ. Cell-based proteome profiling of potential dasatinib targets by use of affinity-based probes. J Am Chem Soc. 2012;134(6):3001-14.

17. Skehan P, Storeng R, Scudiero D, Monks A, McMahon J, Vistica D, et al. New colorimetric cytotoxicity assay for anticancer-drug screening. J Natl Cancer Inst. 1990;82(13):1107-12.

18. Rouillard AD, Gundersen GW, Fernandez NF, Wang Z, Monteiro CD, McDermott MG, et al. The harmonizome: a collection of processed datasets gathered to serve and mine knowledge about genes and proteins. Database. 2016;2016.

19. Nikonova AS, Astsaturov I, Serebriiskii IG, Dunbrack RL, Jr., Golemis EA. Aurora A kinase (AURKA) in normal and pathological cell division. Cell Mol Life Sci. 2013;70(4):661-87.

20. Chou TC. Drug combination studies and their synergy quantification using the Chou-Talalay method. Cancer Res. 2010;70(2):440-6.

21. Duggett NA, Griffiths LA, McKenna OE, de Santis V, Yongsanguanchai N, Mokori EB, et al. Oxidative stress in the development, maintenance and resolution of paclitaxel-induced painful neuropathy. Neuroscience. 2016;333:13-26.

22. Reuter S, Gupta SC, Chaturvedi MM, Aggarwal BB. Oxidative stress, inflammation, and cancer: how are they linked? Free Radic Biol Med. 2010;49(11):1603-16.

23. Goldenson B, Crispino JD. The aurora kinases in cell cycle and leukemia. Oncogene. 2015;34(5):537-45.

24. Willems E, Dedobbeleer M, Digregorio M, Lombard A, Lumapat PN, Rogister B. The functional diversity of Aurora kinases: a comprehensive review. Cell Division. 2018;13(1):7.

25. Du R, Huang C, Liu K, Li X, Dong Z. Targeting AURKA in Cancer: molecular mechanisms and opportunities for Cancer therapy. Molecular Cancer. 2021;20(1):15.

26. O'Shaughnessy J, McIntyre K, Wilks S, Ma L, Block M, Andorsky D, et al. Efficacy and Safety of Weekly Paclitaxel With or Without Oral Alisertib in Patients With Metastatic Breast Cancer: A Randomized Clinical Trial. JAMA Network Open. 2021;4(4):e214103-e.

27. Falchook G, Coleman RL, Roszak A, Behbakht K, Matulonis U, Ray-Coquard I, et al. Alisertib in Combination With Weekly Paclitaxel in Patients With Advanced Breast Cancer or Recurrent Ovarian Cancer: A Randomized Clinical Trial. JAMA Oncology. 2019;5(1):e183773-e.

28. Owonikoko TK, Niu H, Nackaerts K, Csoszi T, Ostoros G, Mark Z, et al. Randomized Phase II Study of Paclitaxel plus Alisertib versus Paclitaxel plus Placebo as Second-Line Therapy for SCLC: Primary and Correlative Biomarker Analyses. J Thorac Oncol. 2020;15(2):274-87.

4. CONNECTING TEXT

In chapters 2 and 3, we demonstrated the feasibility of chemoprobes containing a kinase inhibitor warhead and a biotin tag that could be used to pull down proteins (e.g. kinases) for which the probe has affinity. The studies were performed in cell lysate milieu in which organelles are disrupted to release their contents. Due to their size, these probes cannot be used to image cellular contents without fixation. Thus, we synthesized keeping the same kinase targeting scaffold new fluorescent chemoprobes to visualize the localization of these kinase inhibitors. The molecules were designed to be small in order to facilitate cell penetration. In chapter 4, we described the synthesis of AB20 targeted to MET, AB63 and AB64 to block EGFR, and analyzed their cellular distribution by confocal microscopy. Thus, in chapter 4, we report on the live imaging using kinase targeted probes of multiple colors, green and red.

CHAPTER 4

SYNTHESIS OF NOVEL EPIDERMAL GROWTH FACTOR RECEPTOR (EGFR) AND HEPATOCYTE GROWTH FACTOR RECEPTOR MET TARGETED INHIBITORS RATIONALLY DESIGNED TO CARRY A GREEN OR RED FLUORESCENT LABELS

Alaa Baryyan, Caterina Facchin, and Bertrand Jean-Claude

Cancer Drug Research Laboratory, Department of Medicine, The Research Institute of The McGill University Health Centre, 1001 Decarie Boulevard, Montreal, Quebec, H3A 3J1, Canada

4.1 ABSTRACT

Over the past decade, the epidermal growth factor receptor (EGFR) inhibitors of the quinazoline class have emerged as potent agents in the personalized therapy of lung cancer. Importantly, it is becoming increasingly clear that in cancer cells, the EGFR is not only localized in the membrane but also in the intracellular compartments. Despite the evidence of EGFR localization in multiple compartments inside the cells, little attention is paid to the intracellular distribution of its inhibitors. Interest was more in the kinase profiling of these inhibitors that reveal their ability to bind to multiple kinases. Here we hypothesized that in addition to the target multiplicity of these inhibitors, their primary localization could perhaps influence their biological activities. We also surmised that this could be determined by live imaging of their subcellular distribution, which reflects their macromolecular binding profile. Thus, we designed quinazoline-based molecules to carry a red fluorescence (AB63 and AB64) and studied their distribution in A549 lung cancer cells and A549-GFP-EGFR engineered to endogenously express full length green fluorescent protein (GFP) EGFR. The results showed that the two probes were preferentially distributed in the perinuclear region but not in the membrane where these receptors are activated by their cognate ligands. Furthermore, the hepatocyte growth factor receptor MET expression being associated to resistance to EGFR inhibitors, we also designed a molecule (AB20) in which crizotinib, one of its most potent inhibitors, was labeled with nitrobenzoxadiazole (NBD). Like the EGFR inhibitor, the latter probe was also found localized in the perinuclear region.

4.2 INTRODUCTION

The past twenty years have seen a significant shift of drug discovery from the design of DNA-directed molecules or direct blockade of metabolic enzymes to the targeting of kinases that play specific roles in growth signaling and anti-apoptotic signaling (1-3). Indeed, following the successful development of Gleevec, a kinase inhibitor that targets Bcr-Abl, against CML and gastric cancer (4, 5), a succession of potent kinase inhibitors have received FDA approval for the treatment of many cancers over the past twenty years. These include EGFR and ALK inhibitors for the treatment of lung, pancreas, breast, and other cancers (6-9). However, despite this significant progress, drug resistance to this clinically approved inhibitors often emerge as a major setback (10). Recent strategies to increase the effectiveness of these drugs led to the emergence of a new field termed "personalized medicine" that utilizes pharmacogenomics data to select patients with the greatest probability to benefit from targeted therapy (11). However, as in the case of lung cancer for which patients with specific mutations (e.g. EGFR exon 19 and L858R) were found to be responsive to EGFR inhibitors, durations of survival still remain short (within 1-3 years) (12, 13). One of the reasons put forth to explain these results is the emergence of mutants (e.g. T790M) or expression of receptors (e.g. MET) that mediate redundant signaling. As an example, co-expression of MET with EGFR leads to resistance to their corresponding inhibitors, due to the fact that they both activate the MAPK pathway (14). The complexity of compensatory signaling in these cells has led to a new trend in drug design termed "polypharmacology", that seeks to design drugs capable of blocking multiple targets. While the kinase binding profiles have proven the ability of these drugs to block multiple targets and related signaling pathways, questions remain as to whether their specific location in the cell could play a role in their potency. It is now well known that EGFR and MET are not only localized in the membrane, but can through complex

trafficking, be localized to many organelles including mitochondria, ER, and Golgi (15, 16). They have also been found to be localized in the nucleus. Therefore, here we hypothesized that in addition to the target multiplicity of the drugs, their primary localization could perhaps influence their growth inhibitory potency. We also surmise that this could be determined by live imaging of their subcellular distribution, which could be the result of their macromolecular binding distribution.

In the past, radiolabeling of small molecules was the primary strategy to determine their macromolecular binding, and these did not translate their special distribution in the cells (17). With the advent of fluorescent dyes, the past decade has seen a significant increase in their use as labels to visualize small molecules. Fluorescent labeled small molecules can produce images that result from their target binding profile inside the cells (18). The first fluorescence microscopic study on the subcellular distribution of an EGFR inhibitor was reported by our laboratory (19). We discovered that a blue fluorescent quinazoline inhibitor of EGFR was primarily distributed in the perinuclear region. Recently, we studied the distribution of a rationally designed probe to contain NBD (green fluorescence) (20). However, because of its green color, this probe could not be utilized under conditions where GFP label proteins are endogenously expressed in cells. Therefore, we designed a cell penetrable EGFR targeting probe with a red fluorescent label. This has allowed us to study their interactions with lung cancer cells that endogenously expressing GFP. Here, we report on the synthesis and visualization of these probes in A549 cells wild type and GFP transfected full length EGFR. MET being involved in redundant signaling associated with EGFR signaling (21, 22), we also designed a MET-targeted probe using crizotinib as a kinase warhead. We studied the subcellular distribution of equimolar mixtures of two fluorescent probes: one

designed to target EGFR (red labeled AB64) and MET (green labeled AB20), expecting that perhaps a yellow color would indicate the co-localization of these two receptors. EGFR and MET are are reported to be involved in redundant signaling in cancer cells (22).

4.3 MATERIAL AND METHODS

4.3.1 Cell Culture

To analyze the subcellular distribution of MET and EGFR probes, four cells lines were used: A549-wild type, A549-GFP, NIH3T3-wild type, and NIH3T3-EGRr. The commercially available A549-GFP is a lung cancer cell line engineered to endogenously express the full length EGFR-GFP. The A549 cells also co-express MET. The isogenic NIH3T3 and NIH3T3-EGFR cells were used in our laboratory for the past decade for evaluating EGFR selective targeting. All cell lines were maintained in logarithmic growth as monolayer cultures at 37 C in a humified atmosphere 5% CO2 and 95% air, in DMEM medium supplemented with 10% FBS and antibiotics 10 mM HEPES, gentamycin sulfate and fungizone (all reagents purchased from Wisent Inc., St-Bruno, Canada).

4.3.2 Chemistry

All starting materials were commercially purchased from Sigma Aldrich, or Ark Pharm. Anhydrous solvents were purchased from Sigma Aldrich. NMR spectra were obtained using a Bruker 400 spectrometer at the RIMUHC Drug Discovery Platform. Mass spectra were recorded using the Amazon spectrometer ES-MS instrument, also available at the RIMUHC Drug Discovery Platform.

4.3.2.1 Synthesis of AB20. To synthesize AB20, compound AB8B-B was dissolved in DMF and TEA for 5 minutes, followed by treatment with 4-Chloro-7-nitro-2,1,3-benzoxadiazole (NBD-Cl) dissolved in DMF and slowly dropped over AB8B-B solution and stirred over an oil bath at 70°C for 2 h. Upon reaction completion, the solvent was removed and crude compound was extracted in DCM and dried with sodium sulfate solution. Organic fractions were collected and crude product was purified by column chromatography to yield (R)-N-(2-(4-(4-(6-amino-5-(1-(2,6-dichloro-3-fluorophenyl)ethoxy)pyridin-3-yl)-1H-pyrazol-1-yl)piperidin-1-yl)ethyl)-7-nitrobenzo(c)(1,2,5)oxadiazol-4-amine AB20. ^{1}H NMR (DMSO-d6, 400 MHz, 298 K) δ 9.35 (s, 1H), 8.53 (d, J = 8.9 Hz, 1H), 7.94 (s, 2H), 7.75 (d, J = 1.7 Hz, 2H), 7.57 (q, J = 5.0 Hz, 2H), 7.52 (s, 2H), 7.44 (t, J = 8.7 Hz, 2H), 6.89 (d, J = 1.7 Hz, 2H), 6.48 (d, J = 9.1 Hz, 1H), 6.08 (dd, J = 13.5, 6.7 Hz, 2H), 5.63 (d, J = 5.1 Hz, 3H), 4.11 (t, J = 11.3 Hz, 2H), 3.62 (s, 3H), 3.29 (s, 2H), 3.04 (d, J = 11.5 Hz, 3H), 2.75 – 2.65 (m, 4H), 2.27 – 2.17 (m, 4H), 1.98 (s, 6H), 1.91 (d, J = 10.7 Hz, 4H), 1.80 (d, J = 6.6 Hz, 6H). ES-MS (ESI) *m/z* (%): 656.19 (100) $(M + H)^{+}$.

4.3.2.2 Synthesis of AB63. To synthesize AB63, the method of preparation of compounds **1** and **2** were reported earlier from our laboratory. **3** was coupled with 5-amino-6-hydroxynaphthalene-2-carboperoxoic acid, HOBt in DMF and TEA for 5 minutes, followed by the addition of EDCI and the solution was stirred overnight. Upon reaction completion, the solvent was removed and crude compound was directly purified by column chromatography to give **4** which was treated with para-nitroaniline to give (E)-N-(2-((4-((4-((3-chlorophenyl)amino)quinazolin-6-yl)carbamoyl)benzyl)amino)ethyl)-6-hydroxy-N-methyl-5-((4-nitrophenyl)diazenyl)-2-naphthamide **(AB63)** in a good yield. ^{1}H NMR (DMSO-d6, 400 MHz, 298 K) δ 15.70 (s, 1H),

13.64 (s, 1H), 10.55 (s, 1H), 9.89 (s, 1H), 8.88 (d, J = 1.8 Hz, 2H), 8.60 (s, 1H), 8.51 – 8.37 (m, 1H), 8.26 (d, J = 11.8 Hz, 3H), 8.10 – 7.90 (m, 14H), 7.80 (d, J = 7.8 Hz, 3H), 7.75 (s, 1H), 7.71 (d, J = 8.5 Hz, 2H), 7.53 (t, J = 7.3 Hz, 5H), 7.46 – 7.34 (m, 5H), 7.16 (s, 1H), 6.78 (d, J = 9.7 Hz, 1H). ES-MS (ESI) *m/z* (%): 397.63 (100) $(2M + H)^+$.

4.3.2.3 Synthesis of AB64. Compound **5** was synthesized as previously reported in our laboratory. A homogenous mixture of N4-(3-bromophenyl)-N6-(2-chloroethyl)quinazoline-4,6-diamine **5** and potassium iodide in DMF was added slowly to a mixture of (E)-N,N-dimethyl-4-(2-(pyridin-4-yl)vinyl)aniline in DMF. The reaction was stirred on an oil bath at 70 C for two days. Upon reaction completion, DMF was removed and the crude was purified on preparative TLC plate to yield pure red powder **AB64**. ES-MS (ESI) *m/z* (%): 567.16 (100) $(M + H)^+$.

4.3.3 Microscopic Preparation

Visualization was performed using Zeiss LSM780 laser scanning confocal microscope. Observation was made in a monolayer of cells which were treated with drugs (5 or 10 uM) for 15 minutes prior the live imaging. Confocal images were obtained with the Plan-Neofluar 20x/0.40 LD objective. A 488 nm excitation and the emission in the range of 515-565 nm is for AB20. A 561 nm excitation and the emission in the range of 560-600 nm is for AB64.

4.4 RESULTS

4.4.1 Chemistry

The synthesis of **AB63** proceeded according to Scheme 4.1. Briefly, **1** and **2** were obtained as previously described. Compound **2** was synthesized using a coupling reaction between chloromethyl benzoyl chloride and **1**. Alkylation of **2** in the presence of excess N^1,N^2-dimethylethane-1,2-diamine gave **3**, which was coupled with 5-amino-6-hydroxynaphthalene-2-carboperoxoic acid to give 5-amino-*N*-(2-((4-((4-((3-chlorophenyl)amino)quinazolin-6-yl)carbamoyl)benzyl)(methyl)amino)ethyl)-6-hydroxy-*N*-methyl-2-naphthamide **4**. Diazo coupling of **4** with para-nitroaniline gave **AB63** as a red powder. The other red fluorescent molecule **AB64** was synthesized from a direct reaction between (*E*)-*N*,*N*-dimethyl-4-(2-(pyridin-4-yl)vinyl)aniline and **5** (available in our laboratory) to give **AB64**. (Scheme 4.1). The synthesis of **AB20** was performed according to Scheme 4.1, using direct reaction between (*R*)-5-(1-(1-(2-aminoethyl)piperidin-4-yl)-1*H*-pyrazol-4-yl)-3-(1-(2,6-dichloro-3-fluorophenyl)ethoxy)pyridin-2-amine (NBD-Cl) and compound **6** (synthesis of 6 is reported in chapter 3).

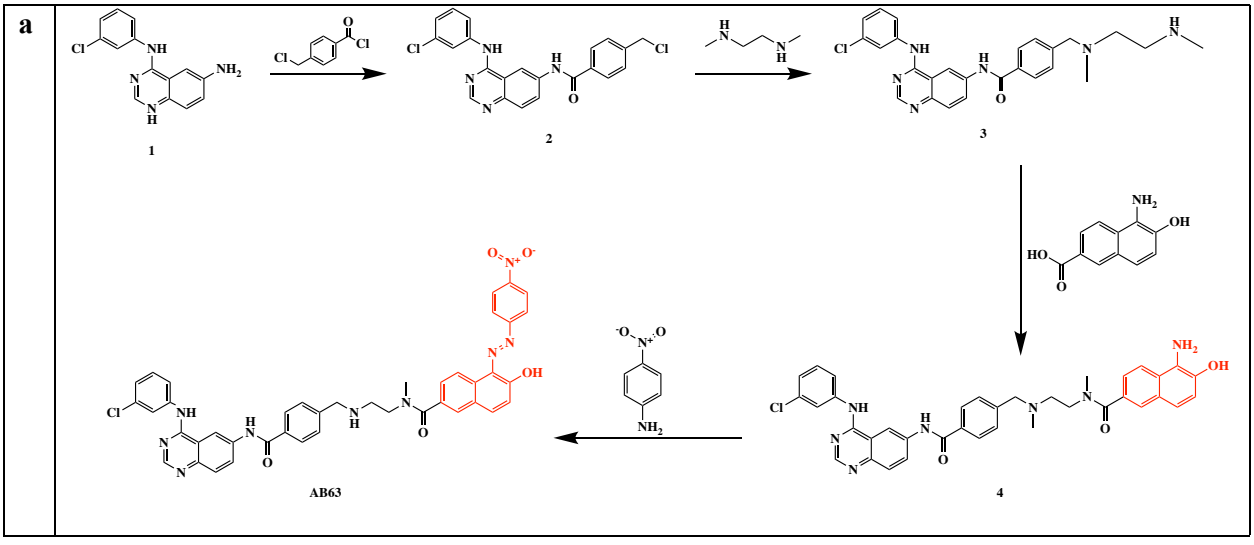

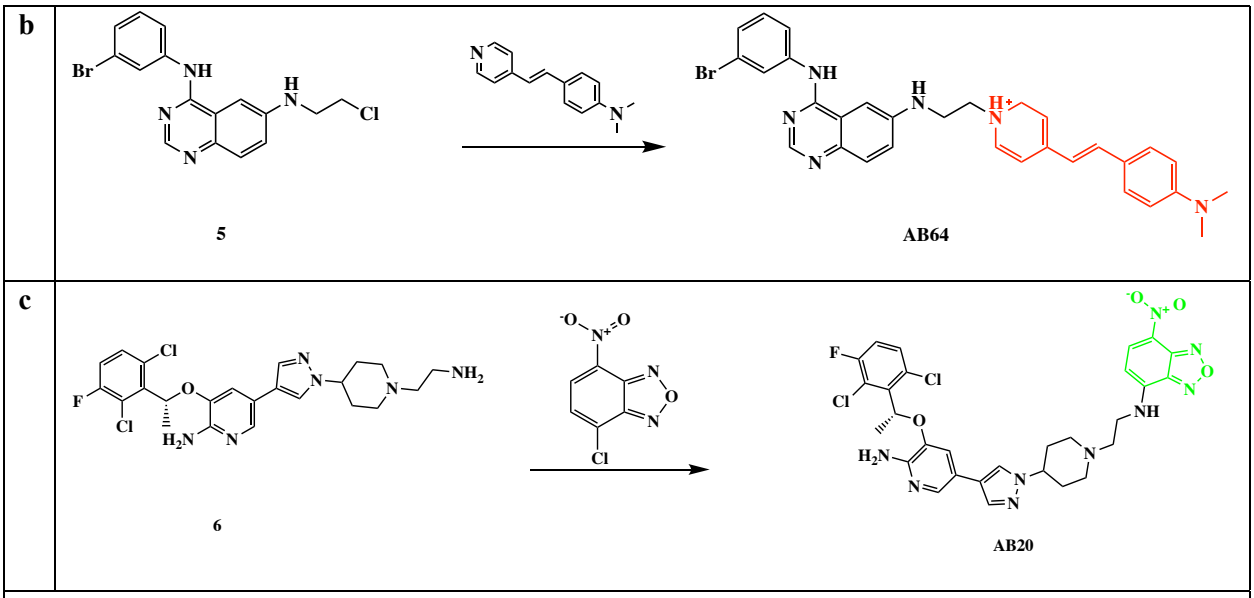

Scheme 4.1. Synthesis of EGFR- (panel **a** and **b**) and MET-targeting (panel **c**) fluorescent labeled molecules.

4.4.2 Biology

4.4.2.1 Isogenic NIH3T3 cells

The cells were exposed to the drug at 10 μM with either AB63 or AB64 for 15 minutes to allow enough time for accumulation inside the cells prior to visualization, and the nuclei was stained with Hoechst 33342. AB64 gave a better staining intensity than AB63 (data not shown), therefore, the latter was adopted for the subsequent staining experiments. AB64 was found to be internalized in both cell types. However, in NIH3T3-wt the distribution was diffused in the cytoplasm, while it has a much more circular appearance around the nucleus in NIH3T3-EGFR, indicating a perinuclear distribution.

4.4.2.2 A549-GFP endogenously expressing full length EGFR

The A549-GFP cell lines was first observed under non-treated conditions and showed a membranal distribution of EGFR. The EGFR function within the cells was validated by the provider using stimulation experiment by EGF that led to internalization of the green fluorescence, and an inhibition of EGFR phosphorylation by EGFR inhibitor (Sigma Aldrich, CLL1141). Interestingly, the green fluorescence was seen in the perinuclear region indicating, the presence of EGFR in the areas close to the nucleus. The natural distribution of the full length EGFR made it the inappropriate model for visualize the subcellular distribution of molecules targeted to EGFR. Interestingly, when the cells were exposed to the red labeled EGFR AB64, the red color was primarily seen in the perinuclear region but did not co-localized with the green fluorescent associated with EGFR in the membrane. Importantly, the study was also carried out with A549 non modified cells. The results showed a similar distribution of the red color of AB64 with no apparent binding to the membrane EGFR.

4.4.2.3 MET staining

Our purpose being to study the co-expression of MET and EGFR, we also used the synthesized AB20, which is a green fluorescent labeled molecule to stain A549-wt cells (which are MET expressing cells) (23). Interestingly, the results showed that the AB20 associated fluorescence was also localized in the perinuclear region and not in the membrane.

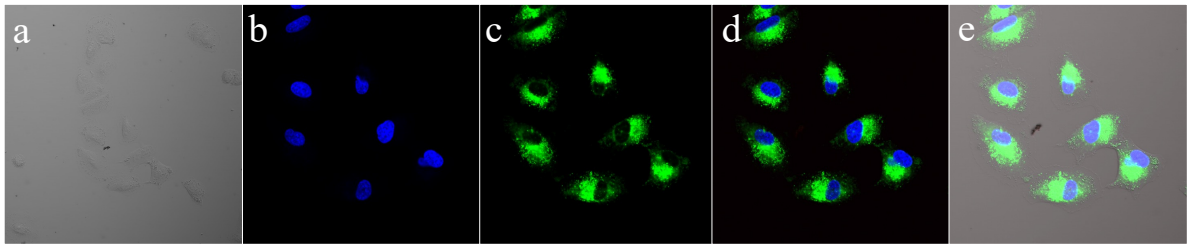

Figure 4.1 Subcellular distribution of AB20 in A549 cells. Cells were grown on an 8-well chamber slide for 24 h, and AB20 (5 uM) added for 15 minutes and observed by confocal microscopy, **(a)** brightfield, **(b)** Nuclear staining with Hoechst 33342, **(c)** distribution of AB20, **(d)** merged images of b and c, **(e)** merged images of a, b, and c.

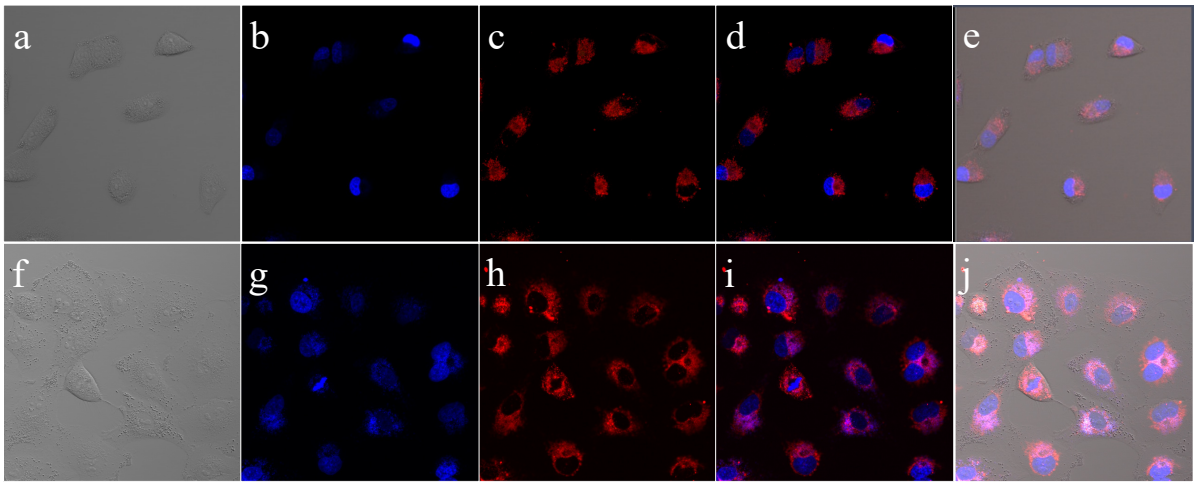

Figure 4.2 Subcellular distribution of AB64 in A549 cells. Cells were grown on an 8-well chamber slide for 24 h and AB64 (10 uM) added for 15 minutes (top panel) and 24 h (bottom panel) and observed by confocal microscopy, **(a/f)** brightfield**, (b/g)** Nuclear staining with Hoechst 33342, **(c/h)** distribution of AB64, **(d/**i**)** merged images of a, b, and c, (**e/j**)

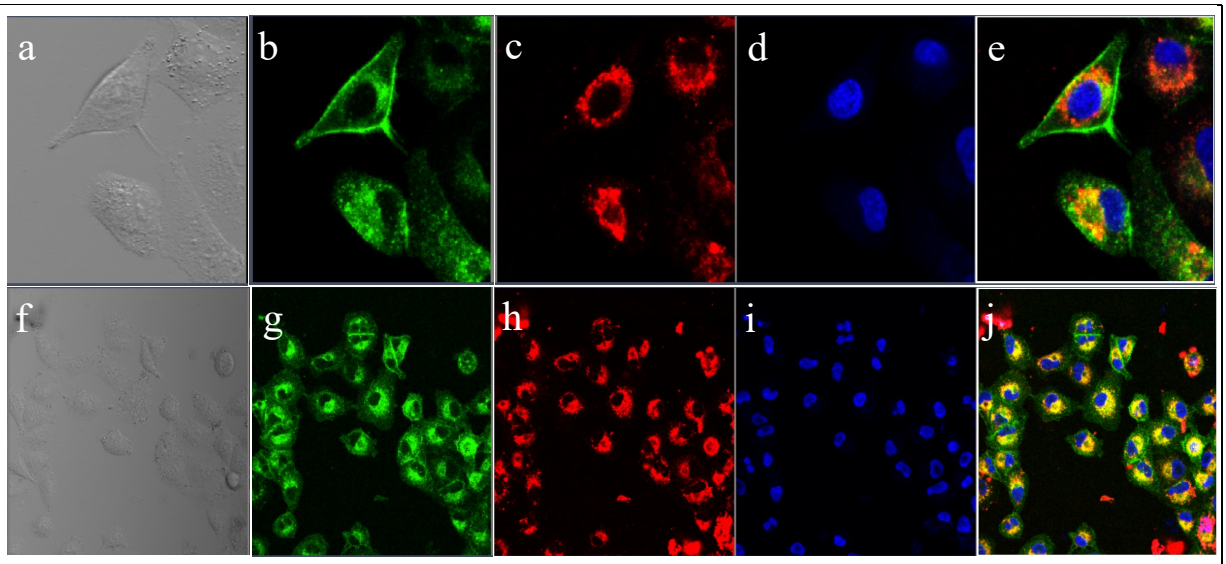

Figure 4.3 Subcellular distribution of AB64 in A549-GFP cells. Cells were grown on an 8-well chamber slide for 24 h, and AB64 (10 uM) added for 15 minutes and observed by confocal microscopy. **(a/f)** brightfield, **(b/g)** EGFR-GFP endogenously expressed, (**c/h**) distribution of AB64, **(d/i)** Nuclear staining with Hoechst 33342, **(e/j)** merged images of b/g, c/h, and d/i.

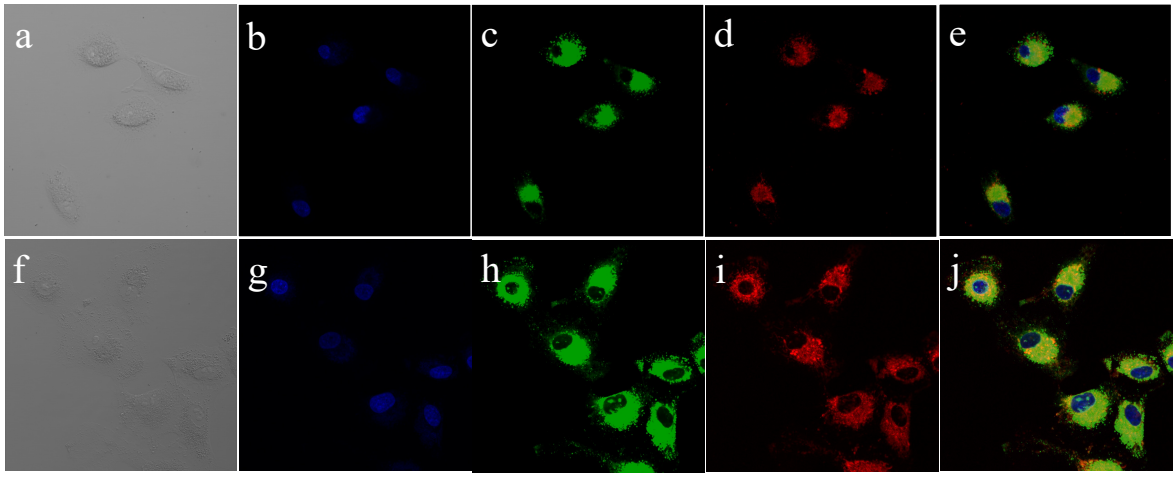

Figure 4.4 Subcellular distribution of a combination of AB20 with AB64 in A549 cells. Cells were grown on an 8-well chamber slide for 24 h, and an equimolar concentration of AB20/AB64 added for 15 minutes (top panel) and 24 h (bottom panel) and observed by confocal microscopy **(a/f)** brightfield, **(b/g)**

Nuclear staining with Hoechst 33342, **(c/h)** distribution of AB20, **(d/i)** distribution of AB20/AB64, (**e/j**) merged images of b/g and c/h, and d/i.

4.5 DISCUSSION

Therapeutic action using kinase inhibitors is directed at either receptor kinases or non-receptor kinases that are involved in multiple signaling pathways. Thus far, there have been reports in the literature on the visualization of kinases targeted to receptors e.g. EGFR and MET, and non-receptor tyrosine kinases e.g. SRC and PI3K (24-29). While visualization of EGFR was attempted by our laboratory and a few other groups, only one publication relates to the visualization of MET receptor (27). Likewise, for the non-receptor tyrosine kinases, only Vetter *et al* (28), and Jiang *et al* (30), attempted to use BODIPY to visualize Src and PI3k. A constant observation by our group and others is the perinuclear distribution of EGFR kinases, or more importantly, the absence of membrane localization of the fluorescent associated with the fluorescence probe. In the past, in the context of studying molecules termed "combi-molecules" designed to be hydrolyzed into DNA damaging species and EGFR inhibitors, we observed perinuclear distribution of the EGFR inhibitors (31). Two subsequent studies were performed by our group: one with a dual fluorescent molecule and a recent one using rationally designed inhibitor to be green fluorescent showed similar observation (24, 31). Studies with lapatinib which is a green fluorescent molecules revealed a similar distribution with absence of membrane localization (32).

The apparent and consistent observation of preferential perinuclear distribution of fluorescent EGFR inhibitors may reveal a distinct property of EGFR or at least its interaction with inhibitors of the quinazoline class. This may be related to the physical state of the EGFR in the membrane

versus the latter in the perinuclear region. In the membrane under serum conditions, the EGFR receptor is activated, indicating that the fluorescent probe may have a greater affinity for the inactivated form of EGFR, a physical state at which it is primarily in the perinuclear region. Also, it is important to mention that Ilmi *et al* (24) and Cao *et al* (33) demonstrated that when EGFR is inhibited, it rapidly translocates into the mitochondria or the Golgi apparatus. Other studies showed that EGFR can retrograde into the endoplasmic reticulum (ER) (34). These organelles e.g. Golgi and ER are the main constituent of the perinuclear region. A very recent paper by Zhang *et al* (26) described fluorescent quinazoline inhibitors as agents that interfere with mitochondrial activities and these have been discovered serendipitously through screening of inhibitors capable of interfering with the mitochondria. The structure identified was a quinazoline-based EGFR inhibitor (Figure 4.5).

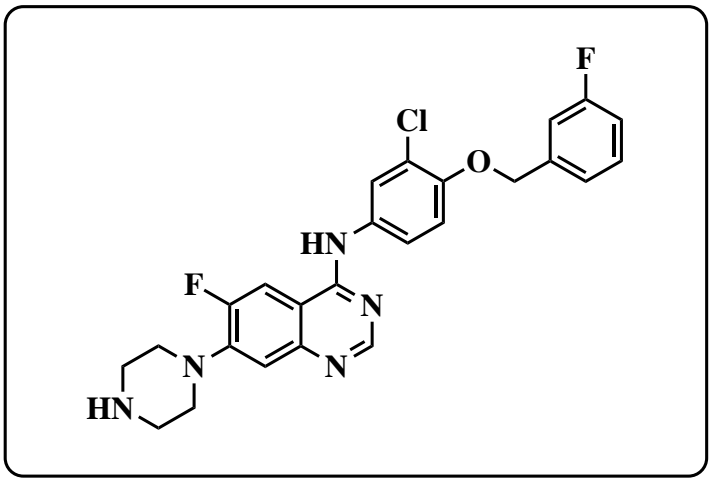

Figure 4.5. The chemical structure of the quinazoline-based molecule observed by Zhang et al to accumulate in the mitochondria of A549 lung cancer cells.

Their visualization studies revealed co-localization of these inhibitors in the mitochondria using Mito-trackers. These results together with our consistent observation of perinuclear distribution of inhibitors of the quinazoline class suggest that, in addition to interference with EGFR mediated cell signaling from the membrane, the mechanism of action of the latter inhibitors may also include interference with mitochondrial functions. Indeed, Cao *et al* (33) suggest that this localization may activate the intrinsic apoptotic pathway. Although our work did not include functional studies, our results are in a agreement with the conclusion that the perinuclear localization of these inhibitors may perhaps have important biological activities.

4.6 REFERENCES

1. Loadman P. Anticancer Drug Development. British Journal of Cancer. 2002;86(10):1665-6.

2. DeVita VT, Chu E. A History of Cancer Chemotherapy. Cancer Research. 2008;68(21):8643-53.

3. Zhong L, Li Y, Xiong L, Wang W, Wu M, Yuan T, et al. Small molecules in targeted cancer therapy: advances, challenges, and future perspectives. Signal Transduction and Targeted Therapy. 2021;6(1):201.

4. Druker BJ, Lydon NB. Lessons learned from the development of an abl tyrosine kinase inhibitor for chronic myelogenous leukemia. J Clin Invest. 2000;105(1):3-7.

5. DeMatteo R, Owzer K, Maki R, Pisters P, Blackstein M, Antonescu C. Gleevec decreases cancer recurrence for patients with primary gastrointestinal stromal tumor. Procs Am Soc Clin Oncol. 2007;25.

6. Starling N, Neoptolemos J, Cunningham D. Role of erlotinib in the management of pancreatic cancer. Ther Clin Risk Manag. 2006;2(4):435-45.

7. Maennling AE, Tur MK, Niebert M, Klockenbring T, Zeppernick F, Gattenlöhner S, et al. Molecular Targeting Therapy against EGFR Family in Breast Cancer: Progress and Future Potentials. Cancers. 2019;11(12):1826.

8. Le T, Gerber DE. Newer-Generation EGFR Inhibitors in Lung Cancer: How Are They Best Used? Cancers (Basel). 2019;11(3).

9. Awad MM, Shaw AT. ALK inhibitors in non-small cell lung cancer: crizotinib and beyond. Clin Adv Hematol Oncol. 2014;12(7):429-39.

10. Lovly CM, Shaw AT. Molecular pathways: resistance to kinase inhibitors and implications for therapeutic strategies. Clinical cancer research : an official journal of the American Association for Cancer Research. 2014;20(9):2249-56.

11. Primorac D, Bach-Rojecky L, Vađunec D, Juginović A, Žunić K, Matišić V, et al. Pharmacogenomics at the center of precision medicine: challenges and perspective in an era of Big Data. Pharmacogenomics. 2020;21(2):141-56.

12. van Veggel B, de Langen AJ, Hashemi S, Monkhorst K, Rosenberg EH, Heideman DAM, et al. Crizotinib treatment for patients with EGFR mutation positive NSCLC that acquire cMET amplification after EGFR TKI therapy results in short-lived and heterogeneous responses. Lung Cancer. 2018;124:130-4.

13. Wang Q, Yang S, Wang K, Sun S-Y. MET inhibitors for targeted therapy of EGFR TKI-resistant lung cancer. Journal of Hematology & Oncology. 2019;12(1):63.

14. Yokokawa M, Morita KI, Oikawa Y, Kayamori K, Sakamoto K, Ikeda T, et al. Co-expression of EGFR and MET has a synergistic effect on the prognosis of patients with oral squamous cell carcinoma. J Oral Pathol Med. 2020;49(3):235-42.

15. Viticchiè G, Muller PAJ. c-Met and Other Cell Surface Molecules: Interaction, Activation and Functional Consequences. Biomedicines. 2015;3(1):46-70.

16. Wang Y-N, Hung M-C. Nuclear functions and subcellular trafficking mechanisms of the epidermal growth factor receptor family. Cell Biosci. 2012;2(1):13-.

17. Waaijer SJH, Kok IC, Eisses B, Schröder CP, Jalving M, Brouwers AH, et al. Molecular Imaging in Cancer Drug Development. Journal of Nuclear Medicine. 2018;59(5):726-32.

18. Terai T, Nagano T. Small-molecule fluorophores and fluorescent probes for bioimaging. Pflugers Arch. 2013;465(3):347-59.

19. Matheson SL, Brahimi F, Jean-Claude BJ. The combi-targetinG concept: intracellular fragmentation of the binary epidermal growth factor (EGFR)/DNA targeting "combi-triazene" SMA41. Biochem Pharmacol. 2004;67(6):1131-8.

20. Bergen JM, Kwon EJ, Shen TW, Pun SH. Application of an environmentally sensitive fluorophore for rapid analysis of the binding and internalization efficiency of gene carriers. Bioconjug Chem. 2008;19(1):377-84.

21. Xu H, Stabile LP, Gubish CT, Gooding WE, Grandis JR, Siegfried JM. Dual blockade of EGFR and c-Met abrogates redundant signaling and proliferation in head and neck carcinoma cells. Clin Cancer Res. 2011;17(13):4425-38.

22. Linklater ES, Tovar EA, Essenburg CJ, Turner L, Madaj Z, Winn ME, et al. Targeting MET and EGFR crosstalk signaling in triple-negative breast cancers. Oncotarget. 2016;7(43):69903.

23. Ma PC, Jagadeeswaran R, Jagadeesh S, Tretiakova MS, Nallasura V, Fox EA, et al. Functional expression and mutations of c-Met and its therapeutic inhibition with SU11274 and small interfering RNA in non–small cell lung cancer. Cancer research. 2005;65(4):1479-88.

24. Ilmi R, Tseriotou E, Stylianou P, Christou YA, Ttofi I, Dietis N, et al. A novel conjugate of bis [((4-bromophenyl) amino) quinazoline], a EGFR-TK ligand, with a fluorescent Ru (II)-bipyridine complex exhibits specific subcellular localization in mitochondria. Molecular pharmaceutics. 2019;16(10):4260-73.

25. Wu Q, Jing Y, Zhao T, Gao J, Cai M, Xu H, et al. Development of small molecule inhibitor-based fluorescent probes for highly specific super-resolution imaging. Nanoscale. 2020;12(42):21591-8.

26. Zhang Y, Hou Q, Li X, Zhu J, Wang W, Li B, et al. Enrichment of novel quinazoline derivatives with high antitumor activity in mitochondria tracked by its self-fluorescence. European journal of medicinal chemistry. 2019;178:417-32.

27. Kim E, Yang KS, Weissleder R. Bioorthogonal Small Molecule Imaging Agents Allow Single-Cell Imaging of MET. PLOS ONE. 2013;8(11):e81275.

28. Vetter ML, Zhang Z, Liu S, Wang J, Cho H, Zhang J, et al. Fluorescent Visualization of Src by Using Dasatinib-BODIPY. ChemBioChem. 2014;15(9):1317-24.

29. Caino MC, Ghosh JC, Chae YC, Vaira V, Rivadeneira DB, Faversani A, et al. PI3K therapy reprograms mitochondrial trafficking to fuel tumor cell invasion. Proceedings of the National Academy of Sciences. 2015;112(28):8638-43.

30. Jiang D, Sims CE, Allbritton NL. Single-cell analysis of phosphoinositide 3-kinase and phosphatase and tensin homolog activation. Faraday Discuss. 2011;149:187-245.

31. Todorova MI, Larroque A-L, Dauphin-Pierre S, Fang Y-Q, Jean-Claude BJ. Subcellular Distribution of a Fluorescence-Labeled Combi-Molecule Designed to Block Epidermal Growth Factor Receptor Tyrosine Kinase and Damage DNA with a Green Fluorescent Species. Molecular Cancer Therapeutics. 2010;9(4):869-82.

32. Hansen MB, Postol M, Tvingsholm S, Nielsen IØ, Dietrich TN, Puustinen P, et al. Identification of lysosome-targeting drugs with anti-inflammatory activity as potential invasion inhibitors of treatment resistant HER2 positive cancers. Cell Oncol (Dordr). 2021;44(4):805-20.

33. Cao X, Zhu H, Ali-Osman F, Lo H-W. EGFR and EGFRvIII undergo stress-and EGFR kinase inhibitor-induced mitochondrial translocalization: a potential mechanism of EGFR-driven antagonism of apoptosis. Molecular cancer. 2011;10(1):1-13.

34. Wang YN, Wang H, Yamaguchi H, Lee HJ, Lee HH, Hung MC. COPI-mediated retrograde trafficking from the Golgi to the ER regulates EGFR nuclear transport. Biochem Biophys Res Commun. 2010;399(4):498-504.

5. CONNECTING TEXT

In the preceding chapters, we demonstrated the feasibility of chemoprobes capable of generating kinase binding profiles and carrying fluorescence tags suitable for live cell imaging. We demonstrated in chapter 3 that the chemoprobe can generate kinase profiles to monitor drug response. We also demonstrated their ability to perform this pull-down in lysates from cells. In chapter 5, we describe their ability to generate pull-down profiles from plasma samples collected from patients, in search for possible signatures that can correlate with outcomes.

CHAPTER 5

APPLICATION OF THE CHEMOPROBE APPROACH TO THE ANALYSIS OF CLINICAL SAMPLES: POTENTIAL DEVELOPMENT AS LIQUID BIOPSY TOOLS

Alaa Baryyan, Kurt Dejgaard, and Bertrand Jean-Claude

Cancer Drug Research Laboratory, Department of Medicine, The Research Institute of The McGill University Health Centre, 1001 Decarie Boulevard, Montreal, Quebec, H3A 3J1, Canada

5.1 ABSTRACT

Targeted therapy of cancer the past decade has benefited from inhibitors of oncogenes that drive tumour progression, e.g. BRAF, EGFR, ALK, and ROS. These inhibitors, while being specific for the canonical target, are capable of binding to a broad spectrum of kinases even non kinases. Mounting these inhibitors scaffold on linkers that allow to capture their bound proteins lead to molecular tools termed “chemoprobe”. Recently, we designed such chemoprobes to read the binding profile of crizotinib, a MET/ALK inhibitor, used in the therapy of lung cancer. Here we test the hypothesis that chemoprobe AB19 can be used as a liquid biopsy tool to read patient samples. As tumours almost always shed fragments e.g. single cells, proteins, DNA, and RNA in various body fluids, we thought it of interest to use our probe to capture molecules in human plasma that can potentially serve as signature for tumour drug response. Here, we analyzed the ability of AB19 to pull-down proteins from patients plasma who were enrolled in clinical trials involving crizotinib two month after treatment. The results showed that AB19 pulled down a large number of lipoproteins and other proteins such as vitronectin (VTNC), fibronectin (FINC), coagulation factor (F13A), etc. Fibronectin was the most significant proteins that appeared in most of the samples, however, it was pulled down by both AB22 and AB19, and the trend was the more fibronectin picked up by both probes, the better the prognosis. While the experiments showed that the probes could generate protein binding profiles, a larger sample size is required to correlate the pull-down results with outcomes. This work can be considered the first proof-of-concept of protein pull-down by chemoprobes from human plasma samples collected from a clinical trial.

5.2 INTRODUCTION

The clinical management of cancer is moving from a one-size-fit-all strategy to a more personalized approach termed "personalized medicine". It has been increasingly clear that patients presenting specific type of mutations (e.g. EGFR L858R for lung cancer) can benefit from EGFR-inhibitor based therapy (1-3). Likewise, patients with advanced anaplastic lymphoma kinase (ALK) rearrangement can benefit from targeted therapy with the MET/ALK inhibitor crizotinib (4-6). Approximately, 5% of all NSCLC patients express ALK and diagnostics is required to indicate crizotinib for their therapy (7). In the future, for patient stratification, the clinical oncologist depends more and more on the availability of specific molecular signatures that can guide the choice of the therapeutic regimen (8). This is being increasingly important with the emergence of targeted therapy with antibodies and kinase inhibitors. Currently, there are several drugs that are directed at important targets that characterize the aggressiveness of the tumour (e.g. EGFR, BRAF, ALK, ROS1, and PARP) (9). In addition to intrinsic signature that can guide the clinical indication, tumours almost always shed fragments e.g. single cells, proteins, DNA, and RNA in various body fluids. It has been shown that the detection of some macromolecules such as circular DNA could be used to track certain mutations of the original tumour (10). This approach which is now called "liquid biopsy" holds a significant promise for non-invasive monitoring of cancer, and may in the future be the primary tool to predict tumour sensitivity or early detection of tumour formation (11). In the latter context that we surmised that a molecular probe designed to capture kinases could generate signatures that are predictive of drug response. We recently designed and made the proof-of-concept of a chemoprobe AB19 designed with crizotinib warhead capable of capturing multiple kinases and other proteins from biological fluids. The molecular pull-down profiles can be developed as specific signatures to predict drug response. The current

work seeks to make a proof-of-concept of the diagnostic capability of AB19 using plasma samples from patients enrolled in a clinical trial in which they receive crizotinib. Their ability of AB19 to capture proteins in the plasma may lead to its development as a liquid biopsy tool.

5.3 MATERIALS AND METHODS

5.3.1 Clinical study

The plasma samples were obtained from patients enrolled in a phase-IV multicentre trial to evaluate resistance mechanism and pharmacokinetics of crizotinib and diagnostic test in advanced ALK positive NSCLC patients (approval # A09-M95-13B). The samples were obtained from patients before and after treatment (n=5) and were available for eight additional patients (n=8) only two month after treatment with crizotinib. Outcomes data were provided as long-term, short-term, normal- and poor-responders. A total of thirteen samples were analysed by mass spectrometry with a proteomics approach. The samples were graciously provided by Dr Jason Agulnik, the principal investigator of the study.

5.3.2 Liquid biopsy preparation

Clinical samples obtained from the crizotinib trial (50 ul) were treated with lysis buffer (Hepes Acetate) supplemented with 1 mM PMSF for 30 min on ice. In parallel, the magnetic streptavidin-coated beads (10 µl) were washed free of the preservative and exposed to AB19 or AB22 (2.5 µM) in a buffer solution (25 µl) for 2 h on a shaker. The resulting functionalized beads were subsequently incubated with 50 µl plasma samples and the beads were washed three times with HEPES (potassium acetate). Bound proteins were digested on bead overnight at 37 °C. The mixture was centrifuged and the supernatant subjected to proteomics analysis.

5.3.3 Proteomics Analysis

For LC-MS analysis, a Q Exactive HF (Thermo Scientific) mass spectrometer was coupled on-line to an EASY-nLC 1000 HPLC system (Thermo Scientific). Rehydrated tryptic peptide fragments were separated on a 25 cm C18 column (Acclaim 75 μm inner diameter, 2 μm particles, Thermo Scientific) fitted upstream with a 2cm trapping column (Acclaim PepMap 100, Thermo Scientific) in a 100 min gradient from 3% to 38% in buffer B (99.9% acetonitrile, 0.1% formic acid) at 350 nL/min, for a total run time of 120 minutes. Mass spectra were acquired in data-dependent mode. Briefly, each survey scan (range 375 to 1,400 m/z, resolution of 120,000 at m/z 200, maximum injection time 60 ms, AGC target of 5E6) was followed by high-energy collisional dissociation based fragmentation (HCD) of the 25 most abundant isotope patterns with a charge ≥ 2 (normalized collision energy of 25, an isolation window of 2.5 m/z, resolution of 15,000, maximum injection time 60 ms, AGC target value of 2E5). Dynamic exclusion of sequenced peptides was set to 3.5 s. All data were acquired using Xcalibur software (Thermo Scientific).

5.4 RESULTS

As mentioned earlier, tumours almost always shed macromolecules in various body fluids including single cells, proteins, DNA, and RNA. Therefore, we believed that our probe, which is designed to bind to specific proteins could potentially capture some tumour specific proteins shed in the plasma. With the hypothesis that perhaps some proteins can be captured by AB19, we probed clinical samples from patients who participated in clinical trials with crizotinib, the warhead of AB19. MET and EGFR are proteins known to be shed in the plasma of patients with lung cancer. Therefore, we analyzed samples obtained from the patients before treatment and after treatment. The results showed that in all the samples analyzed, no MET was captured (Table 5.1). However,

other proteins such as the coagulation factor XIII A chain (F13A) and Testis-specific serine/threonine-protein kinase 4 (TSSK4) could be differentially found between the baseline and the treated patients. Detection of the carboxypeptidase N catalytic chain (CBPN) suggested that perhaps some proteins may be present at lower concentration therefore, we challenged this hypothesis by western blot with the latter proteins to ascertain their levels in the plasma.

5.5 DISCUSSION

Previous work showed that AB19 that carried crizotinib warhead could pull-down a broad profile of kinases or other proteins, many of them being significant oncogenes such as ROS, AXL, EphA2, mTOR, and FAK1. The strong binding of crizotinib to ROS, AXL and ALK has led to its re-classification as MET, ROS, and AXL inhibitor. However , our previous work demonstrated that the crizotinib warhead of AB19 could pull-down non kinase proteins (e.g. fibronectin, 14-3-3S, and apolipoproteins) in cell lysates. However, the latter proteins are sometimes captured by AB22 nonspecific chemoprobe, indicating that the linker side of the chemoprobe may participate in binding through hydrophobic interaction.

AB19 being also a mimic of crizotinib its protein pull-down profile may indicate the protein binding profile of crizotinib when it is administered *in vivo* or to patients. Probably, its kinase inhibitor warhead confers specificity for kinase ATP site and its complex linker may be involved in interaction with other proteins, particularly, the lipoproteins. Given that tumours almost always shed fragments in plasma, we thought it is of interest to tested the ability to read the plasma from patients before receiving the drug (crizotinib) or about two months after drug administration. In the study it appears that AB19 could not capture any kinases from plasma in one patient sample in which the TSSK4 was found. Of all the proteins captured including 14-3-3S, apolipoproteins,

fibronectin, coagulation factor, only fibronectin was consistently captured from all the patients, and could be perhaps given its role in cancer cells be related to patient outcome. When we searched for fibronectin among the proteins captured in cell lysates (e.g. DU145) from previous studies, we found that it could be pulled down by both AB19 and AB22 indicating an involvement of the linker in the mechanism of pull-down. When we analyzed the total number of counts of fibronectin by the two probes, a trend was observed giving higher counts (average 52.5) for patients in the long-term responder group, and counts in the range 25.5 and 17 patients in the normal- and poor-responding groups, respectively.

Fibronectin is a cell surface protein with complex cell surface protein which is cleaved and shed in the plasma during many cellular processes. The role of fibronectin as a predictor of cancer survival is highly controversial, with studies demonstrating that it correlate to poor prognosis and others favorable outcomes. The controversies has been reviewed by Lin *et al.* (12). Nevertheless, although we observed statistical significance between the long-term responders (n=4) and the normal (n=5), or poor responders (n=3), a larger sample size is required to establish a meaningful correlation between fibronectin shed in the plasma and clinical outcomes. These chemical proteomics study is hypothesis generating, suggesting that other more quantitative and sensitive techniques such as western blotting could be used to further ascertain this correlation.

Table 5.1

		Normal Responder				Normal Responder				Poor Responder		unknown		ng-Term Respondng-Term Respondng-Term Respond			Poor Responder		Normal Responde	Normal Responder			ng-Term Respond		Normal Responder				Poor Responder			
		# 2				# 3				# 4		# 5		# 6		# 8	# 9		# 11		# 12	# 15			# 16		# 17			# 23			
		19	22	19	22	19	22	19	22	19	22	19	22	19	22	19	22	19	22	19	22	19	22	19	22	19	22	19	22	19	22
Identified Proteins (312)	Accession Nu	Molecular W	02k19	02k22	02s19	02s22	03k19	03k22	03s19	03s22	04k19	04k22	05s19	05s22	06k19	06k22	08k19	08k22	09s19	09s22	11k19	11k22	12s19	12s22	15k19	15k22	15s19	15s22	16k19	16k22	17k19	17k22	17s19	17s22	23k19	23k22	23s19	23s22
Fibrinogen alpha chain OS=Homo sapiens GN=FGA PE=1 SV=2	FIBA_HUMA	95 kDa	1576	185	502	125	397	57	422	597	767	1223	1587	172	1278	703	64	251	312	1566	1679	1333	458	1592	1162	589	1621	631	1443	772	181	77	1116	303	1216	13	462	403
Fibrinogen beta chain OS=Homo sapiens GN=FGB PE=1 SV=2	FIBB_HUMA	56 kDa	58	34	134	31	90	13	51	98	181	183	72	39	153	167	62	98	66	305	302	157	26	90	75	166	67	119	79	149	22	22	69	67	182	1	85	80
Apolipoprotein A-I OS=Homo sapiens GN=APOA1 PE=1 SV=1	APOA1_HUN	31 kDa	118	27	54	18	47	0	237	22	64	184	135	39	133	60	26	55	6	560	189	27	1	218	388	162	52	51	59	144	47	11	72	17	73	0	14	17
Cluster of Keratin, type II cytoskeletal 1 OS=Homo sapiens GN=KRT1 PE=1 SV=6 (K2C1_HUMAN)	K2C1_HUMA	66 kDa	4	30	8	0	4	0	4	5	41	142	17	0	57	10	12	39	20	228	433	57	0	61	65	19	55	13	135	8	7	0	189	4	111	0	27	14
Fibrinogen gamma chain OS=Homo sapiens GN=FGG PE=1 SV=3	FIBG_HUMA	52 kDa	36	14	47	1	28	0	2	0	18	51	56	11	77	21	46	48	3	290	268	84	6	53	45	78	44	8	57	60	1	10	44	4	33	4	6	5
Cluster of Complement C3 OS=Homo sapiens GN=C3 PE=1 SV=2 (CO3_HUMAN	CO3_HUMAN	187 kDa	28	9	3	11	12	3	23	4	28	38	19	4	61	10	36	28	0	160	357	79	7	61	109	47	41	9	14	9	5	15	22	0	28	0	0	0
Apolipoprotein A-IV OS=Homo sapiens GN=APOA4 PE=1 SV=3	APOA4_HUN	45 kDa	33	0	0	0	15	0	43	3	8	70	35	0	46	1	1	1	0	115	63	46	0	49	210	45	28	3	30	23	1	0	55	4	17	0	0	0
Clusterin OS=Homo sapiens GN=CLU PE=1 SV=1	CLUS_HUMA	52 kDa	20	23	37	0	9	0	27	0	17	33	43	0	39	0	0	17	9	139	51	26	0	92	131	60	9	8	38	17	9	0	43	4	51	0	0	11
Cluster of Keratin, type I cytoskeletal 10 OS=Homo sapiens GN=KRT10 PE=1 SV=6 (K1C10_HUMAN)	K1C10_HUM	59 kDa	2	6	8	0	0	0	4	3	26	61	16	0	27	0	0	6	10	100	237	28	0	22	32	10	33	2	71	0	0	0	73	0	67	0	15	8
Keratin, type I cytoskeletal 9 OS=Homo sapiens GN=KRT9 PE=1 SV=3	K1C9_HUMA	62 kDa	4	31	1	0	1	0	12	0	8	38	14	0	15	5	9	23	12	81	202	35	0	36	35	15	18	10	60	9	8	0	76	5	41	0	18	10
Serum albumin OS=Homo sapiens GN=ALB PE=1 SV=2	ALBU_HUM	69 kDa	1	6	13	0	12	0	0	0	0	6	2	0	9	8	54	38	0	93	313	16	2	3	15	10	0	0	5	1	0	6	1	0	0	0	0	0
Hemopexin OS=Homo sapiens GN=HPX PE=1 SV=2	HEMO_HUM	52 kDa	6	9	12	12	20	5	25	5	11	59	3	34	6	47	28	46	6	22	37	4	13	10	9	19	2	19	1	23	17	24	4	22	19	21	13	11
Apolipoprotein C-III OS=Homo sapiens GN=APOC3 PE=1 SV=1	APOC3_HUN	11 kDa	57	13	12	0	26	0	52	16	12	35	29	0	15	6	0	5	0	49	23	14	0	7	15	17	6	3	41	14	0	0	9	0	54	0	1	0
Alpha-1-antitrypsin OS=Homo sapiens GN=SERPINA1 PE=1 SV=3	A1AT_HUM	47 kDa	0	0	0	0	0	0	0	0	0	63	16	0	21	6	24	0	0	117	174	25	2	14	12	3	0	0	0	0	0	7	0	0	0	0	0	0
Cluster of Serum amyloid A-1 protein OS=Homo sapiens GN=SAA1 PE=1 SV=1 (SAA1_HUMAN)	SAA1_HUM	14 kDa	0	0	0	0	9	3	0	0	0	4	5	0	1	0	0	0	0	2	229	123	0	29	0	0	1	0	2	0	0	0	2	0	13	0	4	7
Fibronectin OS=Homo sapiens GN=FN1 PE=1 SV=4	FINC_HUMA	263 kDa	21	17	27	6	22	0	2	0	12	13	5	0	43	21	19	43	0	32	18	9	13	20	11	20	5	0	17	35	0	10	36	0	0	0	0	0
Apolipoprotein E OS=Homo sapiens GN=APOE PE=1 SV=1	APOE_HUM	36 kDa	54	4	3	0	6	0	10	0	0	37	80	0	18	0	0	4	0	38	54	30	0	18	61	5	5	0	24	16	0	0	10	0	30	0	0	0
Apolipoprotein A-II OS=Homo sapiens GN=APOA2 PE=1 SV=1	APOA2_HUN	11 kDa	14	0	2	0	0	0	18	0	5	22	54	0	7	4	0	10	2	105	32	12	0	38	80	25	8	1	30	6	0	0	8	0	15	0	0	0
Apolipoprotein B-100 OS=Homo sapiens GN=APOB PE=1 SV=2	APOB_HUM	516 kDa	0	2	9	0	2	0	1	0	0	21	12	0	39	0	11	8	0	34	136	4	0	30	52	8	0	0	0	0	0	0	25	0	6	2	0	0
Kininogen-1 OS=Homo sapiens GN=KNG1 PE=1 SV=2	KNG1_HUM	72 kDa	0	14	8	0	10	0	13	0	30	41	0	2	2	28	22	48	0	29	8	3	16	5	4	13	2	0	1	2	0	24	2	0	1	1	2	0
Inter-alpha-trypsin inhibitor heavy chain H2 OS=Homo sapiens GN=ITIH2 PE=1 SV=2	ITIH2_HUMA	106 kDa	7	8	6	1	0	0	0	0	0	23	5	10	18	16	30	32	0	47	37	4	1	17	35	17	0	0	0	12	0	17	8	0	0	0	0	1
Alpha-2-macroglobulin OS=Homo sapiens GN=A2M PE=1 SV=3	A2MG_HUM	163 kDa	8	0	1	0	0	0	7	0	0	0	12	0	28	0	0	0	0	31	136	8	0	17	23	8	2	0	13	0	1	1	8	0	0	0	0	0
Coiled-coil domain-containing protein 87 OS=Homo sapiens GN=CCDC87 PE=1 SV=2	CCD87_HUM	96 kDa	0	0	0	0	0	1	0	0	0	0	0	0	0	0	0	0	0	0	0	0	0	0	0	0	0	0	0	0	0	0	0	0	0	0	0	0
N-alpha-acetyltransferase 25, NatB auxiliary subunit OS=Homo sapiens GN=NAA25 PE=1 SV=1	NAA25_HUN	112 kDa	0	0	0	0	0	0	0	0	0	0	1	0	2	0	0	0	0	0	0	0	0	0	0	0	0	0	0	0	0	0	0	0	1	0	0	0
Cluster of Complement C4-B OS=Homo sapiens GN=C4B PE=1 SV=2 (CO4B_HUMAN)	CO4B_HUM	193 kDa	10	0	0	0	0	0	0	0	15	24	10	0	15	10	1	0	0	57	106	15	0	25	10	7	3	1	0	2	0	0	8	0	3	0	0	0
14-3-3 protein sigma OS=Homo sapiens GN=SFN PE=1 SV=1	1433S_HUM	28 kDa	0	2	9	0	3	0	0	0	4	0	0	0	1	5	0	0	15	41	0	1	0	0	2	3	1	13	0	18	0	0	0	4	0	0	14	8
Cluster of Haptoglobin OS=Homo sapiens GN=HP PE=1 SV=1 (HPT_HUMAN)	HPT_HUMA	45 kDa	0	0	0	0	0	0	0	0	1	0	6	0	9	0	0	5	0	46	139	21	0	13	23	3	6	0	0	0	0	0	4	0	0	0	0	0
Lymphoid-restricted membrane protein OS=Homo sapiens GN=LRMP PE=1 SV=3	LRMP_HUM	62 kDa	0	0	0	3	0	5	0	0	0	0	0	1	0	0	1	0	5	0	0	0	1	0	0	0	0	0	0	0	2	5	0	1	0	2	1	0
Apolipoprotein C-II OS=Homo sapiens GN=APOC2 PE=1 SV=1	APOC2_HUN	11 kDa	27	0	1	0	2	0	15	6	0	20	25	0	4	0	0	0	0	8	12	9	0	10	30	6	18	1	16	0	0	0	11	0	16	0	0	0
Coagulation factor XIII A chain OS=Homo sapiens GN=F13A1 PE=1 SV=4	F13A_HUMA	83 kDa	10	0	0	0	0	0	0	0	8	3	9	0	31	0	0	0	0	4	0	14	0	25	40	2	6	0	0	2	0	0	11	0	4	0	0	0
Apolipoprotein C-I OS=Homo sapiens GN=APOC1 PE=1 SV=1	APOC1_HUN	9 kDa	14	0	0	0	0	0	11	0	9	7	21	0	11	2	0	0	0	14	16	6	0	10	36	4	4	0	4	5	0	0	7	0	2	0	0	0
Cluster of Ig gamma-1 chain C region OS=Homo sapiens GN=IGHG1 PE=1 SV=1 (IGHG1_HUMAN)	IGHG1_HUM	36 kDa	0	0	0	0	0	0	0	0	0	0	0	0	8	0	0	0	0	23	93	5	0	2	2	0	1	0	11	0	0	0	0	0	0	0	0	0
Serum amyloid A-4 protein OS=Homo sapiens GN=SAA4 PE=1 SV=2	SAA4_HUM	15 kDa	11	0	0	0	0	0	5	0	0	11	13	0	6	1	0	0	0	32	5	1	0	8	17	3	7	0	7	3	0	0	3	0	7	0	1	0
Vitronectin OS=Homo sapiens GN=VTN PE=1 SV=1	VTNC_HUM	54 kDa	3	0	0	0	0	0	3	0	0	26	0	0	9	1	0	0	0	5	25	3	0	12	16	4	0	0	0	1	0	0	16	0	5	0	0	1
Apolipoprotein L1 OS=Homo sapiens GN=APOL1 PE=1 SV=5	APOL1_HUM	44 kDa	9	0	0	0	3	0	6	0	5	15	9	0	3	0	0	0	0	20	15	3	0	8	35	5	4	1	5	1	0	0	8	0	4	0	0	0
Inter-alpha-trypsin inhibitor heavy chain H4 OS=Homo sapiens GN=ITIH4 PE=1 SV=4	ITIH4_HUMA	103 kDa	0	0	0	0	0	0	0	0	0	0	3	0	13	0	0	1	0	13	89	24	0	17	10	1	0	0	0	0	0	0	0	0	3	0	0	0
Ig mu chain C region OS=Homo sapiens GN=IGHM PE=1 SV=3	IGHM_HUM	49 kDa	0	10	10	0	0	0	0	0	8	1	0	0	7	12	12	31	0	24	46	9	0	3	5	8	0	0	0	0	0	0	0	0	0	0	0	0
Hemoglobin subunit beta OS=Homo sapiens GN=HBB PE=1 SV=2	HBB_HUMA	16 kDa	21	12	1	0	0	1	0	0	0	1	0	5	0	5	8	0	0	21	15	7	0	7	11	14	6	0	9	0	0	5	8	0	0	0	0	0
Ig kappa chain C region OS=Homo sapiens GN=IGKC PE=1 SV=1	IGKC_HUMA	12 kDa	0	0	0	0	0	0	0	0	0	0	0	0	20	0	0	0	0	23	48	5	0	0	2	0	0	0	8	0	0	0	0	0	0	0	0	0
Hemoglobin subunit alpha OS=Homo sapiens GN=HBA1 PE=1 SV=2	HBA_HUMA	15 kDa	16	0	0	0	0	0	0	0	0	0	0	0	5	0	0	0	0	19	32	8	0	1	12	0	0	0	8	0	0	1	2	0	0	0	0	0
von Willebrand factor OS=Homo sapiens GN=VWF PE=1 SV=4	VWF_HUMA	309 kDa	4	0	1	0	1	0	0	0	0	0	0	0	31	0	1	13	0	1	19	14	0	0	0	0	0	0	6	0	0	0	3	0	0	0	0	0
Protein Shroom3 OS=Homo sapiens GN=SHROOM3 PE=1 SV=2	SHRM3_HUM	217 kDa	2	0	0	0	0	0	3	0	1	9	14	0	9	0	0	0	0	10	1	4	0	10	14	0	7	0	6	0	0	0	8	0	4	0	1	0
Prothrombin OS=Homo sapiens GN=F2 PE=1 SV=2	THRB_HUM	70 kDa	2	0	0	0	0	0	9	0	0	4	0	0	7	0	0	0	0	4	9	3	0	11	5	9	0	0	1	8	0	0	2	1	0	0	1	3
ELAV-like protein 3 OS=Homo sapiens GN=ELAVL3 PE=2 SV=3	ELAV3_HUM	40 kDa	0	0	0	1	0	0	0	0	0	0	0	0	0	0	1	1	0	0	0	0	0	0	0	0	3	0	0	0	0	2	0	1	0	1	0	0
Ig alpha-1 chain C region OS=Homo sapiens GN=IGHA1 PE=1 SV=2	IGHA1_HUM	38 kDa	0	0	0	0	0	0	0	0	0	0	0	0	3	0	0	0	0	24	45	2	0	0	0	1	0	0	0	0	0	0	0	0	0	0	0	0
Ig lambda-2 chain C regions OS=Homo sapiens GN=IGLC2 PE=1 SV=1	LAC2_HUMA	11 kDa	0	0	0	0	0	0	0	0	0	0	15	0	0	0	0	0	0	13	45	9	0	1	5	0	0	0	0	0	0	0	0	0	0	0	0	0
Carboxypeptidase N catalytic chain OS=Homo sapiens GN=CPN1 PE=1 SV=1	CBPN_HUM	52 kDa	0	0	0	0	0	0	0	0	1	24	0	0	5	9	0	6	0	9	1	3	0	7	7	0	0	0	0	0	0	0	0	0	5	0	0	0
StAR-related lipid transfer protein 9 OS=Homo sapiens GN=STARD9 PE=1 SV=3	STAR9_HUM	516 kDa	0	0	0	0	0	0	0	0	0	0	0	0	0	0	0	0	0	0	0	1	0	0	0	0	0	0	0	0	0	0	0	0	0	0	0	0
Coiled-coil domain-containing protein 167 OS=Homo sapiens GN=CCDC167 PE=1 SV=2	CC167_HUM	11 kDa	0	0	0	0	0	0	0	0	0	0	0	0	0	0	0	0	0	0	0	0	0	0	0	0	0	0	0	0	0	0	0	0	3	0	0	0
Alpha-1-antichymotrypsin OS=Homo sapiens GN=SERPINA3 PE=1 SV=2	AACT_HUM	48 kDa	0	0	0	0	0	0	0	0	0	2	0	0	0	0	3	0	0	11	49	4	0	0	0	0	0	0	0	0	0	0	0	0	0	0	0	0
Zinc finger protein basonuclin-2 OS=Homo sapiens GN=BNC2 PE=1 SV=1	BNC2_HUM	122 kDa	0	0	0	0	0	0	0	0	0	0	0	0	0	0	0	0	0	1	0	0	0	0	0	0	0	0	0	0	0	0	0	0	0	0	0	0
Protein WWC3 OS=Homo sapiens GN=WWC3 PE=1 SV=3	WWC3_HUM	123 kDa	8	0	0	0	0	0	0	0	1	0	3	0	0	0	0	0	0	0	9	1	0	1	0	0	0	0	0	0	0	0	0	0	4	0	0	0
Plasminogen OS=Homo sapiens GN=PLG PE=1 SV=2	PLMN_HUM	91 kDa	0	0	0	0	0	0	0	0	0	1	0	0	2	0	0	0	0	1	29	6	0	0	1	0	1	0	0	0	0	0	7	0	1	0	0	0
Complement C1s subcomponent OS=Homo sapiens GN=C1S PE=1 SV=1	C1S_HUMAN	77 kDa	2	0	0	0	0	0	0	0	0	2	0	1	3	0	0	0	0	6	2	0	0	11	17	0	0	0	0	0	0	0	10	0	0	0	0	0
Angiopoietin-related protein 6 OS=Homo sapiens GN=ANGPTL6 PE=1 SV=1	ANGL6_HUM	52 kDa	0	0	0	0	0	0	0	0	0	0	2	0	4	0	0	0	0	0	2	2	0	0	0	0	0	0	0	0	0	0	0	0	0	0	0	0
Serum paraoxonase/arylesterase 1 OS=Homo sapiens GN=PON1 PE=1 SV=3	PON1_HUM	40 kDa	0	0	0	0	0	0	0	0	0	0	5	0	2	0	0	0	0	14	4	1	0	9	19	1	0	0	0	0	0	0	1	0	0	0	0	0
Complement factor B OS=Homo sapiens GN=CFB PE=1 SV=2	CFAB_HUM	86 kDa	0	0	0	0	0	0	0	0	0	0	0	0	1	0	0	0	0	16	27	0	0	3	1	0	0	0	0	0	0	0	0	0	0	0	0	0
40S ribosomal protein S20 OS=Homo sapiens GN=RPS20 PE=1 SV=1	RS20_HUMA	13 kDa	0	0	0	0	0	0	0	0	0	0	0	11	0	4	0	1	0	0	0	0	1	0	0	0	0	0	0	1	0	0	0	10	0	1	0	4
Cluster of Actin, alpha cardiac muscle 1 OS=Homo sapiens GN=ACTC1 PE=1 SV=1 (ACTC_HUMAN)	ACTC_HUMA	42 kDa	0	0	0	0	0	0	0	0	0	0	0	0	8	0	0	0	0	0	1	0	0	3	0	0	5	0	8	4	0	0	0	0	0	0	0	0
Musclebind-like protein 1 OS=Homo sapiens GN=MBNL1 PE=1 SV=2	MBNL1_HUM	42 kDa	0	0	0	0	0	0	0	0	0	0	0	0	0	0	0	0	0	0	0	0	0	0	0	0	2	0	0	0	0	0	0	0	0	0	0	0
Regulatory-associated protein of mTOR OS=Homo sapiens GN=RPTOR PE=1 SV=1	RPTOR_HUM	149 kDa	0	0	0	0	0	0	0	0	0	0	5	0	0	0	0	0	0	0	0	0	0	0	0	0	0	0	3	0	0	0	0	0	0	0	0	0
RalA-binding protein 1 OS=Homo sapiens GN=RALBP1 PE=1 SV=3	RBP1_HUM	76 kDa	0	0	0	0	0	0	0	0	0	1	0	0	0	0	0	0	0	0	0	0	0	0	0	0	0	0	0	0	0	0	0	0	0	0	0	0
Apolipoprotein(a) OS=Homo sapiens GN=LPA PE=1 SV=1	APOA_HUM	501 kDa	0	0	7	0	0	0	0	0	0	0	0	0	0	0	14	1	0	6	0	0	0	0	7	1	0	0	0	0	0	0	0	0	0	0	0	0
Pleckstrin homology domain-containing family A member 8 OS=Homo sapiens GN=PLEKHA8 PE=1 SV=3	PKHA8_HUM	58 kDa	0	0	0	0	0	0	0	0	0	0	0	0	0	0	0	12	0	0	0	0	0	0	0	0	0	0	0	0	0	0	0	0	0	0	0	0
Ceruloplasmin OS=Homo sapiens GN=CP PE=1 SV=1	CERU_HUM	122 kDa	0	0	0	0	0	0	0	0	0	0	0	0	0	0	0	0	0	0	36	0	0	0	0	0	0	0	0	0	0	0	0	0	0	0	0	0
Inter-alpha-trypsin inhibitor heavy chain H1 OS=Homo sapiens GN=ITIH1 PE=1 SV=3	ITIH1_HUM	101 kDa	0	0	0	0	0	0	0	0	0	0	0	0	1	0	0	0	0	5	17	0	0	0	2	0	0	0	0	0	0	0	0	0	0	0	0	0
Centrin-2 OS=Homo sapiens GN=CETN2 PE=1 SV=1	CETN2_HUM	20 kDa	0	0	4	2	0	0	0	0	0	0	1	0	1	0	1	1	0	0	0	0	0	3	0	0	0	0	0	0	1	0	0	0	0	0	0	0
Heparin cofactor 2 OS=Homo sapiens GN=SERPIND1 PE=1 SV=3	HEP2_HUM	57 kDa	0	0	0	0	0	0	0	0	2	0	0	5	0	0	0	0	0	9	11	3	0	1	2	0	0	0	0	0	0	0	0	0	0	0	0	0
Gelsolin OS=Homo sapiens GN=GSN PE=1 SV=1	GELS_HUM	86 kDa	0	0	0	0	0	0	0	0	0	0	0	0	0	0	0	0	0	14	3	0	0	0	0	0	0	0	0	0	0	0	0	0	0	0	0	0
Immunoglobulin lambda-like polypeptide 5 OS=Homo sapiens GN=IGLL5 PE=2 SV=2	IGLL5_HUM	23 kDa	0	0	0	0	0	0	0	0	0	0	0	0	3	0	0	0	0	7	10	0	0	0	0	0	0	0	0	0	0	0	0	0	0	0	0	0
Vitamin K-dependent protein S OS=Homo sapiens GN=PROS1 PE=1 SV=1	PROS_HUM	75 kDa	0	0	0	0	0	0	0	0	4	0	0	1	0	0	3	0	0	6	0	0	0	1	0	0	0	0	0	0	0	5	0	0	0	0	0	0
Alpha-1B-glycoprotein OS=Homo sapiens GN=A1BG PE=1 SV=4	A1BG_HUM	54 kDa	0	0	0	0	0	0	0	0	0	0	0	0	0	0	6	0	0	3	9	0	0	3	0	3	0	0	0	0	0	0	0	0	0	0	0	0
Zinc finger BED domain-containing protein 5 OS=Homo sapiens GN=ZBED5 PE=2 SV=2	ZBED5_HUM	79 kDa	0	0	0	0	0	0	0	0	0	0	0	0	0	0	0	0	0	0	3	0	0	0	0	0	0	0	3	0	0	0	0	0	0	0	0	0

5.6 REFERENCES

1. Krzyszczyk P, Acevedo A, Davidoff EJ, Timmins LM, Marrero-Berrios I, Patel M, et al. The growing role of precision and personalized medicine for cancer treatment. Technology (Singap World Sci). 2018;6(3-4):79-100.

2. Haber D, Bell D, Sordella R, Kwak E, Godin-Heymann N, Sharma S, et al., editors. Molecular targeted therapy of lung cancer: EGFR mutations and response to EGFR inhibitors. Cold Spring Harbor symposia on quantitative biology; 2005: Cold Spring Harbor Laboratory Press.

3. Kobayashi S, Canepa HM, Bailey AS, Nakayama S, Yamaguchi N, Goldstein MA, et al. Compound EGFR mutations and response to EGFR tyrosine kinase inhibitors. J Thorac Oncol. 2013;8(1):45-51.

4. Suryavanshi M, Shah A, Kumar D, Panigrahi MK, Metha A, Batra U. MET Amplification and Response to MET Inhibitors in Stage IV Lung Adenocarcinoma. Oncol Res Treat. 2017;40(4):198-202.

5. Paik PK, Drilon A, Fan PD, Yu H, Rekhtman N, Ginsberg MS, et al. Response to MET inhibitors in patients with stage IV lung adenocarcinomas harboring MET mutations causing exon 14 skipping. Cancer Discov. 2015;5(8):842-9.

6. Salgia R, Sattler M, Scheele J, Stroh C, Felip E. The promise of selective MET inhibitors in non-small cell lung cancer with MET exon 14 skipping. Cancer Treatment Reviews. 2020;87:102022.

7. Chia PL, Mitchell P, Dobrovic A, John T. Prevalence and natural history of ALK positive non-small-cell lung cancer and the clinical impact of targeted therapy with ALK inhibitors. Clin Epidemiol. 2014;6:423-32.

8. Malone ER, Oliva M, Sabatini PJB, Stockley TL, Siu LL. Molecular profiling for precision cancer therapies. Genome Medicine. 2020;12(1):8.

9. Tung NM, Garber JE. BRCA1/2 testing: therapeutic implications for breast cancer management. British Journal of Cancer. 2018;119(2):141-52.

10. Yan Y, Guo G, Huang J, Gao M, Zhu Q, Zeng S, et al. Current understanding of extrachromosomal circular DNA in cancer pathogenesis and therapeutic resistance. Journal of Hematology & Oncology. 2020;13(1):124.

11. Junqueira-Neto S, Batista IA, Costa JL, Melo SA. Liquid Biopsy beyond Circulating Tumor Cells and Cell-Free DNA. Acta Cytol. 2019;63(6):479-88.

12. Lin T-C, Yang C-H, Cheng L-H, Chang W-T, Lin Y-R, Cheng H-C. Fibronectin in Cancer: Friend or Foe. Cells. 2019;9(1):27.

CHAPTER 6

DISCUSSION AND CONTRIBUTION TO KNOWLEDGE

It is becoming increasingly clear that molecular diagnostics has revolutionized modern medicine. It is providing data that are continuously transforming the clinical management of advanced cancers. The discoveries in the context of the current thesis will advance knowledge on new approaches to adapt proteomics and imaging data to the interpretation of drug effect using receptor tyrosine kinase inhibitor scaffolds to read biological systems.

6.1 Chemoprobes as tools to potentially advance knowledge in systems medicine

Systems medicine is defined as an interdisciplinary field that examines the systems of human functions as an integrated whole involving biochemical physiological and environment controlled interactions (244-246). When activities in systems medicine are related to drug effect, it is now referred to as systems pharmacology (247, 248). This is an emerging field that considers an analysis of drug action not on a one-drug-one-target basis, but rather a one-drug-multiple target rationale (249, 250). When a drug is absorbed by a patient, it can be either eliminated and/or interact with specific targets localized at specific organs (251). In the therapy of cancer, in order to induce an effect, the drug has to interact and kill cancerous cells in the tumours to exert favorable pharmacodynamics (252). Cancer cell are characterized by several biochemical pathways that function in tandem in response to drug exposure. The response is mediated by a number of critical targets, which must be blocked in order to arrest the cell cycle and delay tumour growth (253). Classical drug design selects one target with the expectation that it is the main controller of the pharmacodynamics. Recent studies showed that in contrast to the common belief, most drugs have multiple targets that may either play a role in its pharmacodynamics or contribute to its *in vivo* toxicity (159, 237, 254, 255). It is in this context that systems pharmacology is emerging as a dynamic field of interpretation of drug effects (256). Essential to this emergence are biochemical

tools that are required to capture the diversity of targets of a drug (e.g. kinase, metabolic enzyme or DNA repair inhibitors etc.). In this thesis, we demonstrated that we could design and synthesize these tools, and probe biological fluids in order to determine the profile of targeting of two classes of drugs: EGFR and MET inhibitors. More importantly, we took their target profiling one step further, by using them to rationalize drug combination. Furthermore, we executed a proof-of-principle study to demonstrate that these tools could pull-down proteins from patients samples, thereby opening the prospect of developing them as diagnostic tools to monitor drug response retrospectively and prospectively. Our results suggest that the chemoprobe approach has the potential to be used to advance the modern field of systems pharmacology.

6.2 Chemoprobes to visualize target multiplicity

The chemoprobes synthesized in the context of this thesis were designed on the basis of their binding capacity to the ATP pocket of the receptor tyrosine kinases EGFR and MET a PEG linker extension and a biotin tag, using click chemistry for spacing the tag away from the warhead. The latter reaction that has revolutionized bioorthogonal chemistry opened the way to elongating the linker and adding a biotin tag that cannot interfere with the kinase targeting warhead. This given us the opportunity to create innovative and suitable probes for magnetic pull-down (257). Despite their size, these probes could be easily purified by standard column chromatography. Although we could not provide crystallographic evidence of the probe binding to the receptors, we showed by computational modelling that indeed the probes were designed with proper distancing to avoid interactions of the biotin tag with the ATP site of the receptors. The design of the EGFR probe AB31 was based on structure-activity relationship (SAR) discovered in our laboratory that showed the contribution of a hydrogen bond between the N-aminomethylbenzyl nitrogen and Asp776 of

EGFR (258). This unique mode of binding distinguishes AB31 from Sepharose-linked gefitinib-like warheads. Indeed the pull-down profiles of AB31 was markedly different from those previously reported for Sepharose-bead immobilized gefitinib (159).

The design of the MET-targeting probe was made on full retention of the main features of the crizotinib scaffold and revealed a very strong pull-down capacity of MET by the probe. Simulation by molecular modelling also showed proper distancing of the warhead as to the biotin tag. In order to distinguish background pull-down from AB19 specific binding, the crizotinib warhead was replaced by a cyclohexyl group, leading to AB22, a control probe used throughout the study.

Furthermore, in the context of rationally developing live imaging tools that reflects the target multiplicity of MET and EGFR inhibitors, we designed imaging probes that carry the same kinase inhibitor warhead as AB19 (MET targeting), and AB31 (EGFR targeting) but labeled with chromophores of different colors (green or red). We showed that using an endogenously expressed GFP-labeled full length EGFR, that the EGFR-targeted probe could be distributed in the same location as the endogenously expressed EGFR in the intracellular compartment. However, no membrane co-localization was seen. Likewise, we also gave evidence that AB30 a green fluorescent probe designed with the same warhead as AB19 could be synthesized and its associated green fluorescence was primarily localized intracellularly and was not observed in the cell membrane. The results suggest that while the EGFR and MET inhibitors block ligand-mediated signaling at the level of cell membranes, their primary localization is inside the cells and in the perinuclear region. This may have mechanistic significance as recent studies suggest that EGFR and MET are present in organelles such as the mitochondria, the Golgi apparatus and ER. The

localization of an EGFR inhibitor in the mitochondria has recently been associated with its ability to activate the mitochondrial apoptotic pathway (145, 157, 158, 163, 259-261). This is in agreement with our consistent observation of our fluorescent probes in the perinuclear region of the cells.

6.3 Chemoprobes to design drug combination and monitor clinical responses

The MET receptor tyrosine kinase is involved in a number of processes that drive tumour progression including migration, metastasis, invasion, and apoptosis (262, 263). Therefore, we extensively explore the impact of probing the targets of MET in tumour cells from various origins, including prostate and gastric cancer cells. It is now common knowledge that in prostate cancer, loss of androgen sensitivity is associated with MET expression, which activates a number of pathways that increase the aggressiveness of the tumours (264-266). In the advanced stages of prostate cancer, paclitaxel is the most commonly used drug in the clinic (267-270). We have, therefore, used our MET probe to track drug-induced changes in the target profiling of crizotinib that could be exploited to enhance the activity of paclitaxel in castration resistant prostate cancer. Our work led to the discovery that perhaps if crizotinib is given in the clinic and reached the tumour, the following targets could be modulated: RON, SRC, LCK, EPHA2, SLK, FAK1, AURKA, MLKL, AXL, and other non-kinase ones. More importantly, our work suggests that if paclitaxel is given for 24h, and crizotinib is to be subsequently administered, the following targets can be modulated by crizotinib: RON, AURKA, AURKB, and FAK1. This work was not designed to determine the extent of binding of the AB19/crizotinib to the different targets, therefore, we executed experiments wherein each of these targets could be modulated using dose ranges of their corresponding inhibitors. This is the first study that uses drug-induced changes in target profiling,

as revealed by a chemoprobe, to design combinatorial target modulation for augmenting the potency of a standard of care drug in the clinic. Indeed, using computational modelling to detect synergism antagonism (Compusyn), we showed that addition of crizotinib to paclitaxel was not synergistic. However, modulating the following targets AURKA led to a synergistic interaction with paclitaxel. Strikingly, we thought the literature for clinical trial involving paclitaxel and the potent inhibitor alisertib. Interestingly, the discovery was validated by recent clinical trials undertaken with the combination of paclitaxel with the AURKA inhibitor alisertib that showed significant effect in lung and ovarian cancers. The paclitaxel + alisertib combination is now described as one of the most promising combinations in the clinical management of advanced lung and ovarian cancers (271).

6.4 Summary of the versatility of the discovered chemoprobes

As depicted in Figure 6.1, this work has contributed to the discovery of new chemoprobes to pull down kinases from biological medium, and these probes revealed a number of targets under conditions where tumour cells were drug- and non-drug treatment. This translated to the rational discovery of new combinations that were either validated by recent clinical trials or that can be developed in the future (e.g. paclitaxel + mTOR inhibitor torkinib).

We also discovered that these probes could pull down meaningful proteins from patient samples collected from clinical trials. This work has contributed to the reading of drug binding profiles by a magnetic pull-down technology that can be easily applied to not cell lysates but also human plasma. In summary, as per Figure 6.1, we designed and synthesized chemoprobes that were first validated using cell lines expressing high levels of the canonical target, to identify kinases that

were common to the one already available in databases using proteomics analysis. Following the validation, we chose to use the probes to diagnose targeting profiles in normal prostate and cancerous prostate cells. The drug modulations study in the prostate cancer cells led to the discovery of clinically validated combination (alisertib + paclitaxel) and set the basis for the rational design of future combinations with paclitaxel

The chemoprobes could also be used to explore to localization of receptor tyrosine kinase inhibitors through live imaging in a context where proteins are distributed in their corresponding organelles. Further development of the approach will lead to a new rationale for exploring molecular probes as tools to provide data that may be used in Data Science for clinical decision making.

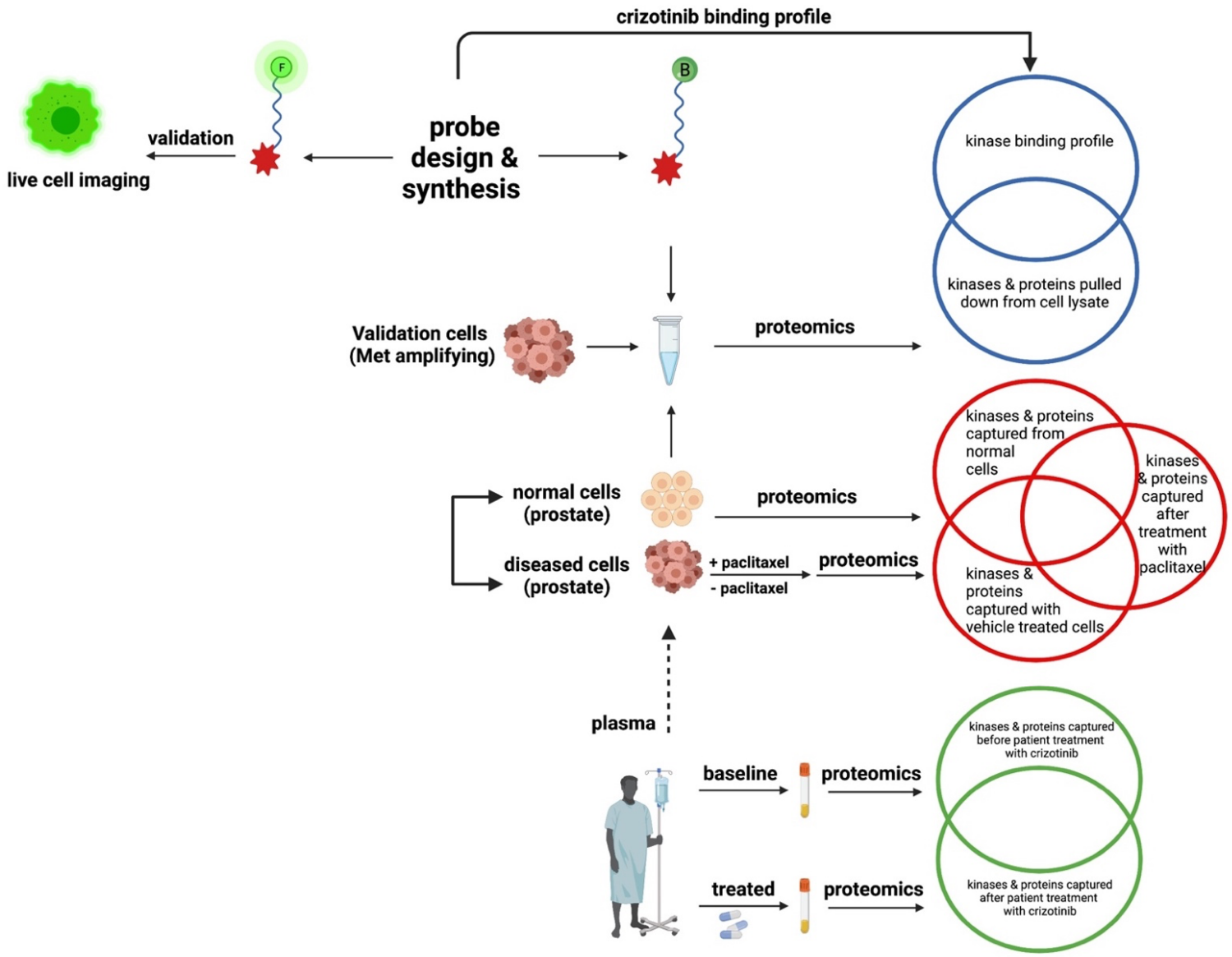

Figure 6.1 Schematic representation of the versatility of the chemoprobes synthesized in the context of this thesis

6.5 REFERENCES

1. Lynch TJ, Bell DW, Sordella R, Gurubhagavatula S, Okimoto RA, Brannigan BW, et al. Activating mutations in the epidermal growth factor receptor underlying responsiveness of non-small-cell lung cancer to gefitinib. N Engl J Med. 2004;350(21):2129-39.

2. Paez JG, Jänne PA, Lee JC, Tracy S, Greulich H, Gabriel S, et al. EGFR mutations in lung cancer: correlation with clinical response to gefitinib therapy. Science. 2004;304(5676):1497-500.

3. Zhong L, Li Y, Xiong L, Wang W, Wu M, Yuan T, et al. Small molecules in targeted cancer therapy: advances, challenges, and future perspectives. Signal Transduction and Targeted Therapy. 2021;6(1):201.

4. Capdeville R, Buchdunger E, Zimmermann J, Matter A. Glivec (STI571, imatinib), a rationally developed, targeted anticancer drug. Nat Rev Drug Discov. 2002;1(7):493-502.

5. Oh HJ, Cho MS, Lee JW, Jang P-S, Chung N-G, Cho B, et al. Efficacy of imatinib mesylate-based front-line therapy in pediatric chronic myelogenous leukemia. Korean journal of pediatrics. 2013;56(8):343.

6. Manning G, Whyte DB, Martinez R, Hunter T, Sudarsanam S. The protein kinase complement of the human genome. Science. 2002;298(5600):1912-34.

7. Cicenas J, Zalyte E, Bairoch A, Gaudet P. Kinases and Cancer. Cancers. 2018;10(3):63.

8. Logue JS, Morrison DK. Complexity in the signaling network: insights from the use of targeted inhibitors in cancer therapy. Genes Dev. 2012;26(7):641-50.

9. Bhullar KS, Lagarón NO, McGowan EM, Parmar I, Jha A, Hubbard BP, et al. Kinase-targeted cancer therapies: progress, challenges and future directions. Molecular cancer. 2018;17(1):1-20.

10. Knapp S. New opportunities for kinase drug repurposing and target discovery. British Journal of Cancer. 2018;118(7):936-7.

11. Hantschel O. Unexpected off-targets and paradoxical pathway activation by kinase inhibitors. ACS chemical biology. 2015;10(1):234-45.

12. Blume-Jensen P, Hunter T. Oncogenic kinase signalling. Nature. 2001;411(6835):355-65.

13. Hunter T. Signaling--2000 and beyond. Cell. 2000;100(1):113-27.

14. Cohen P. Protein kinases--the major drug targets of the twenty-first century? Nat Rev Drug Discov. 2002;1(4):309-15.

15. Matthews DJ, Gerritsen ME. Targeting protein kinases for cancer therapy: John Wiley & Sons; 2011.

16. Manning G, Plowman GD, Hunter T, Sudarsanam S. Evolution of protein kinase signaling from yeast to man. Trends Biochem Sci. 2002;27(10):514-20.

17. Shchemelinin I, Sefc L, Necas E. Protein kinases, their function and implication in cancer and other diseases. Folia biologica. 2006;52(3):81.

18. Greenman C, Stephens P, Smith R, Dalgliesh GL, Hunter C, Bignell G, et al. Patterns of somatic mutation in human cancer genomes. Nature. 2007;446(7132):153-8.

19. Stephens P, Edkins S, Davies H, Greenman C, Cox C, Hunter C, et al. A screen of the complete protein kinase gene family identifies diverse patterns of somatic mutations in human breast cancer. Nature genetics. 2005;37(6):590-2.

20. Levene P, Alsberg C. The cleavage products of vitellin. Journal of Biological Chemistry. 1906;2(1):127-33.

21. Bernard C. Leçons de physiologie expérimentale appliquée à la médecine: faites au Collège de France: JB Baillière et fils; 1855.

22. Young FG. Claude Bernard and the discovery of glycogen. British Medical Journal. 1957;1(5033):1431.

23. Cori GT, Green AA. Crystalline muscle phosphorylase II. Prosthetic group. Journal of Biological Chemistry. 1943;151(1):31-8.

24. Cohen P. The origins of protein phosphorylation. Nature cell biology. 2002;4(5):E127-E30.

25. Burnett G, Kennedy EP. The enzymatic phosphorylation of proteins. Journal of Biological Chemistry. 1954;211(2):969-80.

26. Fischer EH, Graves DJ, Crittenden ERS, Krebs EG. Structure of the site phosphorylated in the phosphorylase b to a reaction. Journal of Biological Chemistry. 1959;234(7):1698-704.

27. Krebs EG, Fischer EH. The phosphorylase b to a converting enzyme of rabbit skeletal muscle. Biochimica et biophysica acta. 1956;20:150-7.

28. Hunter T, Sefton BM. Transforming gene product of Rous sarcoma virus phosphorylates tyrosine. Proc Natl Acad Sci U S A. 1980;77(3):1311-5.

29. Witte ON, Dasgupta A, Baltimore D. Abelson murine leukaemia virus protein is phosphorylated in vitro to form phosphotyrosine. Nature. 1980;283(5750):826-31.

30. Ushiro H, Cohen S. Identification of phosphotyrosine as a product of epidermal growth factor-activated protein kinase in A-431 cell membranes. Journal of Biological Chemistry. 1980;255(18):8363-5.

31. Kasuga M, Karlsson FA, Kahn CR. Insulin stimulates the phosphorylation of the 95,000-dalton subunit of its own receptor. Science. 1982;215(4529):185-7.

32. Yarden Y, Schlessinger J. Self-phosphorylation of epidermal growth factor receptor: evidence for a model of intermolecular allosteric activation. Biochemistry. 1987;26(5):1434-42.

33. Yarden Y, Schlessinger J. Epidermal growth factor induces rapid, reversible aggregation of the purified epidermal growth factor receptor. Biochemistry. 1987;26(5):1443-51.

34. Cooper CS, Park M, Blair DG, Tainsky MA, Huebner K, Croce CM, et al. Molecular cloning of a new transforming gene from a chemically transformed human cell line. Nature. 1984;311(5981):29-33.

35. Nakamura T, Nawa K, Ichihara A. Partial purification and characterization of hepatocyte growth factor from serum of hepatectomized rats. Biochemical and biophysical research communications. 1984;122(3):1450-9.

36. Bottaro DP, Rubin JS, Faletto DL, Chan A, Kmiecik TE, Woude GV, et al. Identification of the hepatocyte growth factor receptor as the c-MET proto-oncogene product. Science. 1991;251(4995):802-4.

37. Ray LB, Sturgill TW. Characterization of insulin-stimulated microtubule-associated protein kinase. Rapid isolation and stabilization of a novel serine/threonine kinase from 3T3-L1 cells. J Biol Chem. 1988;263(25):12721-7.

38. Robinson DR, Wu Y-M, Lin S-F. The protein tyrosine kinase family of the human genome. Oncogene. 2000;19(49):5548-57.

39. Xu H, Stabile LP, Gubish CT, Gooding WE, Grandis JR, Siegfried JM. Dual blockade of EGFR and c-MET abrogates redundant signaling and proliferation in head and neck carcinoma cells. Clin Cancer Res. 2011;17(13):4425-38.

40. Miller MA, Oudin MJ, Sullivan RJ, Wang SJ, Meyer AS, Im H, et al. Reduced proteolytic shedding of receptor tyrosine kinases is a post-translational mechanism of kinase inhibitor resistance. Cancer discovery. 2016;6(4):382-99.

41. Organ SL, Tsao M-S. An overview of the c-MET signaling pathway. Therapeutic advances in medical oncology. 2011;3(1_suppl):S7-S19.

42. Singh B, Carpenter G, Coffey RJ. EGF receptor ligands: recent advances. F1000Research. 2016;5.

43. Lemmon MA, Schlessinger J. Cell signaling by receptor tyrosine kinases. Cell. 2010;141(7):1117-34.

44. Ullrich A, Schlessinger J. Signal transduction by receptors with tyrosine kinase activity. Cell. 1990;61(2):203-12.

45. Schlessinger J. Cell signaling by receptor tyrosine kinases. Cell. 2000;103(2):211-25.

46. Neet K, Hunter T. Vertebrate non-receptor protein–tyrosine kinase families. Genes to Cells. 1996;1(2):147-69.

47. Thomas SM, Brugge JS. Cellular functions regulated by Src family kinases. Annual review of cell and developmental biology. 1997;13(1):513-609.

48. Fischer EH, Krebs EG. Conversion of phosphorylase b to phosphorylase a in muscle extracts. Journal of Biological Chemistry. 1955;216(1):121-32.

49. Hunter T. Protein kinases and phosphatases: the yin and yang of protein phosphorylation and signaling. Cell. 1995;80(2):225-36.

50. Pawson T, Gish GD, Nash P. SH2 domains, interaction modules and cellular wiring. Trends in cell biology. 2001;11(12):504-11.

51. Gocek E, Moulas AN, Studzinski GP. Non-receptor protein tyrosine kinases signaling pathways in normal and cancer cells. Critical reviews in clinical laboratory sciences. 2014;51(3):125-37.

52. Pawson T, Kofler M. Kinome signaling through regulated protein–protein interactions in normal and cancer cells. Current opinion in cell biology. 2009;21(2):147-53.

53. Hantschel O, Superti-Furga G. Regulation of the c-Abl and Bcr–Abl tyrosine kinases. Nature reviews Molecular cell biology. 2004;5(1):33-44.

54. Colicelli J. ABL tyrosine kinases: evolution of function, regulation, and specificity. Science signaling. 2010;3(139):re6-re.

55. Pluk H, Dorey K, Superti-Furga G. Autoinhibition of c-Abl. Cell. 2002;108(2):247-59.

56. Barilá D, Superti-Furga G. An intramolecular SH3-domain interaction regulates c-Abl activity. Nature genetics. 1998;18(3):280-2.

57. Hantschel O, Nagar B, Guettler S, Kretzschmar J, Dorey K, Kuriyan J, et al. A myristoyl/phosphotyrosine switch regulates c-Abl. Cell. 2003;112(6):845-57.

58. Nagar B, Hantschel O, Seeliger M, Davies JM, Weis WI, Superti-Furga G, et al. Organization of the SH3-SH2 unit in active and inactive forms of the c-Abl tyrosine kinase. Mol Cell. 2006;21(6):787-98.

59. Reddy EP, Aggarwal AK. The ins and outs of bcr-abl inhibition. Genes Cancer. 2012;3(5-6):447-54.

60. Gorre ME, Mohammed M, Ellwood K, Hsu N, Paquette R, Rao PN, et al. Clinical resistance to STI-571 cancer therapy caused by BCR-ABL gene mutation or amplification. Science. 2001;293(5531):876-80.

61. Schindler T, Bornmann W, Pellicena P, Miller WT, Clarkson B, Kuriyan J. Structural mechanism for STI-571 inhibition of abelson tyrosine kinase. Science. 2000;289(5486):1938-42.

62. Liu Y, Shah K, Yang F, Witucki L, Shokat KM. A molecular gate which controls unnatural ATP analogue recognition by the tyrosine kinase v-Src. Bioorg Med Chem. 1998;6(8):1219-26.

63. Burmeister T, Schwartz S, Bartram CR, Gökbuget N, Hoelzer D, Thiel E. Patients' age and BCR-ABL frequency in adult B-precursor ALL: a retrospective analysis from the GMALL study group. Blood. 2008;112(3):918-9.

64. Nowell PC, Hungerford DA. Chromosome Studies on Normal and Leukemic Human Leukocytes. JNCI: Journal of the National Cancer Institute. 1960;25(1):85-109.

65. Azam M, Seeliger MA, Gray NS, Kuriyan J, Daley GQ. Activation of tyrosine kinases by mutation of the gatekeeper threonine. Nature structural & molecular biology. 2008;15(10):1109.

66. An X, Tiwari AK, Sun Y, Ding PR, Ashby CR, Jr., Chen ZS. BCR-ABL tyrosine kinase inhibitors in the treatment of Philadelphia chromosome positive chronic myeloid leukemia: a review. Leuk Res. 2010;34(10):1255-68.

67. Buchdunger E, O'Reilly T, Wood J. Pharmacology of imatinib (STI571). Eur J Cancer. 2002;38 Suppl 5:S28-36.

68. Druker BJ, Lydon NB. Lessons learned from the development of an abl tyrosine kinase inhibitor for chronic myelogenous leukemia. J Clin Invest. 2000;105(1):3-7.

69. O'Brien SG, Guilhot F, Larson RA, Gathmann I, Baccarani M, Cervantes F, et al. Imatinib compared with interferon and low-dose cytarabine for newly diagnosed chronic-phase chronic myeloid leukemia. N Engl J Med. 2003;348(11):994-1004.

70. Zheng J, Knighton DR, ten Eyck LF, Karlsson R, Xuong N, Taylor SS, et al. Crystal structure of the catalytic subunit of cAMP-dependent protein kinase complexed with MgATP and peptide inhibitor. Biochemistry. 1993;32(9):2154-61.

71. Mohammadi M, McMahon G, Sun L, Tang C, Hirth P, Yeh BK, et al. Structures of the tyrosine kinase domain of fibroblast growth factor receptor in complex with inhibitors. Science. 1997;276(5314):955-60.

72. Hochhaus A, Larson RA, Guilhot F, Radich JP, Branford S, Hughes TP, et al. Long-Term Outcomes of Imatinib Treatment for Chronic Myeloid Leukemia. New England Journal of Medicine. 2017;376(10):917-27.

73. Hochhaus A, Kreil S, Corbin A, La Rosee P, Müller M, Lahaye T, et al. Molecular and chromosomal mechanisms of resistance to imatinib (STI571) therapy. Leukemia. 2002;16(11):2190-6.

74. Bhamidipati PK, Kantarjian H, Cortes J, Cornelison AM, Jabbour E. Management of imatinib-resistant patients with chronic myeloid leukemia. Ther Adv Hematol. 2013;4(2):103-17.

75. Weisberg E, Manley PW, Breitenstein W, Brüggen J, Cowan-Jacob SW, Ray A, et al. Characterization of AMN107, a selective inhibitor of native and mutant Bcr-Abl. Cancer cell. 2005;7(2):129-41.

76. Zhou T, Commodore L, Huang WS, Wang Y, Thomas M, Keats J, et al. Structural mechanism of the pan-BCR-ABL inhibitor ponatinib (AP24534): lessons for overcoming kinase inhibitor resistance. Chemical biology & drug design. 2011;77(1):1-11.

77. Nicolini FE, Basak GW, Kim D-W, Olavarria E, Pinilla-Ibarz J, Apperley JF, et al. Overall survival with ponatinib versus allogeneic stem cell transplantation in Philadelphia chromosome-positive leukemias with the T315I mutation. Cancer. 2017;123(15):2875-80.

78. Traynor AM, Hewitt M, Liu G, Flaherty KT, Clark J, Freedman SJ, et al. Phase I dose escalation study of MK-0457, a novel Aurora kinase inhibitor, in adult patients with advanced solid tumors. Cancer chemotherapy and pharmacology. 2011;67(2):305-14.

79. Meulenbeld HJ, Mathijssen RH, Verweij J, de Wit R, de Jonge MJ. Danusertib, an aurora kinase inhibitor. Expert Opin Investig Drugs. 2012;21(3):383-93.

80. Cortes J, Talpaz M, Smith HP, Snyder DS, Khoury J, Bhalla KN, et al. Phase 1 dose-finding study of rebastinib (DCC-2036) in patients with relapsed chronic myeloid leukemia and acute myeloid leukemia. Haematologica. 2017;102(3):519-28.

81. Weisberg E, Choi HG, Barrett R, Zhou W, Zhang J, Ray A, et al. Discovery and characterization of novel mutant FLT3 kinase inhibitors. Molecular cancer therapeutics. 2010;9(9):2468-77.

82. Jones JK, Thompson EM. Allosteric Inhibition of ABL Kinases: Therapeutic Potential in Cancer. Molecular cancer therapeutics. 2020;19(9):1763-9.

83. Administration FaD. FDA approves asciminib for Philadelphia chromosome-positive chronic myeloid leukemia
2021 [

84. Attili I, Karachaliou N, Conte P, Bonanno L, Rosell R. Therapeutic approaches for T790M mutation positive non-small-cell lung cancer. Expert Review of Anticancer Therapy. 2018;18(10):1021-30.

85. Engel J, Richters A, Getlik M, Tomassi S, Keul M, Termathe M, et al. Targeting Drug Resistance in EGFR with Covalent Inhibitors: A Structure-Based Design Approach. Journal of Medicinal Chemistry. 2015;58(17):6844-63.

86. Lu X, Yu L, Zhang Z, Ren X, Smaill JB, Ding K. Targeting EGFRL858R/T790M and EGFRL858R/T790M/C797S resistance mutations in NSCLC: Current developments in medicinal chemistry. Medicinal research reviews. 2018;38(5):1550-81.

87. Ciardiello F, Tortora G. A novel approach in the treatment of cancer: targeting the epidermal growth factor receptor. Clin Cancer Res. 2001;7(10):2958-70.

88. Grandis JR, Zeng Q, Tweardy DJ. Retinoic acid normalizes the increased gene transcription rate of TGF–α and EGFR in head and neck cancer cell lines. Nature medicine. 1996;2(2):237-40.

89. Nagatsuka H, Ishiwari Y, Tsujigiwa H, Nakano K, Nagai N. Quantitation of epidermal growth factor receptor gene amplification by competitive polymerase chain reaction in pre-malignant and malignant oral epithelial lesions. Oral oncology. 2001;37(7):599-604.

90. Wong AJ, Ruppert JM, Bigner SH, Grzeschik CH, Humphrey PA, Bigner DS, et al. Structural alterations of the epidermal growth factor receptor gene in human gliomas. Proceedings of the National Academy of Sciences. 1992;89(7):2965-9.

91. Grandis JR, Melhem MF, Barnes EL, Tweardy DJ. Quantitative immunohistochemical analysis of transforming growth factor-α and epidermal growth factor receptor in patients with squamous cell carcinoma of the head and neck. Cancer: Interdisciplinary International Journal of the American Cancer Society. 1996;78(6):1284-92.

92. Rosell R, Moran T, Queralt C, Porta R, Cardenal F, Camps C, et al. Screening for epidermal growth factor receptor mutations in lung cancer. New England Journal of Medicine. 2009;361(10):958-67.

93. Toolabi M, Moghimi S, Bakhshaiesh TO, Salarinejad S, Aghcheli A, Hasanvand Z, et al. 6-Cinnamoyl-4-arylaminothienopyrimidines as highly potent cytotoxic agents: Design, synthesis

and structure-activity relationship studies. European journal of medicinal chemistry. 2020;185:111786.

94. Fukuoka M, Yano S, Giaccone G, Tamura T, Nakagawa K, Douillard J-Y, et al. Multi-institutional randomized phase II trial of gefitinib for previously treated patients with advanced non–small-cell lung cancer. Journal of clinical oncology. 2003;21(12):2237-46.

95. Kawahara A, Azuma K, Sumi A, Taira T, Nakashima K, Aikawa E, et al. Identification of non-small-cell lung cancer with activating EGFR mutations in malignant effusion and cerebrospinal fluid: Rapid and sensitive detection of exon 19 deletion E746-A750 and exon 21 L858R mutation by immunocytochemistry. Lung Cancer. 2011;74(1):35-40.

96. Wang JP, Wu C-Y, Yeh Y-C, Shyr Y-M, Wu Y-Y, Kuo C-Y, et al. Erlotinib is effective in pancreatic cancer with epidermal growth factor receptor mutations: a randomized, open-label, prospective trial. Oncotarget. 2015;6(20):18162-73.

97. Sequist LV, Waltman BA, Dias-Santagata D, Digumarthy S, Turke AB, Fidias P, et al. Genotypic and histological evolution of lung cancers acquiring resistance to EGFR inhibitors. Sci Transl Med. 2011;3(75):75ra26-75ra26.

98. Kobayashi S, Boggon TJ, Dayaram T, Jänne PA, Kocher O, Meyerson M, et al. EGFR Mutation and Resistance of Non–Small-Cell Lung Cancer to Gefitinib. New England Journal of Medicine. 2005;352(8):786-92.

99. Li D, Ambrogio L, Shimamura T, Kubo S, Takahashi M, Chirieac L, et al. BIBW2992, an irreversible EGFR/HER2 inhibitor highly effective in preclinical lung cancer models. Oncogene. 2008;27(34):4702-11.

100. Engelman JA, Zejnullahu K, Gale CM, Lifshits E, Gonzales AJ, Shimamura T, et al. PF00299804, an irreversible pan-ERBB inhibitor, is effective in lung cancer models with EGFR and ERBB2 mutations that are resistant to gefitinib. Cancer Res. 2007;67(24):11924-32.

101. Yang JC, Shih JY, Su WC, Hsia TC, Tsai CM, Ou SH, et al. Afatinib for patients with lung adenocarcinoma and epidermal growth factor receptor mutations (LUX-Lung 2): a phase 2 trial. Lancet Oncol. 2012;13(5):539-48.

102. Liao BC, Lin CC, Yang JC. Second and third-generation epidermal growth factor receptor tyrosine kinase inhibitors in advanced nonsmall cell lung cancer. Curr Opin Oncol. 2015;27(2):94-101.

103. Ramalingam SS, Vansteenkiste J, Planchard D, Cho BC, Gray JE, Ohe Y, et al. Overall Survival with Osimertinib in Untreated, EGFR-Mutated Advanced NSCLC. New England Journal of Medicine. 2019;382(1):41-50.

104. Salgia R. MET in lung cancer: biomarker selection based on scientific rationale. Molecular cancer therapeutics. 2017;16(4):555-65.

105. Fu Y-T, Zheng H-B, Le Zhou D-QZ, Liu X-L, Sun H. Valproic acid, targets papillary thyroid cancer through inhibition of c-MET signalling pathway. American journal of translational research. 2017;9(6):3138.

106. Zhu L, Xiong X, Kim Y, Okada N, Lu F, Zhang H, et al. Acid sphingomyelinase is required for cell surface presentation of MET receptor tyrosine kinase in cancer cells. Journal of cell science. 2016;129(22):4238-51.

107. Liu W-T, Jing Y-Y, Yu G-f, Chen H, Han Z-p, Yu D-d, et al. Hepatic stellate cell promoted hepatoma cell invasion via the HGF/c-MET signaling pathway regulated by p53. Cell Cycle. 2016;15(7):886-94.

108. Zhang Y, Du Z, Zhang M. Biomarker development in MET-targeted therapy. Oncotarget. 2016;7(24):37370.

109. Liang Y, Liu J, Liu T, Yang X. Anti-c-MET antibody bioconjugated with hollow gold nanospheres as a novel nanomaterial for targeted radiation ablation of human cervical cancer cell. Oncology letters. 2017;14(2):2254-60.

110. Maennling AE, Tur MK, Niebert M, Klockenbring T, Zeppernick F, Gattenlöhner S, et al. Molecular Targeting Therapy against EGFR Family in Breast Cancer: Progress and Future Potentials. Cancers. 2019;11(12):1826.

111. Huang X, Gan G, Wang X, Xu T, Xie W. The HGF-MET axis coordinates liver cancer metabolism and autophagy for chemotherapeutic resistance. Autophagy. 2019;15(7):1258-79.

112. Gunasinghe ND, Wells A, Thompson EW, Hugo HJ. Mesenchymal–epithelial transition (MET) as a mechanism for metastatic colonisation in breast cancer. Cancer and Metastasis Reviews. 2012;31(3):469-78.

113. Rucki AA, Xiao Q, Muth S, Chen J, Che X, Kleponis J, et al. Dual inhibition of Hedgehog and c-MET pathways for pancreatic cancer treatment. Molecular cancer therapeutics. 2017;16(11):2399-409.

114. Safaie Qamsari E, Safaei Ghaderi S, Zarei B, Dorostkar R, Bagheri S, Jadidi-Niaragh F, et al. The c-MET receptor: implication for targeted therapies in colorectal cancer. Tumor biology. 2017;39(5):1010428317699118.

115. Hughes PE, Rex K, Caenepeel S, Yang Y, Zhang Y, Broome MA, et al. In vitro and in vivo activity of AMG 337, a potent and selective MET kinase inhibitor, in MET-dependent cancer models. Molecular cancer therapeutics. 2016;15(7):1568-79.

116. Kuang W, Deng Q, Deng C, Li W, Shu S, Zhou M. Hepatocyte growth factor induces breast cancer cell invasion via the PI3K/Akt and p38 MAPK signaling pathways to up-regulate the expression of COX2. American journal of translational research. 2017;9(8):3816.

117. Imura Y, Nakai T, Yamada S, Outani H, Takenaka S, Hamada K, et al. Functional and therapeutic relevance of hepatocyte growth factor/c-MET signaling in synovial sarcoma. Cancer science. 2016;107(12):1867-76.

118. Pilotto S, Carbognin L, Karachaliou N, Ma P, Rosell R, Tortora G, et al. Tracking MET de-addiction in lung cancer: a road towards the oncogenic target. Cancer treatment reviews. 2017;60:1-11.

119. Wu JC, Wang CT, Hung HC, Wu WJ, Wu DC, Chang MC, et al. Heteronemin Is a Novel c-Met/STAT3 Inhibitor Against Advanced Prostate Cancer Cells. The Prostate. 2016;76(16):1469-83.

120. Bahrami A, Shahidsales S, Khazaei M, Ghayour-Mobarhan M, Maftouh M, Hassanian SM, et al. C-MET as a potential target for the treatment of gastrointestinal cancer: Current status and future perspectives. Journal of cellular physiology. 2017;232(10):2657-73.

121. Barrow-McGee R, Kishi N, Joffre C, Ménard L, Hervieu A, Bakhouche BA, et al. Beta 1-integrin–c-MET cooperation reveals an inside-in survival signalling on autophagy-related endomembranes. Nature communications. 2016;7(1):1-18.

122. Yongwen L, Hongyu L, Jun C. Dysregulation of HGF/c-MET signal pathway and their targeting drugs in lung cancer. Zhongguo Fei Ai Za Zhi. 2014;17(8).

123. Yin B, Liu Z, Wang Y, Wang X, Liu W, Yu P, et al. RON and c-MET facilitate metastasis through the ERK signaling pathway in prostate cancer cells. Oncology Reports. 2017;37(6):3209-18.

124. Doa'a GA-, Al-Husein BA, Qasaimeh GR. A mini-review of c-MET as a potential therapeutic target in melanoma. Biomedicine & Pharmacotherapy. 2017;88:194-202.

125. Cecchi F, Rabe DC, Bottaro DP. Targeting the HGF/MET signalling pathway in cancer. European journal of cancer. 2010;46(7):1260-70.

126. Moghul A, Lin L, Beedle A, Kanbour-Shakir A, DeFrances MC, Liu Y, et al. Modulation of c-MET proto-oncogene (HGF receptor) mRNA abundance by cytokines and hormones: evidence for rapid decay of the 8 kb c-MET transcript. Oncogene. 1994;9(7):2045-52.

127. Furge KA, Kiewlich D, Le P, Vo MN, Faure M, Howlett AR, et al. Suppression of Ras-mediated tumorigenicity and metastasis through inhibition of the MET receptor tyrosine kinase. Proceedings of the National Academy of Sciences. 2001;98(19):10722-7.

128. Pennacchietti S, Michieli P, Galluzzo M, Mazzone M, Giordano S, Comoglio PM. Hypoxia promotes invasive growth by transcriptional activation of the MET protooncogene. Cancer cell. 2003;3(4):347-61.

129. Kuniyasu H, Yasui W, Kitadai Y, Yokozaki H, Ito H, Tahara E. Frequent amplification of the c-MET gene in scirrhous type stomach cancer. Biochemical and biophysical research communications. 1992;189(1):227-32.

130. Di Renzo MF, Olivero M, Giacomini A, Porte H, Chastre E, Mirossay L, et al. Overexpression and amplification of the met/HGF receptor gene during the progression of colorectal cancer. Clinical Cancer Research. 1995;1(2):147-54.

131. Harada D, Isozaki H, Kozuki T, Yokoyama T, Yoshioka H, Bessho A, et al. Crizotinib for recurring non-small-cell lung cancer with EML4-ALK fusion genes previously treated with alectinib: A phase II trial. Thorac Cancer. 2021;12(5):643-9.

132. Fallahi P, Ferrari SM, Di Bari F, Materazzi G, Benvenga S, Miccoli P, et al. Cabozantinib in Thyroid Cancer. Recent Pat Anticancer Drug Discov. 2015;10(3):259-69.

133. Rimassa L, Assenat E, Peck-Radosavljevic M, Pracht M, Zagonel V, Mathurin P, et al. Tivantinib for second-line treatment of MET-high, advanced hepatocellular carcinoma (METIV-HCC): a final analysis of a phase 3, randomised, placebo-controlled study. Lancet Oncol. 2018;19(5):682-93.

134. Scagliotti GV, Shuster D, Orlov S, von Pawel J, Shepherd FA, Ross JS, et al. Tivantinib in Combination with Erlotinib versus Erlotinib Alone for EGFR-Mutant NSCLC: An Exploratory Analysis of the Phase 3 MARQUEE Study. J Thorac Oncol. 2018;13(6):849-54.

135. Pant S, Patel M, Kurkjian C, Hemphill B, Flores M, Thompson D, et al. A Phase II Study of the c-MET Inhibitor Tivantinib in Combination with FOLFOX for the Treatment of Patients with Previously Untreated Metastatic Adenocarcinoma of the Distal Esophagus, Gastroesophageal Junction, or Stomach. Cancer Invest. 2017;35(7):463-72.

136. Ueda S, Hatsuse K, Tsuda H, Ogata S, Kawarabayashi N, Takigawa T, et al. Potential crosstalk between insulin-like growth factor receptor type 1 and epidermal growth factor receptor in progression and metastasis of pancreatic cancer. Modern pathology. 2006;19(6):788-96.

137. Wang J, Sinnberg T, Niessner H, Dölker R, Sauer B, Kempf WE, et al. PTEN regulates IGF-1R-mediated therapy resistance in melanoma. Pigment cell & melanoma research. 2015;28(5):572-89.

138. Linklater ES, Tovar EA, Essenburg CJ, Turner L, Madaj Z, Winn ME, et al. Targeting MET and EGFR crosstalk signaling in triple-negative breast cancers. Oncotarget. 2016;7(43):69903.

139. Wang S-C, Hung M-C. Nuclear translocation of the epidermal growth factor receptor family membrane tyrosine kinase receptors. Clinical cancer research : an official journal of the American Association for Cancer Research. 2009;15(21):6484-9.

140. Wang Y-N, Hung M-C. Nuclear functions and subcellular trafficking mechanisms of the epidermal growth factor receptor family. Cell Biosci. 2012;2(1):13-.

141. De Angelis Campos AC, Rodrigues MA, de Andrade C, de Goes AM, Nathanson MH, Gomes DA. Epidermal growth factor receptors destined for the nucleus are internalized via a clathrin-dependent pathway. Biochemical and Biophysical Research Communications. 2011;412(2):341-6.

142. Lippincott-Schwartz J, Roberts TH, Hirschberg K. Secretory protein trafficking and organelle dynamics in living cells. Annual review of cell and developmental biology. 2000;16(1):557-89.

143. Wang X, Li S. Protein mislocalization: mechanisms, functions and clinical applications in cancer. Biochimica et biophysica acta. 2014;1846(1):13-25.

144. Lu J, Yang L, Tao Y, Sun L, Cao Y. Role of epidermal growth factor receptor in DNA damage repair. Chinese Science Bulletin. 2011;56(30):3132.

145. Che T-F, Lin C-W, Wu Y-Y, Chen Y-J, Han C-L, Chang Y-l, et al. Mitochondrial translocation of EGFR regulates mitochondria dynamics and promotes metastasis in NSCLC. Oncotarget. 2015;6(35):37349-66.

146. Giordano S, Di Renzo MF, Narsimhan RP, Cooper CS, Rosa C, Comoglio PM. Biosynthesis of the protein encoded by the c-MET proto-oncogene. Oncogene. 1989;4(11):1383-8.

147. Ancot F, Leroy C, Muharram G, Lefebvre J, Vicogne J, Lemiere A, et al. Shedding-generated MET receptor fragments can be routed to either the proteasomal or the lysosomal degradation pathway. Traffic. 2012;13(9):1261-72.

148. Coleman DT, Gray AL, Kridel SJ, Cardelli JA. Palmitoylation regulates the intracellular trafficking and stability of c-Met. Oncotarget. 2016;7(22):32664.

149. Viticchiè G, Muller PAJ. c-MET and Other Cell Surface Molecules: Interaction, Activation and Functional Consequences. Biomedicines. 2015;3(1):46-70.

150. Kobayashi H, Ogawa M, Alford R, Choyke PL, Urano Y. New strategies for fluorescent probe design in medical diagnostic imaging. Chemical reviews. 2010;110(5):2620-40.

151. Terai T, Nagano T. Small-molecule fluorophores and fluorescent probes for bioimaging. Pflugers Arch. 2013;465(3):347-59.

152. Wu Q, Jing Y, Zhao T, Gao J, Cai M, Xu H, et al. Development of small molecule inhibitor-based fluorescent probes for highly specific super-resolution imaging. Nanoscale. 2020;12(42):21591-8.

153. Matheson SL, Brahimi F, Jean-Claude BJ. The combi-targetinG concept: intracellular fragmentation of the binary epidermal growth factor (EGFR)/DNA targeting "combi-triazene" SMA41. Biochem Pharmacol. 2004;67(6):1131-8.

154. Wikstrand CJ, McLendon RE, Friedman AH, Bigner DD. Cell surface localization and density of the tumor-associated variant of the epidermal growth factor receptor, EGFRvIII. Cancer Res. 1997;57(18):4130-40.

155. Boncompain G, Gareil N, Tessier S, Lescure A, Jones TR, Kepp O, et al. BML-265 and Tyrphostin AG1478 disperse the Golgi apparatus and abolish protein transport in human cells. Frontiers in cell and developmental biology. 2019;7:232.

156. Wilson JN, Liu W, Brown AS, Landgraf R. Binding-induced, turn-on fluorescence of the EGFR/ERBB kinase inhibitor, lapatinib. Organic & biomolecular chemistry. 2015;13(17):5006-11.

157. Zhang Y, Hou Q, Li X, Zhu J, Wang W, Li B, et al. Enrichment of novel quinazoline derivatives with high antitumor activity in mitochondria tracked by its self-fluorescence. European journal of medicinal chemistry. 2019;178:417-32.

158. Ilmi R, Tseriotou E, Stylianou P, Christou YA, Ttofi I, Dietis N, et al. A novel conjugate of bis [((4-bromophenyl) amino) quinazoline], a EGFR-TK ligand, with a fluorescent Ru (II)-bipyridine complex exhibits specific subcellular localization in mitochondria. Molecular pharmaceutics. 2019;16(10):4260-73.

159. Brehmer D, Greff Z, Godl K, Blencke S, Kurtenbach A, Weber M, et al. Cellular Targets of Gefitinib. Cancer Research. 2005;65(2):379.

160. Vetter ML, Zhang Z, Liu S, Wang J, Cho H, Zhang J, et al. Fluorescent Visualization of Src by Using Dasatinib-BODIPY. ChemBioChem. 2014;15(9):1317-24.

161. Golabi N, Larroque AL, Peyrard L, Williams C, Jean-Claude BJ. Subcellular distribution and mechanism of action of AL906, a novel and potent EGFR inhibitor rationally designed to be green fluorescent. Invest New Drugs. 2021;39(1):240-50.

162. Todorova MI, Larroque A-L, Dauphin-Pierre S, Fang Y-Q, Jean-Claude BJ. Subcellular Distribution of a Fluorescence-Labeled Combi-Molecule Designed to Block Epidermal Growth Factor Receptor Tyrosine Kinase and Damage DNA with a Green Fluorescent Species. Molecular Cancer Therapeutics. 2010;9(4):869-82.

163. Kim E, Yang KS, Weissleder R. Bioorthogonal Small Molecule Imaging Agents Allow Single-Cell Imaging of MET. PLOS ONE. 2013;8(11):e81275.

164. Zou HY, Li Q, Lee JH, Arango ME, Burgess K, Qiu M, et al. Sensitivity of Selected Human Tumor Models to PF-04217903, a Novel Selective c-MET Kinase Inhibitor. Molecular Cancer Therapeutics. 2012;11(4):1036-47.

165. Patrinos GP, Ansorge W, Danielson PB. Molecular diagnostics. Amsterdam ;: Academic Press is an imprint of Elsevier; 2016. Available from: https://public.ebookcentral.proquest.com/choice/publicfullrecord.aspx?p=4730426 https://www.sciencedirect.com/science/book/9780128029718 http://0-www.sciencedirect.com.pugwash.lib.warwick.ac.uk/science/book/9780128029718

http://www.vlebooks.com/vleweb/product/openreader?id=none&isbn=9780128029886.

166. Hsiao SJ. Sources of error in molecular diagnostic analyses. Accurate Results in the Clinical Laboratory: Elsevier; 2019. p. 337-47.

167. Poste G. Molecular diagnostics: a powerful new component of the healthcare value chain. Expert Review of Molecular Diagnostics. 2001;1(1):1-5.

168. Burtis CA, Ashwood ER, Bruns DE. Tietz Textbook of Clinical Chemistry and Molecular Diagnostics - E-Book: Elsevier Health Sciences; 2012.

169. Kan YW, Golbus MS, Dozy AM. Prenatal diagnosis of alpha-thalassemia. Clinical application of molecular hybridization. N Engl J Med. 1976;295(21):1165-7.

170. Strimbu K, Tavel JA. What are biomarkers? Curr Opin HIV AIDS. 2010;5(6):463-6.

171. Saiki RK, Scharf S, Faloona F, Mullis KB, Horn GT, Erlich HA, et al. Enzymatic amplification of beta-globin genomic sequences and restriction site analysis for diagnosis of sickle cell anemia. Science. 1985;230(4732):1350-4.

172. Hamburg MA, Collins FS. The path to personalized medicine. N Engl J Med. 2010;363(4):301-4.

173. Kan YW, Lee KY, Furbetta M, Angius A, Cao A. Polymorphism of DNA sequence in the beta-globin gene region. Application to prenatal diagnosis of beta 0 thalassemia in Sardinia. N Engl J Med. 1980;302(4):185-8.

174. Kan YW, Dozy AM. Polymorphism of DNA sequence adjacent to human beta-globin structural gene: relationship to sickle mutation. Proceedings of the National Academy of Sciences. 1978;75(11):5631-5.

175. Woo SL, Lidsky AS, Güttler F, Chandra T, Robson KJ. Cloned human phenylalanine hydroxylase gene allows prenatal diagnosis and carrier detection of classical phenylketonuria. Nature. 1983;306(5939):151-5.

176. Farrall M, Rodeck C, Stanier P, Lissens W, Watson E, Law H-Y, et al. First-trimester prenatal diagnosis of cystic fibrosis with linked DNA probes. The lancet. 1986;327(8495):1402-5.

177. Orkin SH, Kazazian HH, Jr., Antonarakis SE, Ostrer H, Goff SC, Sexton JP. Abnormal RNA processing due to the exon mutation of beta E-globin gene. Nature. 1982;300(5894):768-9.

178. Persselin JE, Stevens RH. Anti-Fab antibodies in humans. Predominance of minor immunoglobulin G subclasses in rheumatoid arthritis. J Clin Invest. 1985;76(2):723-30.

179. Kaplan G, Gaudernack G. In vitro differentiation of human monocytes. Differences in monocyte phenotypes induced by cultivation on glass or on collagen. The Journal of experimental medicine. 1982;156(4):1101-14.

180. Busslinger M, Moschonas N, Flavell RA. Beta + thalassemia: aberrant splicing results from a single point mutation in an intron. Cell. 1981;27(2 Pt 1):289-98.

181. Treisman R, Orkin SH, Maniatis T. Specific transcription and RNA splicing defects in five cloned β-thalassaemia genes. Nature. 1983;302(5909):591-6.

182. Myers RM, Lumelsky N, Lerman LS, Maniatis T. Detection of single base substitutions in total genomic DNA. Nature. 1985;313(6002):495-8.

183. Collins M, Myers RM. Alterations in DNA helix stability due to base modifications can be evaluated using denaturing gradient gel electrophoresis. Journal of molecular biology. 1987;198(4):737-44.

184. Orkin SH, Markham AF, Kazazian HH, Jr. Direct detection of the common Mediterranean beta-thalassemia gene with synthetic DNA probes. An alternative approach for prenatal diagnosis. The Journal of Clinical Investigation. 1983;71(3):775-9.

185. Mullis KB, Faloona FA. [21] Specific synthesis of DNA in vitro via a polymerase-catalyzed chain reaction. Methods in enzymology. 1987;155:335-50.

186. Domon B, Aebersold R. Mass spectrometry and protein analysis. Science. 2006;312(5771):212-7.

187. Jungbauer A, Hahn R. Ion-exchange chromatography. Methods Enzymol. 2009;463:349-71.

188. Voedisch B, Thie H. Size exclusion chromatography. Antibody Engineering: Springer; 2010. p. 607-12.

189. Hage DS, Anguizola JA, Bi C, Li R, Matsuda R, Papastavros E, et al. Pharmaceutical and biomedical applications of affinity chromatography: recent trends and developments. Journal of pharmaceutical and biomedical analysis. 2012;69:93-105.

190. Lequin RM. Enzyme immunoassay (EIA)/enzyme-linked immunosorbent assay (ELISA). Clinical chemistry. 2005;51(12):2415-8.

191. Kurien BT, Scofield RH. Western blotting. Methods. 2006;38(4):283-93.

192. Dunn MJ, Burghes AH. High resolution two-dimensional polyacrylamide-gel electrophoresis. Gel Electrophoresis of Proteins: Elsevier; 1986. p. 203-61.

193. Issaq HJ, Veenstra TD. Two-dimensional polyacrylamide gel electrophoresis (2D-PAGE): advances and perspectives. Biotechniques. 2008;44(5):697-700.

194. Marouga R, David S, Hawkins E. The development of the DIGE system: 2D fluorescence difference gel analysis technology. Analytical and bioanalytical chemistry. 2005;382(3):669-78.

195. Sutandy FR, Qian J, Chen CS, Zhu H. Overview of protein microarrays. Current protocols in protein science. 2013;72(1):27.1. 1-.1. 16.

196. Yates III JR. A century of mass spectrometry: from atoms to proteomes. nature methods. 2011;8(8):633-7.

197. Smith JB. Peptide sequencing by Edman degradation. e LS. 2001.

198. Shiio Y, Aebersold R. Quantitative proteome analysis using isotope-coded affinity tags and mass spectrometry. Nature protocols. 2006;1(1):139-45.

199. Ong S-E, Blagoev B, Kratchmarova I, Foster LJ, Andersen JS, Mann M. Stable isotope labeling by amino acids in cell culture for quantitative proteomics. Cell Biology: Elsevier; 2006. p. 427-36.

200. Wiese S, Reidegeld KA, Meyer HE, Warscheid B. Protein labeling by iTRAQ: a new tool for quantitative mass spectrometry in proteome research. Proteomics. 2007;7(3):340-50.

201. Kroksveen AC, Jaffe JD, Aasebø E, Barsnes H, Bjørlykke Y, Franciotta D, et al. Quantitative proteomics suggests decrease in the secretogranin-1 cerebrospinal fluid levels during the disease course of multiple sclerosis. Proteomics. 2015;15(19):3361-9.

202. Aebersold R, Mann M. Mass spectrometry-based proteomics. Nature. 2003;422(6928):198-207.

203. Yamashita M, Fenn JB. Electrospray ion source. Another variation on the free-jet theme. The Journal of Physical Chemistry. 1984;88(20):4451-9.

204. Ong SE, Mann M. Mass spectrometry-based proteomics turns quantitative. Nat Chem Biol. 2005;1(5):252-62.

205. Bondarenko PV, Chelius D, Shaler TA. Identification and relative quantitation of protein mixtures by enzymatic digestion followed by capillary reversed-phase liquid chromatography-tandem mass spectrometry. Anal Chem. 2002;74(18):4741-9.

206. Cox J, Hein MY, Luber CA, Paron I, Nagaraj N, Mann M. Accurate proteome-wide label-free quantification by delayed normalization and maximal peptide ratio extraction, termed MaxLFQ. Mol Cell Proteomics. 2014;13(9):2513-26.

207. Carrillo B, Yanofsky C, Laboissiere S, Nadon R, Kearney RE. Methods for combining peptide intensities to estimate relative protein abundance. Bioinformatics. 2010;26(1):98-103.

208. Hultin-Rosenberg L, Forshed J, Branca RM, Lehtiö J, Johansson HJ. Defining, comparing, and improving iTRAQ quantification in mass spectrometry proteomics data. Mol Cell Proteomics. 2013;12(7):2021-31.

209. Webb-Robertson BJ, Wiberg HK, Matzke MM, Brown JN, Wang J, McDermott JE, et al. Review, evaluation, and discussion of the challenges of missing value imputation for mass spectrometry-based label-free global proteomics. J Proteome Res. 2015;14(5):1993-2001.

210. Mann M, Kulak NA, Nagaraj N, Cox J. The coming age of complete, accurate, and ubiquitous proteomes. Mol Cell. 2013;49(4):583-90.

211. Lazar C, Gatto L, Ferro M, Bruley C, Burger T. Accounting for the Multiple Natures of Missing Values in Label-Free Quantitative Proteomics Data Sets to Compare Imputation Strategies. J Proteome Res. 2016;15(4):1116-25.

212. Wei R, Wang J, Su M, Jia E, Chen S, Chen T, et al. Missing Value Imputation Approach for Mass Spectrometry-based Metabolomics Data. Sci Rep. 2018;8(1):663.

213. Meier F, Brunner AD, Koch S, Koch H, Lubeck M, Krause M, et al. Online Parallel Accumulation-Serial Fragmentation (PASEF) with a Novel Trapped Ion Mobility Mass Spectrometer. Mol Cell Proteomics. 2018;17(12):2534-45.

214. Ong SE, Blagoev B, Kratchmarova I, Kristensen DB, Steen H, Pandey A, et al. Stable isotope labeling by amino acids in cell culture, SILAC, as a simple and accurate approach to expression proteomics. Mol Cell Proteomics. 2002;1(5):376-86.

215. Gygi SP, Rist B, Gerber SA, Turecek F, Gelb MH, Aebersold R. Quantitative analysis of complex protein mixtures using isotope-coded affinity tags. Nat Biotechnol. 1999;17(10):994-9.

216. Li Z, Adams RM, Chourey K, Hurst GB, Hettich RL, Pan C. Systematic comparison of label-free, metabolic labeling, and isobaric chemical labeling for quantitative proteomics on LTQ Orbitrap Velos. J Proteome Res. 2012;11(3):1582-90.

217. Lanucara F, Holman SW, Gray CJ, Eyers CE. The power of ion mobility-mass spectrometry for structural characterization and the study of conformational dynamics. Nature chemistry. 2014;6(4):281-94.

218. Yi EC, Marelli M, Lee H, Purvine SO, Aebersold R, Aitchison JD, et al. Approaching complete peroxisome characterization by gas-phase fractionation. Electrophoresis. 2002;23(18):3205-16.

219. Pfammatter S, Bonneil E, McManus FP, Prasad S, Bailey DJ, Belford M, et al. A Novel Differential Ion Mobility Device Expands the Depth of Proteome Coverage and the Sensitivity of Multiplex Proteomic Measurements. Mol Cell Proteomics. 2018;17(10):2051-67.

220. Bantscheff M, Scholten A, Heck AJ. Revealing promiscuous drug–target interactions by chemical proteomics. Drug discovery today. 2009;14(21-22):1021-9.

221. Carlson SM, White FM. Using small molecules and chemical genetics to interrogate signaling networks. ACS chemical biology. 2011;6(1):75-85.

222. Sadaghiani AM, Verhelst SH, Bogyo M. Tagging and detection strategies for activity-based proteomics. Current opinion in chemical biology. 2007;11(1):20-8.

223. Yamamoto K, Yamazaki A, Takeuchi M, Tanaka A. A versatile method of identifying specific binding proteins on affinity resins. Analytical biochemistry. 2006;352(1):15-23.

224. Cravatt BF, Wright AT, Kozarich JW. Activity-based protein profiling: from enzyme chemistry to proteomic chemistry. Annu Rev Biochem. 2008;77:383-414.

225. Liang X, Hajivandi M, Veach D, Wisniewski D, Clarkson B, Resh MD, et al. Quantification of change in phosphorylation of BCR-ABL kinase and its substrates in response to Imatinib treatment in human chronic myelogenous leukemia cells. Proteomics. 2006;6(16):4554-64.

226. Lee AY, Paweletz CP, Pollock RM, Settlage RE, Cruz JC, Secrist JP, et al. Quantitative analysis of histone deacetylase-1 selective histone modifications by differential mass spectrometry. Journal of proteome research. 2008;7(12):5177-86.

227. Song D, Chaerkady R, Tan AC, García-García E, Nalli A, Suárez-Gauthier A, et al. Antitumor activity and molecular effects of the novel heat shock protein 90 inhibitor, IPI-504, in pancreatic cancer. Molecular cancer therapeutics. 2008;7(10):3275-84.

228. Domon B, Aebersold R. Options and considerations when selecting a quantitative proteomics strategy. Nature biotechnology. 2010;28(7):710-21.

229. Zhang Y, Fonslow BR, Shan B, Baek M-C, Yates III JR. Protein analysis by shotgun/bottom-up proteomics. Chemical reviews. 2013;113(4):2343-94.

230. Yates III JR. The revolution and evolution of shotgun proteomics for large-scale proteome analysis. Journal of the American Chemical Society. 2013;135(5):1629-40.

231. Catherman AD, Skinner OS, Kelleher NL. Top down proteomics: facts and perspectives. Biochemical and biophysical research communications. 2014;445(4):683-93.

232. Toby TK, Fornelli L, Kelleher NL. Progress in top-down proteomics and the analysis of proteoforms. Annual review of analytical chemistry. 2016;9:499-519.

233. Gao Y, Yates III JR. Protein Analysis by Shotgun Proteomics. Mass Spectrometry-Based Chemical Proteomics2019. p. 1-38.

234. Bantscheff M, Eberhard D, Abraham Y, Bastuck S, Boesche M, Hobson S, et al. Quantitative chemical proteomics reveals mechanisms of action of clinical ABL kinase inhibitors. Nature biotechnology. 2007;25(9):1035-44.

235. Klaeger S, Heinzlmeir S, Wilhelm M, Polzer H, Vick B, Koenig PA, et al. The target landscape of clinical kinase drugs. Science. 2017;358(6367).

236. Medard G, Pachl F, Ruprecht B, Klaeger S, Heinzlmeir S, Helm D, et al. Optimized chemical proteomics assay for kinase inhibitor profiling. J Proteome Res. 2015;14(3):1574-86.

237. Konecny GE, Pegram MD, Venkatesan N, Finn R, Yang G, Rahmeh M, et al. Activity of the dual kinase inhibitor lapatinib (GW572016) against HER-2-overexpressing and trastuzumab-treated breast cancer cells. Cancer research. 2006;66(3):1630-9.

238. Fonović M, Bogyo M. Activity-based probes as a tool for functional proteomic analysis of proteases. Expert Rev Proteomics. 2008;5(5):721-30.

239. Budin G, Moune-Dimala M, Leriche G, Saliou JM, Papillon J, Sanglier-Cianférani S, et al. Nondenaturing chemical proteomics for protein complex isolation and identification. ChemBioChem. 2010;11(17):2359-61.

240. Shi H, Zhang CJ, Chen GY, Yao SQ. Cell-based proteome profiling of potential dasatinib targets by use of affinity-based probes. J Am Chem Soc. 2012;134(6):3001-14.

241. Ursuegui S, Recher M, Krężel W, Wagner A. An in vivo strategy to counteract post-administration anticoagulant activity of azido-Warfarin. Nature communications. 2017;8(1):1-8.

242. Ku X, Heinzlmeir S, Liu X, Médard G, Kuster B. A new chemical probe for quantitative proteomic profiling of fibroblast growth factor receptor and its inhibitors. Journal of proteomics. 2014;96:44-55.

243. Koch H, Busto MEDC, Kramer K, Médard G, Kuster B. Chemical proteomics uncovers EPHA2 as a mechanism of acquired resistance to small molecule EGFR kinase inhibition. Journal of proteome research. 2015;14(6):2617-25.

244. Schleidgen S, Fernau S, Fleischer H, Schickhardt C, Oßa A-K, Winkler EC. Applying systems biology to biomedical research and health care: a précising definition of systems medicine. BMC health services research. 2017;17(1):1-16.

245. Federoff HJ, Gostin LO. Evolving From Reductionism to Holism: Is There a Future for Systems Medicine? JAMA. 2009;302(9):994-6.

246. Kudva PB. Systems medicine – Evolution of a new era in health care. J Indian Soc Periodontol. 2016;20(3):232-3.

247. Zhang W, Huai Y, Miao Z, Qian A, Wang Y. Systems Pharmacology for Investigation of the Mechanisms of Action of Traditional Chinese Medicine in Drug Discovery. Front Pharmacol. 2019;10:743-.

248. Vicini P, van der Graaf PH. Systems pharmacology for drug discovery and development: paradigm shift or flash in the pan? Clin Pharmacol Ther. 2013;93(5):379-81.

249. Casas AI, Hassan AA, Larsen SJ, Gomez-Rangel V, Elbatreek M, Kleikers PW, et al. From single drug targets to synergistic network pharmacology in ischemic stroke. Proceedings of the National Academy of Sciences. 2019;116(14):7129-36.

250. Pritchard K, Martin D, Naylor S. Systems pharmacology: when multi-targeting is advantageous. Drug Discovery World. 2019;2018:33-43.

251. Vrbanac J, Slauter R. Chapter 3 - ADME in Drug Discovery. In: Faqi AS, editor. A Comprehensive Guide to Toxicology in Nonclinical Drug Development (Second Edition). Boston: Academic Press; 2017. p. 39-67.

252. Ratain MJ, Schilsky RL, Conley BA, Egorin MJ. Pharmacodynamics in cancer therapy. J Clin Oncol. 1990;8(10):1739-53.

253. Joly JH, Chew BT, Graham NA. The landscape of metabolic pathway dependencies in cancer cell lines. PLoS Computational Biology. 2021;17(4):e1008942.

254. Giordano S, Petrelli A. From single-to multi-target drugs in cancer therapy: when aspecificity becomes an advantage. Current medicinal chemistry. 2008;15(5):422-32.

255. Ramsay RR, Popovic-Nikolic MR, Nikolic K, Uliassi E, Bolognesi ML. A perspective on multi-target drug discovery and design for complex diseases. Clinical and translational medicine. 2018;7(1):1-14.

256. Zhang W, Huai Y, Miao Z, Qian A, Wang Y. Systems Pharmacology for Investigation of the Mechanisms of Action of Traditional Chinese Medicine in Drug Discovery. Front Pharmacol. 2019;10:743.

257. Wright M, Sieber S. Chemical proteomics approaches for identifying the cellular targets of natural products. Natural product reports. 2016;33(5):681-708.

258. Larroque-Lombard AL, Ning N, Rao S, Lauwagie S, Halaoui R, Coudray L, et al. Biological Effects of AL622, a Molecule Rationally Designed to Release an EGFR and ac-Src Kinase Inhibitor. Chemical biology & drug design. 2012;80(6):981-91.

259. Boerner JL, Demory ML, Silva C, Parsons SJ. Phosphorylation of Y845 on the epidermal growth factor receptor mediates binding to the mitochondrial protein cytochrome c oxidase subunit II. Molecular and cellular biology. 2004;24(16):7059-71.

260. Cao X, Zhu H, Ali-Osman F, Lo H-W. EGFR and EGFRvIII undergo stress-and EGFR kinase inhibitor-induced mitochondrial translocalization: a potential mechanism of EGFR-driven antagonism of apoptosis. Molecular cancer. 2011;10(1):1-13.

261. Guo T, Zhu Y, Gan CS, Lee SS, Zhu J, Wang H, et al. Quantitative proteomics discloses MET expression in mitochondria as a direct target of MET kinase inhibitor in cancer cells. Molecular & Cellular Proteomics. 2010;9(12):2629-41.

262. Gentile A, Trusolino L, Comoglio PM. The MET tyrosine kinase receptor in development and cancer. Cancer Metastasis Rev. 2008;27(1):85-94.

263. Johnson M, Koukoulis G, Matsumoto K, Nakamura T, Iyer A. Hepatocyte growth factor induces proliferation and morphogenesis in nonparenchymal epithelial liver cells. Hepatology. 1993;17(6):1052-61.

264. Liu T, Mendes DE, Berkman CE. From AR to c-Met: Androgen deprivation leads to a signaling pathway switch in prostate cancer cells. International journal of oncology. 2013;43(4):1125-30.

265. Verras M, Lee J, Xue H, Li TH, Wang Y, Sun Z. The androgen receptor negatively regulates the expression of c-Met: implications for a novel mechanism of prostate cancer progression. Cancer Res. 2007;67(3):967-75.

266. Nakazawa M, Paller C, Kyprianou N. Mechanisms of Therapeutic Resistance in Prostate Cancer. Curr Oncol Rep. 2017;19(2):13-.

267. Antonarakis ES, Armstrong AJ. Evolving standards in the treatment of docetaxel-refractory castration-resistant prostate cancer. Prostate Cancer Prostatic Dis. 2011;14(3):192-205.

268. Berry W, Friedland D, Fleagle J, Jackson D, Ilegbodu D, Boehm KA, et al. A phase II study of weekly paclitaxel/estramustine/carboplatin in hormone-refractory prostate cancer. Clin Genitourin Cancer. 2006;5(2):131-7.

269. Kelly WK, Curley T, Slovin S, Heller G, McCaffrey J, Bajorin D, et al. Paclitaxel, estramustine phosphate, and carboplatin in patients with advanced prostate cancer. Journal of clinical oncology. 2001;19(1):44-53.

270. Obasaju C, Hudes GR. Paclitaxel and docetaxel in prostate cancer. Hematology/Oncology Clinics. 2001;15(3):525-45.

271. Scharer CD, Laycock N, Osunkoya AO, Logani S, McDonald JF, Benigno BB, et al. Aurora kinase inhibitors synergize with paclitaxel to induce apoptosis in ovarian cancer cells. J Transl Med. 2008;6:79-.

VII APPENDIX

McGill

Faculty of Medicine
3655 Promenade Sir William Osler #633
Montreal, QC H3G 1Y6

Faculté de médecine
3655, Promenade Sir William Osler #633
Montréal, QC H3G 1Y6

Fax/Télécopieur: (514) 398-3870
Tél/Tel: (514) 398-3124

CERTIFICATION OF ETHICAL ACCEPTABILITY FOR RESEARCH INVOLVING HUMAN SUBJECTS

The Faculty of Medicine Institutional Review Board (IRB) is a registered University IRB working under the published guidelines of the Tri-Council Policy Statement, in compliance with the Plan d'action ministériel en éthique de la recherche et en intégrité scientifique, (MSSS, 1998) and the Food and Drugs Act (17 June 2001); and acts in accordance with the U.S. Code of Federal Regulations that govern research on human subjects. The IRB working procedures are consistent with internationally accepted principles of good clinical practice.

At a full Board meeting on September 23, 2013, the Faculty of Medicine Institutional Review Board, consisting of:

Frances Aboud, PhD	Pierre Deschamps, BCL, LScR
Carolyn Ells, PhD	Marigold Hyde, B.Sc.
Adrian Langleben, MD	Sally Mann, MS
Kathleen Montpetit, MS	Shahad Salman, LL.B., JD

Harvey Sigman, MD

Examined the research project **A09-M95-13B** titled: *A phase IV, multicenter trial to evaluate the resistance mechanisms and real-world pharmacoeconomics of crizotinib and its companion diagnostic test in advanced ALK-positive non-small cell lung cancer (NSCLC) patients [McG 1327]*

As proposed by: Dr. Jason Agulnik (Applicant) to _____ (Granting Agency, if any)

And consider the experimental procedures to be acceptable on ethical grounds for research involving human subjects.

6 December 2013	Carolyn Ells	R. Reinhart
Date	Chair, IRB	Dean of Faculty

Institutional Review Board Assurance Number: FWA 00004545